Recombinant Expression, Purification and Characterisation of *Tz*CATB and *Tz*stefinB from *Trichinella zimbabwensis*

by

Ryan Woodgate

BSc (Hons) in Biochemistry

In fulfilment of the academic requirements of:

MSc in Biochemistry

Department of Biochemistry

School of Life Sciences

University of KwaZulu-Natal

Pietermaritzburg

2024

Preface

The experimental work described in this dissertation was carried out in the School of Life Sciences, University of KwaZulu-Natal, Pietermaritzburg, under the supervision of Professor THT Coetzer. The study represents the original work by the author and has not otherwise been submitted in any other form to another University. Where use has been made of the work of others, it has been duly acknowledged in the text.

Ryan Woodgate

As the candidates Supervisor I agree to the submission of this dissertation.

Prof. Theresa H. T. Coetzer

Declaration – Plagiarism

I, Ryan Woodgate, declare that:

1. The research reported in this dissertation, except where otherwise indicated, is my original research.

2. This dissertation has not been submitted for any degree or examination at any other university.

3. This dissertation does not contain other persons' data, pictures, graphs or other information, unless specifically acknowledged as being sourced from other persons.

4. This dissertation does not contain other persons' writing, unless specifically acknowledged as being sourced from other researchers. Where other written sources have been quoted, then:

a. Their words have been re-written, but the general information attributed to them has been referenced.

b. Where their exact words have been used, then their writing has been placed in italics and inside quotation marks and referenced.

5. This dissertation does not contain text, graphics or tables copied and pasted from the Internet, unless specifically acknowledged, and the source being detailed in the dissertation and in the Reference section.

Ryan Woodgate

Acknowledgements

I would like to extend my most sincere and heart-felt gratitude to my supervisor, Professor Theresa HT Coetzer. Her guidance, undying support, patience, teaching of new techniques, and perspective on how to analyse scientific literature and lab results, are all things I am truly grateful to have been given during my years working in her laboratory. I had no doubt at all in my choice of supervisor in the beginning and I remain with no regrets, I have felt truly at home working in Lab 45 and it will remain in my heart forever.

Thank you to my fellow researchers in Lab 45. Arishka, you provided me with guidance many times, and I will always appreciate your willingness to lend your knowledge. Faiaz, you were always extremely helpful and always seemed ready to take on the task of helping out with anyone else's scientific challenges while no doubt being busy enough with your own work. Thank you to Lucky (may his soul rest in peace). You were taken away from us all so suddenly and unexpectedly. You were one of if not the kindest person I met in my years as a student, and you like Faiaz were also always so helpful at any time. You were also so intelligent and hard-working. You are greatly missed by all who got to know you at Lab 45.

I would like to thank the National Research Foundation for funding this research project and giving me this amazing opportunity to expand myself as a student and a scientist.

I would like to thank my loving partner, Caitlin, for her never-ending support throughout my years of study. Throughout every moment where I felt like I had hit a brick-wall, was utterly confused and frustrated with research and felt more stressed than I ever had before, she was there every time and despite not always knowing exactly what was going on in the lab, she was always able to reassure me, stabilise me, and set me back on the right track, allowing me to regain my motivation. Thank you so much for being so patient with me and supporting me throughout these years.

Thank you to my parents for supporting my studies, believing in my ability, and motivating me to push further and further than what I ever originally thought possible.

Thank you to my amazing daughter, Arabella May Woodgate. Through many of the darkest days, you have been the light that keeps me going, shining the way forward. I am so incredibly proud of you and forever will be. There were countless times when I felt overwhelmed and like my motivation might have been fading, but thinking of you gave me the strength and motivation to keep going, keep trying, and to never stop, regardless of any hurdles along the way.

Abstract

Parasitic roundworms of the genus *Trichinella*, the causative agents of Trichinellosis, are highly successful parasites evident by their broad geographical and host ranges and their ability to manipulate the host immune system. The focal species of this study was *T. zimbabwensis*; a lesser studied member of the genus prevailing in Sub-Saharan Africa. Although not yet reported in humans, in the absence of a diagnostic test for this species of *Trichinella*, it poses a risk to human health and economic well-being. Research on different antigens expressed across all the stages of the parasite lifecycle may identify diagnostic, drug and vaccination targets. Cysteine proteases and protease inhibitors are particularly valuable targets for these purposes due to their essential functions in the parasite's lifecycle, such as penetration of the small intestinal wall, nutrient acquisition and immune evasion amongst others. The aim of the present study was to recombinantly express and characterise cathepsin B (*Tz*CATB) and stefin B (*Tz*stefinB) from *T. zimbabwensis*. Recombinant *Tz*CATB was expressed in the pET-28a and pCold-1 expression vectors as insoluble proteins at 43 and 42 kDa, respectively. After solubilisation and nickel immobilised metal affinity chromatography (Ni-IMAC) purification of these proteins, no proteolytic activity was detected. Recombinant *Tz*CATB was subsequently expressed in the pCold-TF expression vector as a soluble protein 90 kDa protein, which was purified using immunoaffinity chromatography and the attached trigger factor fusion protein removed with thrombin cleavage. However, this preparation of *Tz*CATB also did not have hydrolytic activity but was detected by chicken anti-*Tz*CATB IgY antibodies in a western blot, but not by rabbit anti-human cathepsin B antibodies. Recombinant *Tz*stefinB was expressed in the pET-28a expression vector as a soluble 16 kDa protein and purified with IMAC. Purified *Tz*stefinB was used to raise IgY antibodies in chickens, which were confirmed to detect the protein in ELISA and western blotting. These antibodies did not detect sheep stefin B. Purified *Tz*stefinB inhibited the hydrolysis of Z-Phe-Arg-AMC by the plant cysteine protease papain as well as by cathepsin L from the parasite *Trypanosoma congolense*. The inhibition of papain by TzstefinB was also detected with reverse zymography. The inhibitory activity of recombinant *Tz*stefinB was shown to be stable from pH 5.0 to pH 9.0, was rapidly inactivated with incubation at 99 ºC, and was retained after storage at both 4 ºC and room temperature for up to 3 weeks. Thus, *Tz*CATB was recombinantly expressed but was inactive, *Tz*stefinB was recombinantly expressed and demonstrated to have inhibitory activity that is stable across a broad pH range but sensitive to high temperature, and both of these proteins have potential as diagnostic markers.

Table of Contents

List of Figures

List of Tables

Abbreviations

2 x YT	yeast extract, tryptone
A_{280}	absorbance (280 nm)
ABTS	2,2-azino-di-[3-ethylbenzthiazoline sulfonate]
AMC	7-amino-4-methylcoumarin
AMT	acetate-MES-tris
bp	base pairs
BSA	bovine serum albumin
CATB	cathepsin B
CATL	cathepsin L
cDNA	complementary deoxyribonucleic acid
C-terminal	carboxy terminal
dH_2O	distilled water
dNTP	deoxynucleotide triphosphate
DTT	dithiothreitol
E. coli	*Escherichia coli*
E-64	L-trans-epoxysuccinyl-leucylamido (4-guanidino) butane
EDTA	ethylenediaminetetra-acetic acid
ELISA	enzyme-linked immunosorbent assay
Em	emission
ER	endoplasmic reticulum
ES	excretory-secretory
Ex	excitation
g	g-force (RCF)
h	Hours
HCl	hydrogen chloride
HRPO	horseradish peroxidase
IFN-γ	interferon gamma
Ig	immunoglobulin
IPTG	isopropyl-β-D-thiogalactopyranoside
kDa	kilodalton
M	molecular weight
min	minute (s)
mRNA	messenger RNA
NCBI	National Centre for Biotechnology Information
N-terminal	amino terminal

OD_{600}	optical density (at 600 nm)
PAGE	polyacrylamide gel electrophoresis
PBS	phosphate buffered saline
PCE	sarkosyl elution buffer
PCL	sarkosyl lysis buffer
PCR	polymerase chain reaction
PCW	sarkosyl wash buffer
PDB	Protein Data Bank
PEG	polyethylene glycol
RT	room temperature
s	second (s)
sarkosyl	N-lauroyl sarcosine sodium salt
SBTI	soya bean trypsin inhibitor
SDS	sodium dodecyl sulfate
TAE	tris-acetate-EDTA
TBS	tris-buffered saline
Tfh	follicular T-helper cells
Th	T-helper cells
Tris	2-amino-2-(hydroxymethyl)-1,3-propandiol
U	units
UV	ultraviolet
V	volts
X-gal	isopropyl-β-D-thiogalactopyranoside
Z-Arg-Arg-AMC	benzyloxycarbonylargininylarginine-7-amino-4-methylcoumarin
Z-Phe-Arg-AMC	benzyloxycarbonylphenylalanylarginine-7-amino-4-methylcoumarin

Chapter One

Literature Review

1.1 Introduction

Nematodes (commonly known as roundworms) are diverse and abundant in nature. They are highly adaptable and can exist as free-living organisms in many habitats (playing an important role in nutrient recycling) or, in the case of more than half of the phylum, as parasites within an array of hosts including plants and animals (Cooper and Eleftherianos, 2016; Iqbal and Jones, 2017). Over 300 species have been reported to infect humans with infections mostly occurring in tropical and/or developing countries. Within the phylum Nematoda exists a highly successful parasitic genus known as *Trichinella*, the most common species of which (*T. spiralis*) was first formally reported in 1835, and the genus has in recent years been determined through research to contain 13 different genotypes with 10 of them being classified as distinct species (Zarlenga et al., 2020). These parasites infect a wide range of animals including humans, in which they cause the food-borne disease known as Trichinellosis (Pozio et al., 2003). These parasites are listed by the World Health Organisation/United Nations Food and Agriculture Organisation as one of the most important food-borne parasites (Sharma et al., 2021).

The disease arises from the consumption of undercooked meat where *Trichinella* larvae reside in the striated muscle; pork being a notorious source of infection (Vutova et al., 2020; Khurana et al., 2021; Zhang et al., 2022). *Trichinella* infections cause numerous symptoms, such as diarrhoea, muscle pain and fever, which makes diagnosis of Trichinellosis difficult. Like other parasitic helminths, *Trichinella* parasites can modulate the host immune system (immunomodulation) whereby they make use of functional proteins and excretory-secretory (ES) products that have functions such as tissue penetration and anti-inflammatory activity. Examples include proteases and protease inhibitors from *T. spiralis*; serine proteases being most common, along with cysteine, aspartyl and metalloproteases (Todorova et al., 1995; Todorova, 2000; Sofronic-Milosavljevic et al., 2015; Xu et al., 2021). These proteins are vital for the parasitism of *Trichinella* and thus have become valuable targets for the development of diagnostic tests, drugs and vaccines. In addition, *Trichinella* muscle larvae survive in the host by existing within a modified “nurse” cell which protects and supports growth of the parasite (Despommier, 1998; Wu et al., 2013).

Trichinella zimbabwensis, which is the focal species in this study, was first discovered in 1995 in farmed Nile crocodiles from Zimbabwe (Pozio et al., 2007). Three *Trichinella* species belong to the non-encapsulated clade of the genus, which refers to the absence of a collagen capsule

around the nurse cell, produced by the majority of *Trichinella* species including *T. spiralis* (Park et al., 2016). *Trichinella zimbabwensis* prevails in Eastern and Southern sub-Saharan Africa in reptilian and mammalian hosts (with predatory scavengers being especially important hosts), and while it has not been officially reported in humans, there is concern for this due to its infectivity in experimental primates as well as domestic pigs (La Grange et al., 2010; La Grange and Mukaratirwa, 2020; Ndlovu et al., 2023). This species of *Trichinella* was found to have higher prevalence in carnivores than other species known to circulate in South Africa and can be regarded as a high-risk food safety concern (La Grange and Mukaratirwa, 2020).

There is currently no diagnostic test for infection by *T. zimbabwensis* and it poses a risk to human health and economic well-being especially in poor, developing countries. Despite being studied for a long time, Trichinellosis remains a public health hazard. The discovery of new species within the genus as well as new hosts, emphasise the need to study different members of the genus to obtain a better understanding of Trichinellosis beyond the typical *T. spiralis* model (Bruschi and Murrell, 2002). Numerous disease outbreaks caused by other species such as *T. britovi*, *T. pseudospiralis* and *T. paupae* have been reported (Jongwutiwes et al., 1998; Ranque et al., 2000; Khumjui et al., 2008; Pavic et al., 2020). It is important that the biology of the different members of the genus is understood to ensure advances in diagnosis, treatment and prevention of infections.

1.2 Classification and distribution of *Trichinella*

The term “helminth” translates to “worm”, and these lifeforms can be classified as Cestodes, Trematodes and Nematodes based upon morphology (Castro, 1996) Cestodes and Trematodes comprise the platyhelminths (flatworms) and refer to tapeworms and flukes, respectively, while Nematodes are roundworms. The phylum Nematoda consists of the classes Chromadorea and Enoplea (Fig. 1.1) which are subdivided into three sub-classes being Chromadoria, Enoplia and Dorylamia (De Ley, 2006). Dorylamia consists of a variety of free-living and parasitic nematodes, including those of the genus *Trichinella* (Smythe et al., 2019) which belong to the order Trichinellida, as part of the Trichinellidae family within the Trichinelloidea superfamily. To date 13 species of *Trichinella* (T1-T13) have been classified between two clades within the genus: the majority being within the encapsulated clade and three within the non-encapsulated clade (T4, T10 and T11), including *T. zimbabwensis* (Pozio et al., 2002; Sharma et al., 2021).

The encapsulated and non-encapsulated species are similar in their modes of infection in that they both induce dedifferentiation of host muscle cells into nurse cells, but are distinct in that the encapsulated members induce the nurse cell to produce a protective collagen capsule

(Pozio et al., 2001). This capsule is beneficial to the survival of the members of this clade as it allows them to survive for longer periods, remaining infective within rotting muscle tissue.

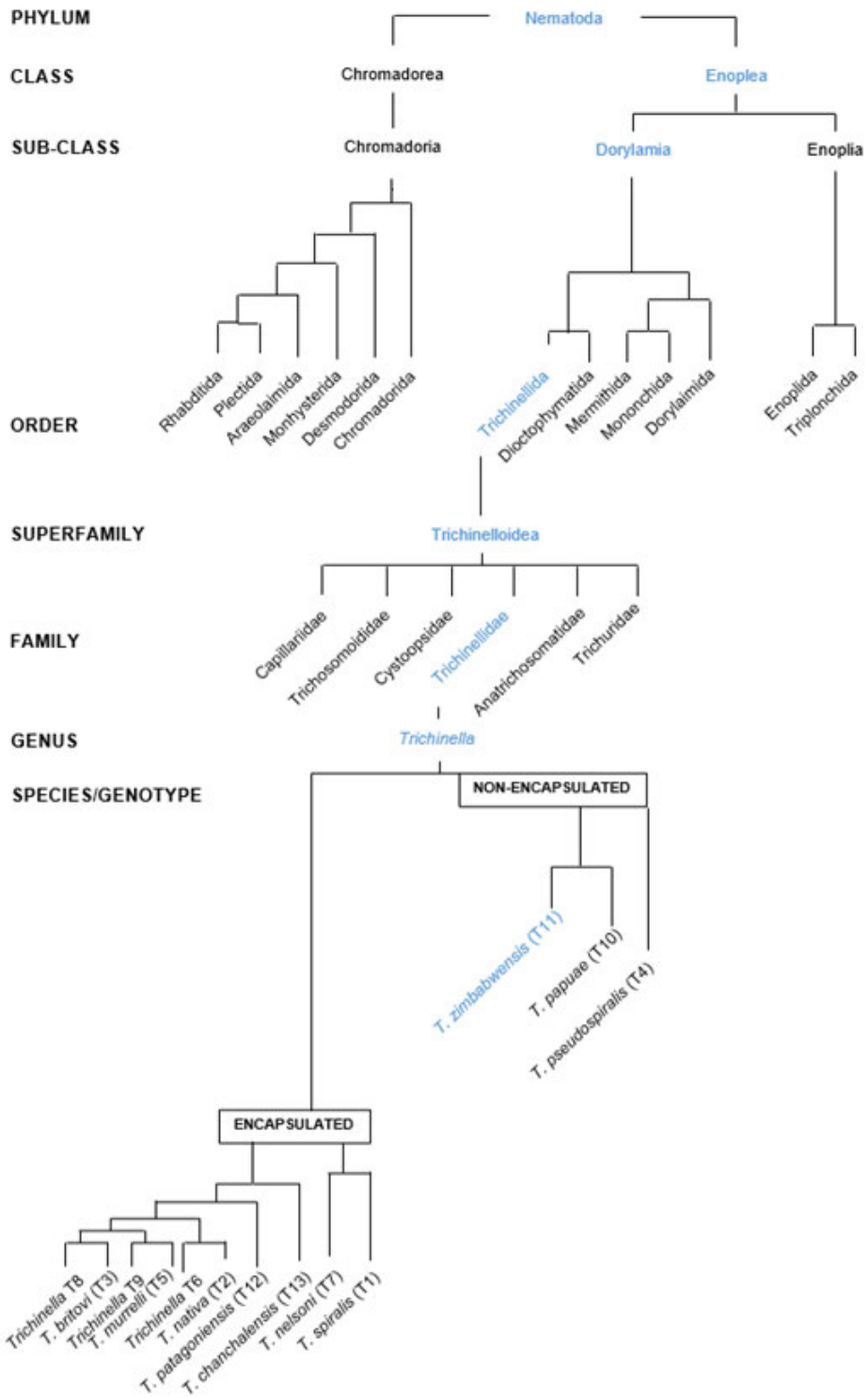

Figure 1.1: Classification and phylogeny of *Trichinella* compiled from (Pozio et al., 2002; De Ley, 2006; Smythe et al., 2019; Sharma et al., 2021)

Trichinella parasites have been discovered across a broad geographical range in an array of different hosts (Table 1.1). All *Trichinella* species have been reported to infect mammals, while *T. zimbabwensis* and *T. papuae* also infect reptiles and *T*. *pseudospiralis* has been reported in birds. Interestingly, it is observed that only non-encapsulated members of the genus are capable of infecting reptilian hosts (*T. zimbabwensis* and *T. papuae* which are the only species capable of infecting both homeothermic and poikilothermic hosts) and avian hosts (*T. pseudospiralis*), while encapsulated members are limited to mammalians hosts (Zarlenga et al., 2020).

1.3 Life cycle of *Trichinella* and the host immune response

The life cycle of *Trichinella* starts with the consumption of undercooked meat (Section 1.1) as shown in Figure 1.2 (Mitreva and Jasmer, 2006). Undercooked meat eaten by a human or animal host is digested by pepsin and hydrochloric acid in the stomach. This results in the release of adult muscle larvae from the nurse cells and is known as the enteral phase of infection (Capó and Despommier, 1996). Freed *Trichinella* larvae pass into the small intestine and migrate through the columnar epithelium (migratory/intestinal phase) where larvae mature into adult worms through four successive moults, which takes 30-34 hours. Thereafter mating occurs resulting in the release of new-born larvae one to two days post infection which are passed into blood vessels or into the lymphatic system (Mitreva and Jasmer, 2006; Andrade-Becerra et al., 2017). The larvae reach the skeletal muscle tissue via the bloodstream, invade myofibres and develop into L1 muscle larvae which complete the lifecycle of the infection. The muscle phase of infection begins when individual myotubes are infected; here the larvae induce an alteration of gene expression in the host myotube, causing the cell to re-enter the cell cycle, alter the cytoplasmic matrix and produce a collagen capsule in the case of encapsulated species (Fabre et al., 2009). This change in host genomic expression is suggested to be induced by the release of glycosylated peptides known as tyvelosylated peptides (Despommier, 1998).

Tyvelose is a highly antigenic sugar molecule (3,6-dideoxy arabinohexose). These tyvelosylated peptides are suspected of playing an important role in directing nurse cell formation. They are produced only by L1 muscle larvae and are directed into subcellular components including the cytoplasm during nurse cell formation. Additionally, anti-tyvelose antibodies produced during the humoral response induced in the host, provide protection against infection by expulsion of muscle larvae within the small intestine (Bolás-Fernandez and Corral Bezara, 2006; Bolas-Fernández et al., 2009). There is also an array of other proteins amongst the excretory-secretory (ES) products from muscle larvae, including

proteases, which have been suggested to play a role in inducing muscle cell de-differentiation, followed by re-differentiation and nurse cell formation (Hernández-Ancheyta et al., 2018).

Table 1.1: Reported host range and distribution of *Trichinella*

Species/Genotype	Host Range	Geographical distribution
Non-encapsulated		
T. zimbabwensis	Reptiles including Nile crocodiles and monitor lizards; mammals including rodents, monkeys, and lions (1,2)	Zimbabwe, South Africa, Ethiopia, Mozambique (1-3)
T. paupae	Reptiles including crocodiles, caimans, lizards and turtles; mammals including domestic pigs, rodents, cats, and wild boar (4-7)	Papua New Guinea, Thailand, Cambodia (4-7)
T. pseudospiralis	Mammals including pigs, rodents, marsupials, and humans; birds (8-10)	Tasmania, Europe, Thailand, North America, India (8-10)
Encapsulated		
T. spiralis	Vast array of mammals including pigs, rats, and foxes. (11, 12)	Europe, North and South America, Asia, Indonesia, New Zealand, Africa (11-13)
T. nativa	Mammals including bears, polar bears, walruses, seals, wild boars, foxes and wolverines (14-17)	Arctic and subarctic regions; North America, Canada, Europe, Asia (14-17)
T. britovi	Mammals including wild boars, foxes, bears, wolves, rodents (18- 20)	Europe, Asia, South America, North and West Africa (18-23)
T. murelli	Mammals including bears and bobcats (24, 25)	USA and Canada (25, 26)
Trichinella T6	Mammals including wolverines (17)	USA and Canada (17, 27)
T. nelsoni	Mammals including lions, jackals, hyenas, cheetah, leopard, bush pig and warthog (28, 29)	Sub-Saharan Africa, (28, 29)
Trichinella T8	Mammals including lions and hyenas (28, 30)	South Africa (28, 30)
Trichinella T9	Mammals including foxes, bears and raccoons (31-33)	Japan (31-33)
T. patagoniensis	Cougars (34)	Argentina (34)
T. chanchalensis	Wolverines (35)	Canada (35)

1: (Pozio et al., 2007); 2: (La Grange et al., 2010); 3: (Mukaratirwa et al., 2013); 4: (Pozio et al., 1999); 5: (Khumjui et al., 2008); 6: (Caron et al., 2020); 7: (Pozio et al., 2005); 8: (Beveridge and Spratt, 1996); 9: (Ranque et al., 2000); 10: (Jongwutiwes et al., 1998); 11: (Pozio et al., 2009); 12: (Bilska-Zając et al., 2020); 13: (Feidas et al., 2014); 14: (Diemert, 2012); 15: (Pozio and Kapel, 1999); 16: (Chmurzyńska et al., 2013); 17: (Reichard et al., 2008); 18: (Aoun et al., 2012); 19: (Dilcheva and Petkova, 2018); 20: (Van Der Giessen et al., 1998); 21: (Pozio, 2001) 22: (Krivokapich et al., 2019); 23: (Bruschi and Pozio, 2019); 24 :(Satoskar et al., 2009); 25: (Reichard et al., 2021); 26: (Sharma et al., 2018); 27: (Gajadhar and Forbes, 2010); 28: (Marucci et al., 2009); 29: (Pozio, 2001); 30: (Pozio et al., 1992); 31: (Kanai et al., 2006); 32: (Tominaga et al., 2021); 33: (Kobayashi et al., 2007); 34: (Gottstein et al., 2009); 35: (Sharma et al., 2020)

Proteases and protease inhibitors from *Trichinella* have numerous functions throughout the lifecycle of the parasite. After release of L1 larvae from infected tissue and migration to the small intestine, both cysteine and serine proteases (Section 1.5) facilitate larval penetration of the small intestinal wall (Han et al., 2020; Song et al., 2022) by hydrolysing junction proteins of the epithelial monolayer. Proteases have also been shown to play a role in adult worm development and fecundity in the intestinal wall where mating occurs (Hu et al., 2021). Likewise, protease inhibitors have also been shown to play a role in larval penetration, worm development and fecundity (Yang et al., 2019). Proteases and protease inhibitors were found to be functional proteins and ES products of muscle larvae (Nagano et al., 2009) where these proteins play a role in degradation of the cellular matrix for muscle cell remodelling (Park et al., 2012). Both proteases and protease inhibitors are important throughout the lifecycle in evading the host immune system by immunomodulation (Yang et al., 2015; Xu et al., 2017; Liu et al., 2022). Certain proteases and inhibitors, such as a cathepsin B-like protease and a cysteine protease inhibitor from *T. spiralis*, have been identified at all stages of the parasite lifecycle (Zhan et al., 2013; Tang et al., 2015).

Infections of experimental animals with *T. spiralis* have been shown to induce a brief Th1 (T-helper 1) immune response followed by a predominant Th2 immune response as well as regulatory T-cell (Treg) responses (Ilic et al., 2012; Farid et al., 2019; Wang et al., 2020) which inhibit the Th1 immune response, preventing worm expulsion. Following experimental *T. spiralis* infection in pigs there were increased percentages of CD3+ T cells, CD4+ T cells, B cells, Treg cells, Th17 cells and neutrophils, as well as increased levels of the Th2, Treg and Th17 cytokines IL-4, IL-10 and IL-17A. This was observed along with decreased percentages of CD8+ T cells and decreased levels of Th1 cytokine IL-2 (Wang et al., 2020). While encapsulated and non-encapsulated species are similar and survive within the same niches, the manner in which they do so and the way in which the host immune system responds, is not entirely the same. Infection with *T. spiralis* induces stronger inflammatory responses than infection with *T. pseudospiralis*, which produces more IL-10 than the former (Asano et al., 2016). Infection by *T. pseudospiralis* does not induce a strong Th2 response, but instead impairs Tfh- (follicular helper T-) cell differentiation resulting in decreased antigen-specific IgG levels, which dampens the humoral immune response. Infection of mice with *T. zimbabwensis* was shown to induce a mixed Th1/Th2 response (Onkoba et al., 2016) in which a mix of pro-inflammatory and anti-inflammatory conditions favours the survival of the parasite. These findings emphasise a need to conduct research on all members of the genus to understand different parasite-host interactions.

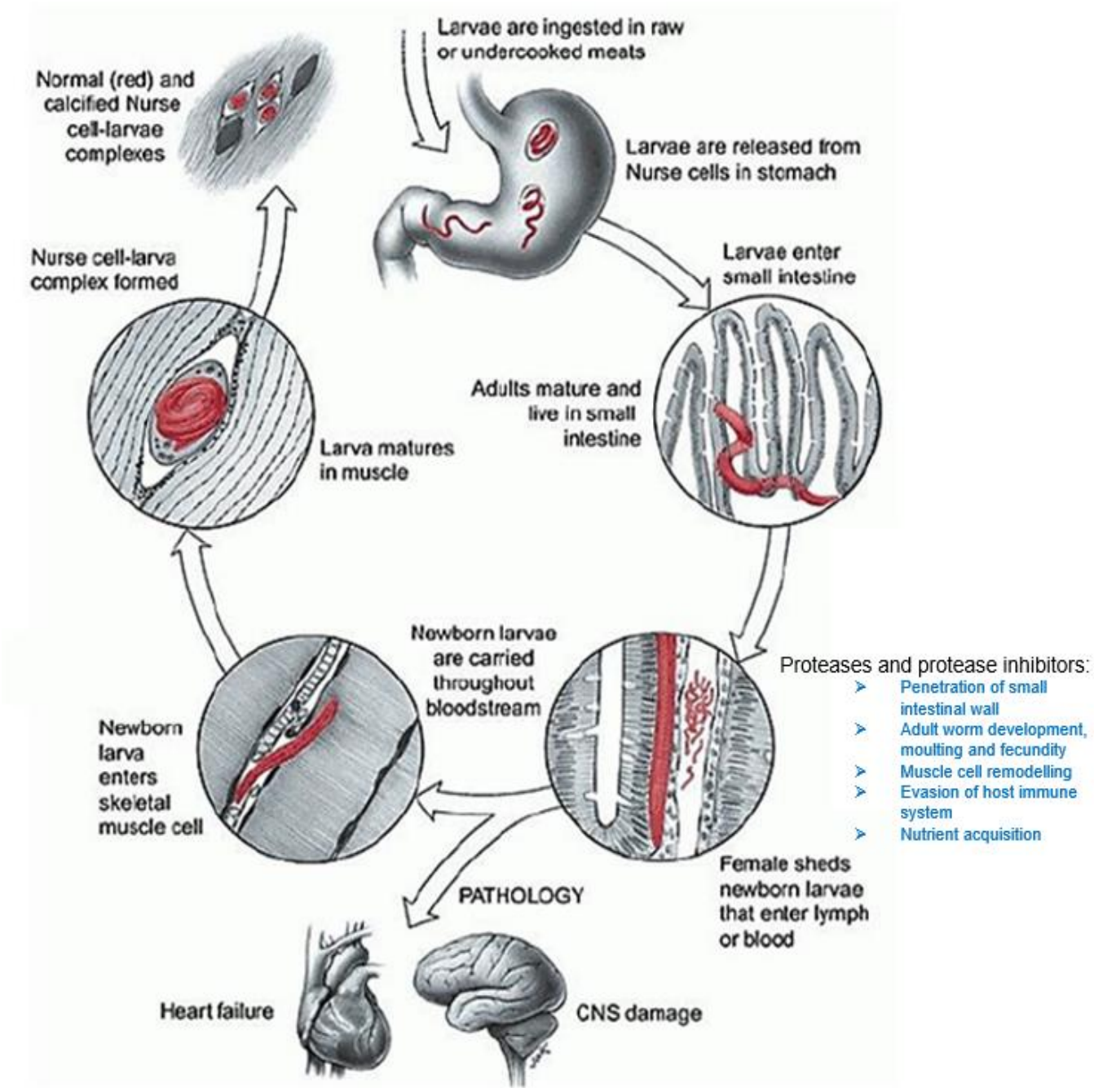

Figure 1.2: Stages of the *Trichinella* lifecycle (Mitreva and Jasmer, 2006)

1.4 ES products from *Trichinella*

Trichinella parasites make use of ES products for numerous functions and these ES products include proteases and protease inhibitors (Section 1.3). Excretory-secretory products released by the parasite during the enteric phase assist in establishing the infection (Han et al., 2019) where they alter the Th1/Th2 host immune response by inhibition or suppression of the functioning of macrophages and dendritic cells. They have been shown to maintain the

parasite within the host muscle tissue by coordinating the formation of the protective nurse cell and by communicating with and modulating the host immune system to promote the survival of the parasite as well as to prevent excessive harm to the host (Gruden-Movsesijan et al., 2011; Ilic et al., 2012).

Their involvement in these processes which are vital to the parasite as well as their tendency to be highly antigenic, makes ES products of particular interest and value to researchers (Wu et al., 2016b). They have become desirable targets for the development of diagnostics as well as targets for drug and vaccine development. A number of proteases and inhibitors from *Trichinella* species (particularly *T. spiralis*) have been recombinantly expressed and studied to understand their functioning and determine their antigenicity, including cathepsins and cystatins. Results from a study on cathepsin B from *T. spiralis* (TsCB) suggested that the protease plays a role in larval penetration of the small intestine via interaction with epithelial cells (Han et al., 2020). A cathepsin B-like protease (TsCPB) from *T. spiralis* was found to be expressed at all stages of the parasite lifecycle and was identified as a circulating antigen in the sera of *T. spiralis*-infected mice (Zhan et al., 2013) suggesting that this protease has potential as a diagnostic marker of infection by *T. spiralis*. A study on another cathepsin B-like protease (TsCPB2) from *T. spiralis* showed that it could provide protective immunity to mice that were later infected with *T. spiralis*, showing its potential as a vaccine candidate (Yang et al., 2018). Cystatins from *T. spiralis* have been found to play important functions including immunomodulation of the host immune system by suppressing inflammatory responses by macrophages (Kobpornchai et al., 2020) and inhibition of cathepsins which function in antigen presentation (Nutman, 2015). Cystatins have been found to be expressed at all stages of the parasite lifecycle (Tang et al., 2015). These findings are valuable as there is a need to identify as many antigens as possible across different stages of the parasite's lifecycle to make advancements in diagnosis, treatment and prevention of Trichinellosis.

1.5 Proteases and protease inhibitors

Proteases (also known as proteolytic enzymes or peptidases) digest proteins by hydrolysing peptide bonds (Powers et al., 2002). These enzymes are abundant in nature as they are essential in many important physiological processes and vary in their exact nature of enzymatic activity. Proteases are divided into different catalytic classes based upon their mechanism of peptide bond cleavage. These are cysteine, serine, threonine and glutamic proteases based upon the amino acid residue used in nucleophilic attack of peptide bonds, as well as aspartyl and metalloproteases which make use of an activated water molecule as the nucleophile (Lecaille et al., 2002; Rawlings et al., 2011). A seventh class, asparagine peptide lyases, are self-cleaving proteases where Asn is involved in the nucleophilic elimination

reaction to cleave internal peptide. Across the first six classes of proteases there is a conserved mechanistic model observed: making use of a nucleophile, base and acid in peptide hydrolysis. This is referred to as the nucleophile-base-acid model or catalytic triad (Polgár, 2005) with histidine and aspartate/asparagine in the active site commonly functioning as the base and acid, respectively. In this triad, the nucleophile and histidine form an ion pair which is stabilised by aspartate/asparagine (Brömme, 2000). Variations of this catalytic site structure have been observed among proteases, such as active site dyads instead of triads.

While these classifications by catalytic activity are useful, they do not reflect evolutionary relationships. Proteolytic enzymes can be divided into clans based upon their tertiary protein structure, into families based upon sequence similarity and into protein-species based upon numerous characteristics including phylogeny and subcellular location amongst others (Rawlings, 2020). Members of a clan or a family are identified by virtue of their similarity (in tertiary structure or protein sequence respectively) to a type-example designated for that clan/family, and one clan may contain one or more different families (see Section 1.5.1).

Protease inhibitors, which can be proteins or small molecules, are common in natural systems as they are essential for the regulation of proteolytic activity of both endogenous proteases and those from invading microorganisms (Boris et al., 2002). Protease inhibitors typically function by binding to residues of catalytic importance such as the nucleophile or base (Powers et al., 2002) which blocks the catalytic binding site of the enzyme. These inhibitors are also abundant across different lifeforms and are utilised by invading microorganisms to inhibit host proteases, some of which are key in antigen processing and other immune processes (Kędzior et al., 2016).

The focus of this study is on a *Trichinella* cysteine protease and cysteine protease inhibitor, therefore general information on these proteins is provided in the sub-sections that follow.

1.5.1 Cysteine proteases

Cysteine proteases, traditionally known as thiol proteases, have 96 families (more than any other catalytic class) identified (Rawlings, 2020), with family C1 (the papain family) having the most enzymes identified (Rawlings and Barrett, 1994; Otto and Schirmeister, 1997). These include plant and protozoan proteases as well as lysosomal cathepsins that play roles in numerous physiological and pathological processes. This family along with family C2 (the calpain family) and family C10 (the streptopain family) belong to clan A or the papain-like superfamily, being the best-studied group of cysteine proteases. Whereas the papain family proteases are usually lysosomal or secreted (Rawlings and Barrett, 1994), members of the

calpain family are intracellular, being localised in the cytosol (Sorimachi et al., 2013) and are distinct in that they rely on calcium ions for their activity.

Papain, after which family C1 and the papain-like superfamily are named, is a plant protease originally extracted from papaya latex (Kimmel and Smith, 1954). This protease has been of particular commercial value due to its potent catalytic activity across broad reaction conditions and its broad substrate specificity (Fernández-Lucas et al., 2017). Papain was the first protease to have its structure determined and is the archetype for the papain-like family of cysteine proteases (Storer and Ménard, 2013; Tacias-Pascacio et al., 2021). Early studies on the enzyme advanced understanding of cysteine proteases as well as enzymes in general (Storer and Ménard, 2013). Cysteine proteases share the common feature of relying on the sulfur anion on the sidechain of L-cysteine as the nucleophile (Buttle and Mort, 2013). In the three-dimensional structure (Kim et al., 1992) of papain (Fig. 1.3), Cys25 is shown to be the nucleophile that acts along with His159 to form a catalytic dyad (Brömme, 2000; Novinec and Lenarčič, 2013). The catalytic triad previously discussed (Section 1.5) is typically found in serine proteases, however cysteine proteases are considered to have a catalytic dyad consisting of a Cys-His ion pair with additional residues playing roles in catalytic activity (Novinec and Lenarčič, 2013). Residue Asn175 has a similar function to the aspartate residue in the catalytic triad of serine proteases, forming a hydrogen bond to His-159, but is not essential for activity. This residue and Gln19 play a role in proper positioning of the catalytic dyad. Residue Trp177 has also been suggested to function in generating the nucleophilic character of the catalytic dyad (Novinec and Lenarčič, 2013).

A well-studied group of papain-like proteases, of interest in the present study, is the cysteine cathepsins. The term “cathepsin” refers to an intracellular protease, usually localised in lysosomes, and active at acidic pH (Otto and Schirmeister, 1997). The cathepsins are mostly cysteine proteases, however there are also serine and aspartic cathepsins (Turk et al., 2012; Brix, 2018) and despite being typically lysosomal these proteases have also been identified in other locations, often being secreted by cells, and in addition have been identified in the cytosol and nucleus (Brix, 2018). Cysteine cathepsins have numerous functions and are important in an array of physiological pathways in the mammalian host as specific processing enzymes and are utilised as non-specific hydrolases for protein turnover (Novinec and Lenarčič, 2013).

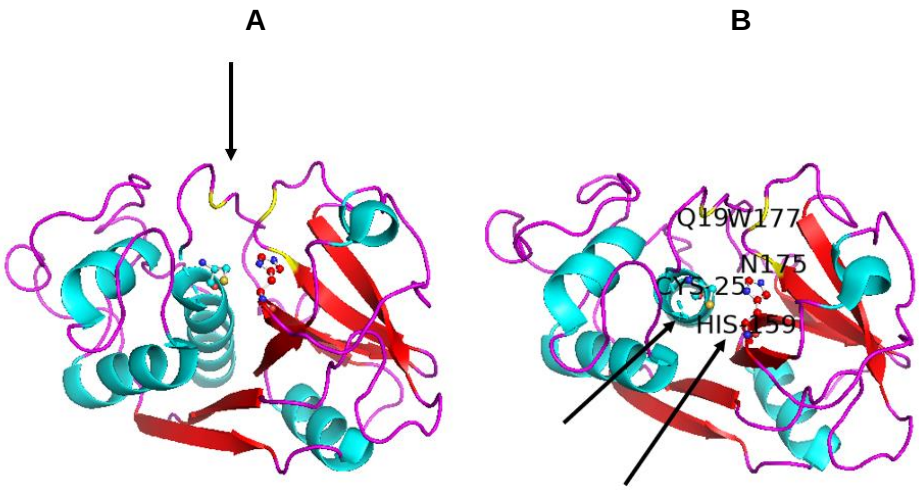

Figure 1.3: The three-dimensional structure of papain. Entry 1PPP (https://doi.org/10.2210/pdb1PPP/pdb) from the PDB (Protein Data Bank) was visualised in PyMOL. **(A):** Papain structure observed in the standard orientation with the active site cleft (indicated by the arrow) facing upwards. **(B):** Papain observed facing towards the active site cleft. Residues of the catalytic dyad, Cys25 and His159 (in ball-and-stick format), are labelled with their three-letter code and indicated by arrows. Additional residues of importance (yellow) are labelled with their one-letter codes (Asn175, Asn177 and Gln19).

Cathepsin B is an example of a lysosomal cysteine cathepsin and is one of several proteases within the lysosome that are responsible for protein turnover (Demchik et al., 1999; Cavallo-Medved et al., 2011; Aggarwal and Sloane, 2014), thus playing a role in homeostasis. In humans the protease has been implicated in antigen processing, bone turnover, hormone and enzyme activation, inflammatory responses, tissue remodelling and apoptosis (Mort and Buttle, 1997; Cavallo-Medved et al., 2011). Like all papain-like cysteine proteases, it has a similar structure to papain. In the three-dimensional structure of cathepsin B (Turk et al., 1995), the active site is at the interface of the bi-lobal structure and the catalytic dyad is comprised of cysteine and histidine (Fig. 1.4), with additional residues contributing, but not essential to activity (Musil et al., 1991; Cavallo-Medved et al., 2011; Aggarwal and Sloane, 2014). Cysteine proteases have a conserved GC-X-GG motif in their amino acid sequence, while cathepsin B is distinguishable by having this motif only and not an additional ERFIN motif found in other cysteine proteases (Karrer et al., 1993; Zhou et al., 2023). Cathepsin B also differs from other cysteine cathepsins by the presence of an occluding loop which allows the protease to have a dual activity. At acidic pH, the occluding loop forms two salt bridges with the active site that block the entry of larger substrates, resulting in exopeptidase activity. At neutral/alkaline pH, the occluding loop is displaced allowing for endopeptidase activity (Cavallo-Medved et al., 2011; Aggarwal and Sloane, 2014). The inactive cathepsin B known as a pre-proenzyme or zymogen is synthesised in the rough endoplasmic reticulum (ER) and differs from its active form due to the presence of an N-terminal signal peptide as well as a propeptide preceding the catalytic domain in the primary structure. The propeptide functions to stabilise the

protease, to inhibit it by blocking the active site and to ensure correct folding of the catalytic domain (Khan and James, 1998; Aggarwal and Sloane, 2014; Petushkova et al., 2022). The N-terminal signal peptide traffics the protease into the lumen of the rough ER where the signal peptide is removed to form the proenzyme (with the propeptide still present), which is transported to the Golgi apparatus. Here it is glycosylated at two asparagine residues with mannose-6-phosphate containing oligosaccharides. Glycosylated procathepsin B binds to mannose-6-phosphate receptors of the trans-Golgi network allowing for transport to lysosomes. Within the lysosome, the acidic pH allows for autocatalytic cleavage of the propeptide, producing the active form of cathepsin B (Aggarwal and Sloane, 2014).

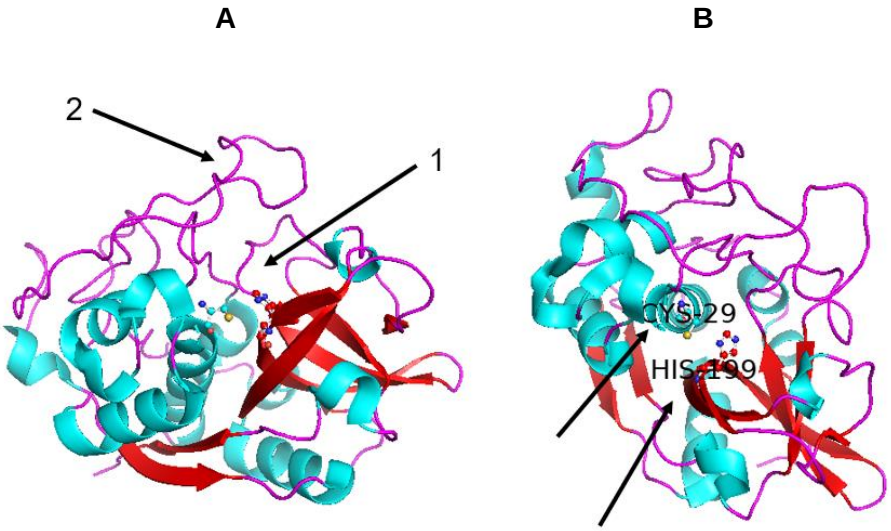

Figure 1.4: The three-dimensional structure of human cathepsin B. Entry 1CSB (https://doi.org/10.2210/pdb1CSB/pdb) from the PDB was visualised in PyMOL. **(A):** Cathepsin B structure observed in the standard orientation with the active site cleft (indicated by arrow 1) facing upwards. Arrow 2 shows the position of the occluding loop. **(B):** Cathepsin B structure observed facing towards the active site cleft. Residues of the catalytic dyad, Cys29 and His199 (in ball-and-stick format), are labelled with their three-letter code and indicated by arrows.

The catalytic mechanism of papain-like cysteine proteases (Fig. 1.5A) involves a nucleophilic attack by the ion pair on the deprotonated sulfhydryl on the carbonyl carbon of the scissile bond in the protein substrate. This forms a tetrahedral intermediate which is resolved by acylation, releasing the first product in this reaction (the N-terminal portion of the peptide substrate) and producing an acyl enzyme. Hydrolysis results in a second tetrahedral intermediate which then releases the final C-terminal peptide product via de-acylation, reforming the free enzyme (Brömme, 2000).

Residues that line the substrate binding site of a protease are responsible for the specificity of the enzyme by allowing for binding of certain substrate amino acids (Rawlings, 2020). Subsites

on the enzyme on the N-terminal side of the scissile bond of the substrate are denoted S1-4 and S1'-4' on the C-terminal side (Fig. 1.5B). On the corresponding substrate, the amino acids which bind these sites are denoted P1-4 on the N-terminal side of the scissile bond and P1'-4' on the C-terminal side (Schechter and Berger, 1967). In papain-like cysteine proteases, the S2/P2 subsite interaction is important in that it determines the primary specificity of the enzyme (Brömme, 2000). Typically this subsite accepts hydrophobic residues however there are some enzymes which have alternative specificities, such as cathepsin B which can bind basic residues in its P2 subsite (Novinec and Lenarčič, 2013).

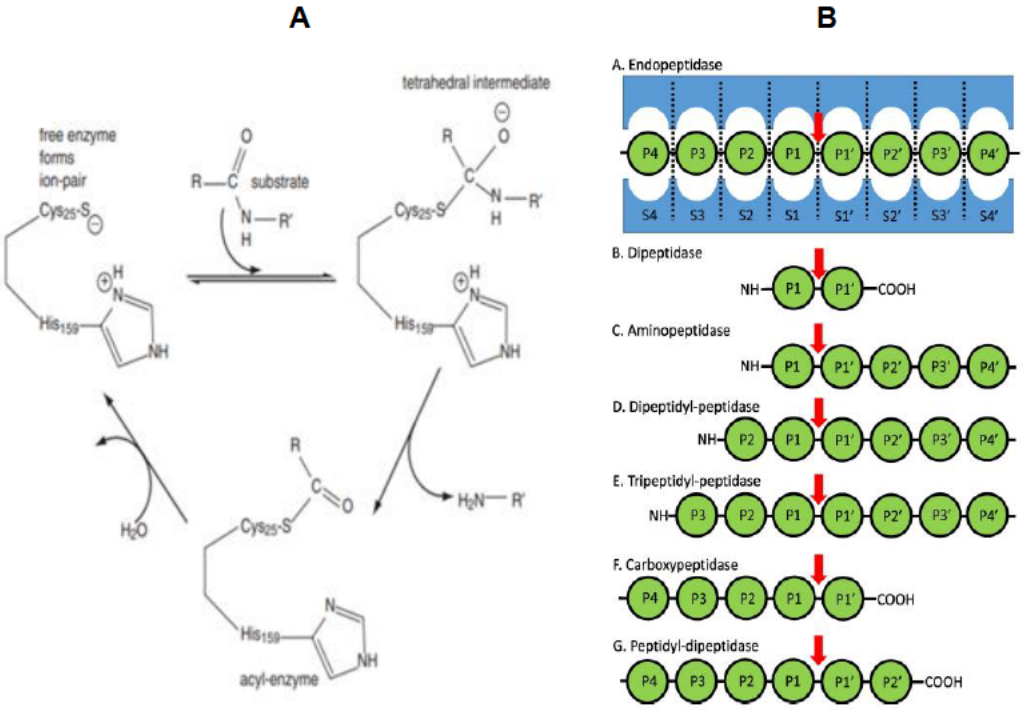

Figure 1.5: Mechanism of substrate hydrolysis by papain-like cysteine proteases and Schechter and Berger nomenclature of peptidases. (A): Diagrammatic representation of the mechanism of substrate hydrolysis by cysteine proteases (Brömme, 2000). **(B):** Schechter and Berger nomenclature of peptidase substrate binding sites and substrate residues (Rawlings, 2020).

1.5.2 Cysteine protease inhibitors

In situ off-target activity of cysteine cathepsins is potentially harmful. The regulation of these proteases is therefore essential and is accomplished by zymogen activation and pH regulation (Section 1.5.1), as well as inhibition by endogenous protease inhibitors known as cystatins which are the main regulators of cysteine cathepsins and other papain-like cysteine proteases (Turk et al., 2019). Cystatins are typically competitive and reversible inhibitors, which function not only to regulate endogenous proteases but also to inhibit those from invading microorganisms. Likewise, the cystatins of microorganisms (including parasites) inhibit host

proteases to modulate the host immune response (Turk et al., 2019). The cystatin family constitutes three subfamilies based on protein sequence and tertiary protein structure: the stefin family (I25A), the cystatin family (I25B) and the kininogens (I25C) (Otto and Schirmeister, 1997; Turk et al., 2019; Ramirez Merlano and Almeida, 2022). The stefin and cystatin families represent low molecular weight cysteine protease inhibitors while the kininogens are large multifunctional inhibitors. Members of the stefin family lack disulfide bridges, carbohydrate residues and signal peptides, thus they are typically intracellular. Members of this family include cystatins/stefins A and B. Inhibitors of the cystatin family are extracellular and have disulfide bridges. This group includes cystatins C, D, E/M, F, G, S, SA and SN. (Otto and Schirmeister, 1997; Turk et al., 2019; Ramirez Merlano and Almeida, 2022).

Certain residues and structural domains are highly conserved between stefins and cystatins and are of importance for their inhibitory activity. These include one or two N-terminal glycine residues, a Q-x-V-x-G motif on one hairpin loop and a proline-tryptophan motif at the C-terminus of a second hairpin loop (Turk et al., 2019; Ramirez Merlano and Almeida, 2022). Together these structural elements form a “wedge-shaped hydrophobic tripartite edge” that has a complementary structure to the V-shaped active site cleft of papain-like cysteine proteases. The N-terminal glycine residues block the S1-S3 subsites on the enzyme (Fig. 1.5B) as a substrate would bind, the following peptide segment turns away from the active site to prevent being cleaved, and the two hairpin loops block subsites S1’-4’ on the enzyme. Molecular docking of chicken egg-white cystatin to papain first suggested the mechanism of interaction between cysteine proteases and cystatin-like inhibitors (Turk et al., 2019) which was later confirmed by docking of human stefin B and papain (Fig. 1.6). In the case of stefin B there is less contribution from the second hairpin loop.

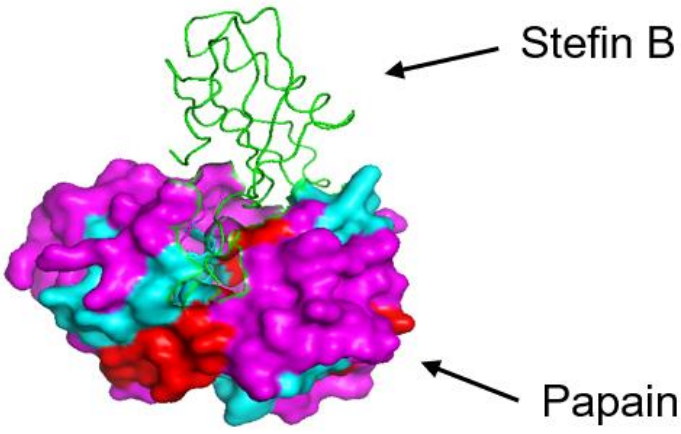

Figure 1.6: Human stefin B bound to the active site of papain. Entry 1STF (https://doi.org/10.2210/pdb1STF/pdb) from the PDB was visualised in PyMOL. Papain is observed in the standard orientation with the active cleft facing up, with human stefin B bound.

1.6 Cathepsin B and cystatins (stefins) from parasitic helminths

Cysteine proteases play a number of biological roles in parasitic organisms from unicellular protozoa up to multicellular helminths such as *Trichinella* (Yang et al., 2023). Numerous examples of such proteases have been recombinantly expressed in prokaryotic and eukaryotic systems to conduct research on these proteins due to their potential value as diagnostic markers, drug targets and vaccine candidates.

A cathepsin B-like cysteine protease (HC58) from the parasitic nematode *Haemonchus contortus* was PCR (polymerase chain reaction) cloned from cDNA (complementary DNA) which was produced using RACE-PCR from parasite RNA (Muleke et al., 2006). This protease was expressed in *Escherichia coli* from the pET-28a expression vector which produced a 27 kDa His-tagged HC58. The proteolytic activity of HC58 was inhibited by E-64 as expected of a cysteine protease. The protease digested different protein substrates depending upon pH, such as haemoglobin, goat IgG heavy chain and azocasein at low pH and fibrinogen at a more basic pH. Another cathepsin B-like protease (AcCBL1) from the parasitic nematode *Angiostrongylus cantonensis* was expressed in *E. coli* from the pET-30 expression vector producing a 38 kDa His-tagged AcCBL1 (Cheng et al., 2012). Similar results to that of HC58 were obtained, as AcCBL1 was shown to digest haemoglobin and IgG at acidic pH, having optimal activity at pH 5.0. The study suggested that the cysteine protease may play a role in parasite nutrient uptake. A 65 kDa recombinant GST-tagged cathepsin B from *Schistosoma japonicum* (SjCB2) was expressed in *E. coli* using the pGEX-h-6t-1 expression vector (Zhu et al., 2020). This cysteine protease had optimal activity at pH 4.0, was inhibited by E-64, and was shown to digest collagen, fibronectin, elastin, keratin, immunoglobulins A, G and M, complement C3, as well as protein components of the epidermis and immune system. The study suggested that SjCB2 plays a role in parasitic invasion of the skin. A recent study on cathepsin B from *Trichinella spiralis* (TsCB) entailed its expression in the pGEX-4T-1 expression vector at a 63 kDa recombinant GST-tagged protein (Zao et al., 2024). Recombinant TsCB was shown to target and digest collagenase type I and to have optimal activity at pH 5.5 that was inhibited by E-64.

A cystatin from *Angiostrongylus cantonensis* (AcCystatin) was expressed as a 14 kDa recombinant GST-tagged protein (Liu et al., 2010). The recombinant AcCystatin was shown to inhibit cathepsin B activity with maximal inhibition after pre-incubation at pH 8.0 and was also shown to increase nitric oxide production by IFN-ɣ activated macrophages. Another study showed the potential of this cystatin for repurposing as an anti-inflammatory agent for the treatment of airway inflammation in asthmatic patients (Ji et al., 2015). A cystatin from *Schistosoma japonicum* (SjCystatin) was expressed in the pET-28a expression vector as an

11 kDa recombinant His-tagged protein (He et al., 2011). This recombinant cystatin was used to immunise mice, antibodies from which showed that SjCystatin was expressed at both the egg and adult stages of the parasite's lifecycle using western blotting. Cysteine protease inhibitory activity of SjCystatin was also used to inhibit the cysteine protease papain. A cystatin from *Haemonchus contortus* (HCcyst-2) was expressed in the pET-32a expression vector as a 34 kDa recombinant His-tagged and TRX-tagged protein (Wang et al., 2017a). This cystatin was shown to inhibit papain, cathepsin B and cathepsin L and also shown to modulate the activity and cytokine expression of goat monocytes. Another cystatin from the same helminth (HCcyst-3) was also expressed in the pET-32a expression vector (at 35 kDa) and the similar findings obtained as those for HCcyst-2 (Wang et al., 2017b).

1.7 Diagnosis of *Trichinella*

Methods used for the detection of *Trichinella* infections in both animals and humans can be distinguished as indirect and direct methods (Gómez-Morales et al., 2014). Diagnosis of infections in animals is essential in assuring that meat is safe for human consumption (Nöckler et al., 2000; Gajadhar et al., 2009) and in humans it is important for infections to be appropriately treated and for the impact and prevalence of the disease to be understood. In many countries the impact of the disease is not known due to lack of early diagnosis (Gottstein et al., 2009).

Serological methods are indirect methods that detect antibodies raised against *Trichinella* antigens during the host immune response. Antibodies (IgG or IgM) or antigens are detected in blood samples or within meat juices from slaughter animals. Although blood is preferred, blood quality is an issue as haemolysis and bacterial infection may interfere with serological tests. These methods are therefore only useful for epidemiological investigations in animals and are not appropriate for meat inspection (Nöckler et al., 2000; Nöckler et al., 2009). The most used method for antibody detection is the ELISA (Enzyme Linked Immunosorbent Assay) which is a highly sensitive method, however this test can lack specificity with false positives being a common pitfall. The method can be supplemented with a western blot to confirm results. Another serological method developed for diagnosis of *Trichinella* infection utilises gold-labelled ES antigens on a lateral flow strip which detects anti-*Trichinella* antibodies (Bai et al., 2017). This method provides an easy and fast alternative to the ELISA.

Direct methods are those which detect *Trichinella* muscle larvae directly within the skeletal muscle tissue. In animals, the muscle tissue is observed following conducting a biopsy. This can be done both post-mortem and ante-mortem however direct methods in live animals are unfavourable because they are painful and invasive (Nöckler et al., 2000). These methods are useful as post-mortem inspections for the surveillance of meat samples for human

consumption. Direct methods include Trichinoscopy, which involves compressing two thin films of meat tissue between two glass slides and observing for muscle larvae using microscopy at 15-40x magnification, and the pepsin digestion method which releases the larvae from the muscle tissue (Nöckler et al., 2000; Franssen et al., 2017). The larvae are then isolated using filtration and sedimentation after which they can be observed at 40-100x magnification under a light microscope.

With regard to diagnosis in humans, direct methods are not preferred for obvious reasons and therefore indirect methods (discussed above) are required along with observation of clinical symptoms. Such diagnosis comes with numerous difficulties. Medical practitioners in many countries are unfamiliar with Trichinellosis and even those who are familiar with the infection can have difficulty with diagnosis due to symptoms being very similar to those of other diseases (Gottstein et al., 2009; Mukaratirwa et al., 2019). Serological methods such as ELISA utilise *Trichinella* ES antigens as they have important functions for parasitism as discussed (Sections 1.3 and 1.4), but these methods have certain pitfalls. Antibodies raised against ES antigens from adult larvae will not be able to recognise ES antigens from muscle larvae and vice versa (Liu et al., 2016). Cross-reactivity of antibodies (raised against *Trichinella* ES antigens) with antigens from other parasitic infections reduces the specificity of ELISA tests due to false positive results (Cui et al., 2015). In addition, human IgG produced against *Trichinella* infection cannot be used to differentiate between current and past infections as these antibodies are continually secreted even up to a year post-infection (Zhan et al., 2013).

There is a need to identify ES antigens from *Trichinella* which are both specific to this parasite and which are present at all stages of the lifecycle. These antigens may provide effective early diagnosis of infection which would allow for great advancement in food safety and human health. These antigens may also prove to be effective targets for drug and vaccine development.

1.8 Treatment and prevention of Trichinellosis

There are two types of drugs that would be considered for treatment upon positive diagnosis of Trichinellosis; i.e. anthelmintics and glucocorticosteroids (Kocięcka, 2000; Pozio et al., 2003). Anthelmintics are a group of drugs used against helminth infection and the most common are albendazole and mebendazole. These are effective in killing parasitic worms, however efficacy depends on the time elapsed since infection. This is because these drugs are effective in killing intestinal worms and less so in killing muscle larvae due to poor drug absorption by the intestinal lumen (Pozio et al., 2003) which is only possible at higher, toxic dosages. Higher dosages administered over a longer time are used for chronic infections, however this will likely be ineffective in removing muscle larvae. This further indicates a need

for early diagnosis so that treatment may be administered quickly. Glucocorticosteroids are steroid hormones which bind to glucocorticoid receptors and reduce inflammatory symptoms as well as fever during Trichinellosis, the most common drug being prednisolone (Kocięcka, 2000) which reduces symptoms, but does not clear the infection. These drugs, except for Pyrantel, are not safe for use by pregnant women. Pyrantel is especially poorly absorbed by the intestinal lumen (Pozio et al., 2003).

There are numerous ways in which the spread of *Trichinella* can be controlled. In the agricultural sector, farmers should be made aware of practices to identify *Trichinella* and/or prevent infected meat from entering the market. These include slaughter testing for infection, processing methods such as cooking, freezing, curing and irradiating (in certain areas the possible presence of freeze-resistant species of *Trichinella* must be considered) as well as maintaining an appropriate, controlled and hygienic environment on the farm to prevent possible infection, rodent control being particularly important (Gamble et al., 2000). Vaccines are a desirable solution to control *Trichinella* in livestock as they circumvent the need for drugs which may affect meat quality. Development of such a vaccine will require using multiple *Trichinella* antigens which are essential in the invasive and parasitic processes of the larvae, and which induce a Th-2 type response in the host (Zhang et al., 2018). Antigens including ES products and functional proteins such as proteases and their inhibitors are potentially valuable vaccine candidates. An example of such an antigen is a cathepsin-B like protease from *T. spiralis* which was shown to provide protective immunity against infection in mice (Section 1.4). It is important that many different antigens from *Trichinella* species are studied for their potential as vaccine candidates. A “cocktail” vaccine made up of several antigens from different stages of the parasite lifecycle would be of great value as it would be able to provide protection against the parasite at all stages of its lifecycle.

1.9 Rationale, Aims and Objectives of the study

1.9.1 Rationale of study

Trichinellosis poses a risk to humans by infection through consumption of contaminated meat which may arise with intercalation of the sylvatic and domestic cycles of *Trichinella* infection, whereby these parasites may be passed from wild animals to those that are domesticated. This is a public health hazard and a socioeconomic problem, especially in resource-poor third-world countries. There is a need to identify and characterise as many functionally important and immunogenic antigens from *Trichinella* as possible for advancement in diagnosis, treatment and vaccination. Such studies on antigens from *T. zimbabwensis* will be of value as this species like many others is not as well studied as *T. spiralis*. Advancement in diagnosis as well as drug and vaccine development will be advantageous in monitoring and treating

human infections as well as in monitoring the prevalence and spread of the infection amongst domestic and wild animals, which would allow for its spread to be controlled.

1.9.2 Aim and objectives

The aim of the present study was to recombinantly express cathepsin B (*Tz*CATB) and stefin B (*Tz*stefinB) from *Trichinella zimbabwensis*, to characterise their activity and to evaluate them as potential diagnostic markers.

Objectives:

1. To identify the genes which encode *Tz*CATB and *Tz*stefinB and use bioinformatic analyses to predict their biophysical properties and compare their sequences with those from other species of *Trichinella*.
2. To have the gene which codes for *Tz*CATB commercially synthesised and PCR amplify the gene which codes for *Tz*stefinB.
3. To clone these genes in *E. coli* JM109 cells and subclone them into expression vectors.
4. To recombinantly express *Tz*CATB and *Tz*stefinB in *E. coli* BL21 (DE3) cells.
5. To purify his-tagged r*Tz*CATB and r*Tz*stefinB using Nickel Immobilised Affinity Chromatography.
6. To immunise chickens with purified r*Tz*stefinB and isolate anti-stefinB-IgY antibodies from yolks of eggs collected using filtration and PEG (polyethylene glycol) precipitation.
7. To evaluate chicken anti-stefinB-IgY antibodies using ELISA and western blotting against r*Tz*stefinB.
8. To characterise the proteolytic activity of r*Tz*CATB in synthetic substrate assays in the presence of different inhibitors and at different pH levels.
9. To test r*Tz*CATB for hydrolysis of gelatin using zymography, and test for hydrolysis of other protein substrates.
10. To characterise the inhibitory activity of r*Tz*stefinB using synthetic substrate assays and reverse zymography, testing its inhibition of r*Tz*CATB and other cysteine proteases.

Chapter Two

Methodology

2.1 Materials

Table 2.1: Materials used and manufacturers

Buffer salts and other common reagents were purchased from Sigma (USA) Merck (Germany) and were of the highest purity available.

Method	Material	Manufacturer
Parasite isolation, RNA isolation and cDNA synthesis	Pepsin	Sigma-Aldrich
	Direct-Zol™ RNA miniprep plus kit Lunascript™ RT Supermix kit	ZymoResearch, CA, USA
Molecular cloning and recombinant expression	6x MassRuler DNA loading dye O'GeneRuler™ 1 kb DNA ladder Fast digest EcoRI, BamHI, XhoI 10x Fast Digest buffer BamHI, SalI 10x Tango buffer (with BSA) 2x Ligation buffer T4 DNA ligase	Thermo Fisher Scientific, Lithuania
	GeneJET Plasmid Miniprep Kit	Thermo Fisher Scientific, USA
	FIREpol® Taq polymerase PCR reaction buffer B 25 mM $MgCl_2$	Solis Biodyne, Estonia
	EmeraldAmp® GT PCR Master Mix pMD-19 cloning vector pCold-1 expression vector pCold-TF expression vector	TaKaRa (CA, USA)
	ZymoClean™ Gel DNA Recovery Kit	ZymoResearch, USA
	pET-28a expression vector	Novagen, Germany
	10 mM dNTP mixture *E. coli* JM109 cells *E. coli* BL21 (DE3) cells	New England Biolabs, USA
	Bacteriological agar Tryptone Yeast extract	Merck Biolab, Germany
	Kanamycin Ampicillin	Gibco, UK

	Isopropyl-β-D-thiogalactopyranoside (X-gal) 5-bromo-4-chloro-3-indolyl-β-D-galactopyranoside (IPTG)	Fermentas, Lithuania
SDS-PAGE	Whatman No. 1 filter paper	Whatman International Ltd, UK
	Pierce™ Unstained Protein MW Marker PageRuler™ Unstained Low Range Protein Ladder	Thermo Fisher Scientific, USA
Western blot	Nitrocellulose	PALL Corp, USA
	4- chloro-1 naphthol	Sigma, USA
	Fat free milk powder	Amresco, USA
Purification	(Ni-NTA) agarose resin	Qiagen, Germany
	UltraLink™ Hydrazide Resin	Thermo Fisher Scientific, USA
	Thrombin	Novagen, Germany
	p-Aminobenzamidine agarose	Sigma, USA
	Amicon® Ultra centrifugal filter	Merck Biolab, Germany
Enzymatic characterisation	Dithiothreitol (DTT)	Fermentas, Lithuania
	Papain Gelatin H-D-Ala-Leu-Lys-7-amino-4-methylcoumarin (AMC) Z-Phe-Arg-AMC Z-Arg-Arg-AMC *trans*-Epoxysuccinyl-L-leucylamido(4-guanidino) butane (E-64)	Sigma, USA
	Black FluoroNunc™ 96-well plates	Nunc Intermed, Denmark
	*Tc*CATL	In-house
ELISA	2, 2'-azinobis (3-ethyl-3, dihydrobenzithiazole-6-sulfonate) (ABTS)	Roche, Germany
	Nunc-Immuno™ Maxisorp 96-well plates	Nunc Intermed, Denmark

Antibodies used in ELISA and western blotting	Mouse anti-6xHis IgG-horseradish peroxidase	Sigma, USA
	Rabbit anti-chicken IgY-HRPO Goat anti-mouse IgG-HRPO Goat anti-rabbit IgG HRPO	Jackson ImmunoResearch Inc, USA
	Chicken anti-*Tz*CATB IgY	In-house

Nomenclature of restriction enzymes as per Roberts et al. (2003). In-house antibodies raised in a past study (Zondo, 2019).

2.2 Bioinformatic analyses

The genes encoding *Tz*CATB and *Tz*stefinB were obtained from NCBI Genbank (https://www.ncbi.nlm.nih.gov/genbank/) and aligned with sequences of these proteins from other *Trichinella* species using Clustal Omega multiple sequence alignment (https://www.ebi.ac.uk/Tools/msa/clustalo/). This was done to confirm the presence of residues and motifs that are conserved amongst cysteine proteases and cysteine protease inhibitors, some of which are of importance for their activity, and to observe the sequence similarity between different species of *Trichinella*. In addition, the biophysical properties of *Tz*CATB and *Tz*stefinB were predicted using the ExPasy server (https://www.expasy.org/).

2.3 Protein quantification

Protein concentration in experimental samples was obtained using the Bradford method (Bradford, 1976) which involves the binding of dye to basic amino acid residues producing an absorbance which can be measured at 595 nm. In triplicate samples, bovine serum albumin (BSA) was diluted to 100 µL with distilled water to obtain desired concentrations (0-100 µg/mL) followed by the addition of 900 µL of Bradford reagent [0.06 % (w/v) Coomassie Brilliant Blue, 2 % (v/v) perchloric acid]. Samples were mixed by vortexing and the absorbance measured at 595 nm. Absorbance readings were used for calibration of a standard curve to be utilised for determination of protein concentrations in samples with unknown concentration.

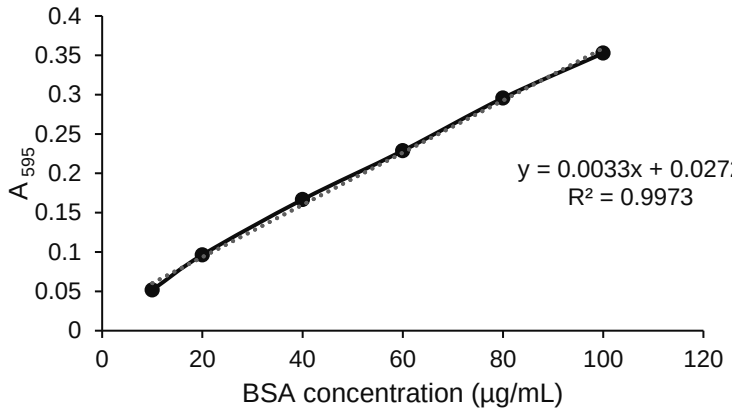

Figure 2.1: Standard curve of BSA concentration against absorbance at 595 nm obtained in the Bradford assay. Bovine serum albumin was diluted with distilled water to obtain 10-100 µg/mL in triplicate samples and combined with Bradford reagent. Absorbance was measured at 595 nm to obtain readings for the standard curve.

2.4 Cultivation of *Trichinella zimbabwensis* parasites and isolation from rat muscle tissue

All protocols involving animals for research were approved by the UKZN Research Ethics committee (approval number: AREC/00004250/2022). *Trichinella zimabwensis* muscle larvae were obtained from Professor Sam Mukaratirwa, School of Life Sciences, UKZN Westville Campus. Male Sprague-Dawley (SD) rats were 90 – 150 g at the time of infection unless otherwise stated and were orally infected with 300 – 500 *T. zimbabwensis* larvae in 1% (w/v) saline solution. An infected rat was sacrificed using carbon dioxide three months post infection (pi) and the infected muscle tissue was digested using the pepsin-HCl digestion method (Pozio et al., 2002). Muscle tissue was weighed and mixed with warm distilled water in a 5 L beaker (2 L per 100 g rat muscle) and upon confirming that temperature of the mixture was 42 °C, digestion was facilitated by the addition of pepsin (20 g per 100 g rat muscle) and 37% (v/v) HCl (8 ml per 2 L distilled water) and the mixture was stirred for 30 min, now being referred to as the digestion fluid. The digestion fluid was sieved through 800 µm followed by 250 µm sieves to remove undigested solids, and then was poured into 2 L separating funnels and left to stand for 40 min to allow sedimentation of parasites. Following sedimentation, 50 mL of digestion fluid was collected per separating funnel into beakers and each diluted with an equal volume of distilled water. The diluted digestion fluid was further sedimented within the beaker in 15 min intervals after which 30 mL was aspirated and the rest checked for the presence of parasites using a light microscope. The aspiration process was continued until 5 mL of the digestion fluid remained which was confirmed to contain parasites by microscopy. This fluid was further aspirated to 1 mL and stored at –70 °C until used for RNA extraction.

2.5 Extraction of *Trichinella zimbabwensis* mRNA and synthesis of cDNA

Parasites (100 µL) were thawed and suspended in Tri-reagent (300 µL) from the Direct-zol RNA miniprep plus R2070 kit. The resultant mixture was ground using a chilled pestle and mortar containing liquid nitrogen. This process was repeated until the parasite mixture was ground into a fine powder which was transferred to a microfuge tube. The ground powder was dissolved in Tri-reagent (100 µL) and 500 µL of 100% (v/v) ethanol. Subsequently, RNA was isolated using the kit according to the manufacturer's instructions. This RNA was then used in cDNA synthesis using the LunaScript R Supermix kit. Briefly, isolated RNA (8 µL) was mixed with oligo primer (2 µL) or random primer (2 µL) to assess which primer yield the highest concentration of synthesised cDNA. The RNA-oligo primer and RNA-random primer mixtures were incubated at 70°C for 5 min for RNA denaturation. Subsequently, cDNA was synthesised as per the manufacturer's instruction.

2.6 PCR amplification of the *Tz*stefinB gene from cDNA

PCR amplification allows for a desired gene sequence to be amplified to large numbers for analytical and cloning purposes. The gene encoding *Tz*stefinB was PCR amplified from cDNA (Section 2.5) using primers (Table 2.2) designed in a past study (Maseko, 2019) of this protein and synthesised by Inqaba Biotechnical Industries (Pretoria, RSA). The correct gene sequence was confirmed on GenBank and the primers were checked against it using Primer BLAST. The forward primer contains an EcoRI restriction site and the reverse primer contains a XhoI restriction site.

Table 2.2: *Tz*stefinB gene primer sequences

Primer	Nucleotide sequence (5' – 3')	Annealing temp.
*Tz*stefinB Fwd	AAGAATTC ATG AGT AAC ATA TGC GGA GGT GT	51.7 ºC
*Tz*stefinB Rev	AACTCGAG CTA AAA ATA TTC GAG CTT ATC AGA ATG TTT TTT ACC A	

Underlined residues represent restriction sites for EcoRI in the forward primer and XhoI in the reverse primer.

PCR was conducted using the EmeraldAmp® GT PCR Master Mix (TaKaRa) already containing polymerase, dNTP's and $MgCl_2$. Two reactions were carried out, each using 12.5 µL of master mix, with 0.5 µL of cDNA (Section 2.5) added as well as gene primers at a final concentration of 0.2 µM, with the final volume of the reactions at 25 µL. The PCR thermal cycle was as follows: initial denaturation at 95 °C for 5 min, followed by 34 cycles of

denaturation at 95 °C for 3 min, annealing at 51.7 °C for 30 s, and extension at 72 °C for 5 min. This was followed by a final extension at 72 °C for 5 min. PCR products were analysed by agarose gel electrophoresis (Section 2.7).

2.7 Analysis of DNA by agarose gel electrophoresis

The PCR amplicons obtained from cDNA were analysed on an agarose gel by electrophoresis, a separation which is made possible due to the negative charge present on the DNA backbone (Maity et al., 2022). A 1 % (w/v) agarose gel was prepared by adding 0.5 g of agarose powder to 50 mL of 1 x TAE buffer (40 mM Tris, 20 mM acetic acid, 1 mM EDTA, pH 8.3) and dissolving the agarose by heating the solution. The gel solution was allowed to cool to touch, 2.5 µL of GelRed was added to allow visualization of DNA fragments, and then the gel solution was poured and allowed to set. To each PCR sample, 1x loading dye buffer was added and samples were run alongside the O'Gene 1 kb DNA ladder (Thermo Fisher Scientific) at 80 V until the dye front had reached at least ¾ of the distance down the gel. The gel was then visualised under UV light in a G-Box system (SynGene). A standard curve (Fig. 2.2) of relative mobility against log (bp) was calibrated using the distances traveled by the bands of the DNA molecular weight marker.

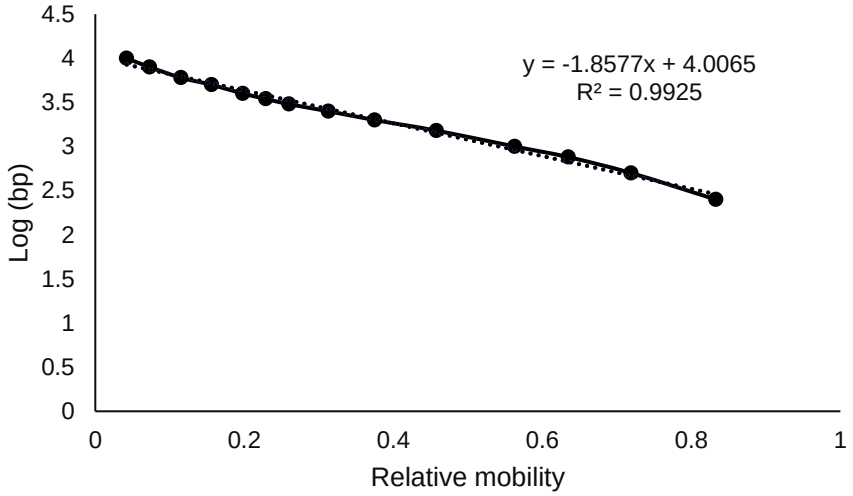

Figure 2.2: Standard curve of relative mobility against log (molecular weight) of DNA fragments. The O'Gene Ruler (1 kb) electrophoresed on a 1 % (w/v) agarose gel at 80 V. Distance run by fragments was measured, and relative mobility plotted against respective log (molecular weight).

2.8 Cloning of the *Tz*CATB and *Tz*stefinB genes

The correct *Tz*CATB gene sequence was confirmed on Genbank and was then commercially synthesised by Thermo Fisher Scientific within the cloning vector pMA-RQ to alleviate early steps of cloning used for *Tz*stefinB.

2.8.1 Preparation of competent cells

Competent *E. coli* cells for transformation of gene constructs were prepared by a chemical method (Liu et al., 2014). *E*. *coli* JM109 and BL21 (DE3) cells were each used to inoculate 5 mL of 2 x YT liquid medium [1.6 % (w/v) tryptone, 1% (w/v) yeast extract, 0.5 % (w/v) NaCl] without antibiotic, and cultures grown at 37 ºC for 16 h with agitation at 200 rpm. Cultures were diluted 1:100 up to 50 mL and grown at 37 ºC with 200 rpm agitation until reaching an OD_{600} of 0.4, after which they were centrifuged (2700 x g, 10 min, 4 ºC) and the supernatant discarded. Pelleted JM109 and BL21 (DE3) cells were each diluted in ice-cold sterile 100 mM $MgCl_2$ (2 mL) and 100 mM $CaCl_2$ (1 mL). Resuspended samples were then centrifuged (2700 x g, 10 min, 4 ºC) and resuspended in ice-cold sterile 100 mM $CaCl_2$ (2 mL). Competent cell samples were aliquoted to 500 µL samples and to each an equal volume of sterile 60 % (v/v) glycerol was added. Glycerol stocks of competent cells were stored at -80 ºC.

2.8.2 Ligation of *Tz*stefinB to pMD-19 simple

The purified PCR product from amplification of *Tz*stefinB (Section 2.6) was ligated to pMD-19 simple cloning vector (50 ng) using a 3:1 ratio of insert to vector. Taq polymerase used in PCR leaves a 3’ adenine overhang on the PCR product (Zhou and Gomez-Sanchez, 2000) which allows for ligation to T-vectors which have complementary 3’ thymine overhangs (Fig. 2.3). Ligation was conducted in the presence of 1 x ligation buffer and 1 x T4 DNA ligase at RT for 16 h. The ligation mixture was kept at -20 °C until used to transform competent cells.

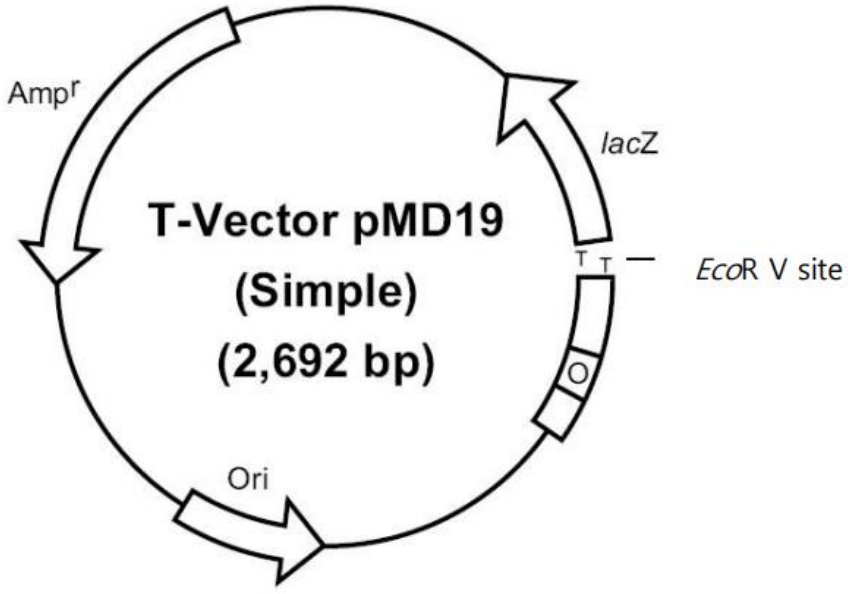

Figure 2.3: pMD-19 simple T-vector cloning map. T-vectors utilise 3’ thymine overhangs for TA cloning, whereby PCR products can be directly ligated (Khan et al., 2016).

2.8.3 Transformation into *E. coli* JM109 cells

The *Tz*CATB-pMA-RQ and *Tz*stefinB-pMD-19 constructs were transformed into competent *E. coli* JM109 cells (Section 2.8.1) to maintain and clone them to high numbers. Transformation was conducted by separately adding 5 µL of *Tz*CATB-pMA-RQ and 2.5 µL of ligation mixture (Section 2.8.2) to 30 µL of competent JM109 cells (volumes optimised) and incubating on ice for 30 min. The mixtures were then heat shocked at 42 °C for 90 s and placed on ice for 5 min. Following this, 80 µL of SOC medium [2% (w/v) tryptone, 0.5 % (w/v) yeast extract, 10 mM NaCl, 2.5 mM KCl, 10 mM $MgSO_4$, 20 mM glucose] was added to each transformation mixture which were then incubated in an orbital incubator at 37 °C with 200 rpm agitation for 1 h. The transformation mixtures were then plated onto two 2 x YT agar [1.6 % (w/v) tryptone, 1% (w/v) yeast extract, 0.5 % (w/v) NaCl, 1% (w/v) bacteriological agar] plates containing 50 µg/mL ampicillin and incubated at 37 °C for 16 h. To allow blue-white screening, 20 mg/ml X-gal (40 µL) and 100 mM IPTG (10 µL) were spread on the surface of agar plates and allowed to absorb at 37 ºC for 30 min, prior to plating transformation mixtures. White colonies were picked and used to screen for the presence of the *Tz*CATB and *Tz*stefinB inserts.

2.8.4 Isolation of plasmid DNA by miniprep

To screen *Tz*CATB-pMA-RQ colonies for the presence of the *Tz*CATB gene insert, restriction digests on isolated plasmid were required due to lack of specific gene primers. Bacterial colonies obtained from transformation of *Tz*CATB (Section 2.8.3) were each used to inoculate 6 mL of 2 x YT liquid medium containing 50 µg/mL ampicillin and incubated at 37 °C with 200 rpm of agitation for 16 h. From each culture, 700 µL was removed and added separately to 300 µL of sterile 50 % v/v glycerol to create glycerol stocks which were stored at -80 ºC. The remaining volumes of each culture were used to isolate plasmid using the GeneJET Plasmid Miniprep Kit (Thermo Fisher Scientific) as per the manufacturer's instructions.

2.8.5 Restriction digestion to confirm presence of *Tz*CATB gene

The pMA-RQ-*Tz*CATB construct was synthesised with BamHI and XhoI restriction sites on the 5' and 3' sides of the gene sequence, respectively. Restriction digests were conducted on isolated pMA-RQ-*Tz*CATB (Section 2.8.4) to confirm the presence of the *Tz*CATB gene insert at the correct size. In 10 µL reaction mixtures, 300 ng of pMA-RQ-*Tz*CATB (from each clone) was digested with 0.3 µL of FastDigest BamHI and XhoI in the presence of 1 x FastDigest buffer (Thermo Fisher Scientific). Digestions were carried out at 37 ºC for 1 h, after which digestion products were analysed using agarose gel electrophoresis (Section 2.7).

2.8.6 Colony PCR to confirm *Tz*stefinB gene presence

Recombinant *Tz*stefinB-pMD-19 colonies (Section 2.8.3) were diluted in 10 µL of sterile distilled water. These were used to inoculate cultures for preparation of glycerol stocks (Section 2.8.4) and to conduct colony PCR which utilises gene-specific primers to amplify and detect a desired gene sequence in bacterial colonies. Colony PCR was used to screen for the presence of the *Tz*stefinB gene with the same thermal cycle as previously described (Section 2.6) but with 24 cycles. The reaction components are listed in Table 2.3.

Table 2.3: Colony PCR components for detection of the *Tz*stefinB gene insert

Component	Final concentration	Volume (µL)
10 x Buffer B	1 x	1.25
dNTP's (10 mM)	200 µM	0.25
Forward primer (10 µM)	0.2 µM	0.5
Reverse primer (10 µM)	0.2 µM	0.5
$MgCl_2$ (25 mM)	2 mM	1
dH_2O	-	8.375
Template	-	0.5
FIREpol® Taq polymerase (5U/µL)	0.05	0.125

Separate reactions were conducted for each colony and the products were analysed using agarose gel electrophoresis (Section 2.7).

2.9 Sub-cloning of the *Tz*CATB gene into the pET-28a, pCold-1 and pCold-TF expression vectors and the *Tz*stefinB gene into the pET-28a expression vector

Cloned pMA-RQ-*Tz*CATB and pMD-19-*Tz*stefinB as well as the pET-28a, pCold-1 and pCold-TF expression vectors were isolated using miniprep (Section 2.8.4). Plasmids were restriction digested to produce compatible ends for ligation of gene inserts to expression vectors. The pMA-RQ-*Tz*CATB construct and the pET-28a expression vector (2000 ng) were restriction digested at 37 ºC for 1 h, using 1 µL of FastDigest BamHI and XhoI (Thermo Fisher Scientific) with 1 x FastDigest buffer in 20 µL reactions. The same was done to the pCold-1 and pCold-TF expression vectors (2000 ng) but with BamHI and SalI (Thermo Fisher Scientific) in 1 x Tango buffer. The pCold-1 vector used in the present study already had a gene insert present from an unrelated study; this was removed by the double restriction digestion. The *Tz*stefinB-pMD-19 construct and the pET-28a expression vector (2000 ng) were digested under the same conditions but using FastDigest EcoRI and XhoI. Restriction digestion products were

analysed using agarose gel electrophoresis (Section 2.7) and upon observing the expected fragments in the gel, the *Tz*CATB and *Tz*stefinB gene inserts as well as the digested expression vectors were excised from the gels and gel extracted using the Zymogen DNA gel extraction kit (Zymo Research) according to the manufacturer's protocol. The *Tz*CATB gene was then ligated to pET-28a, pCold-1 and pCold-TF, and the *Tz*stefinB gene was ligated to pET-28a (Section 2.8.2). Ligation mixtures were used for transformation (Section 2.8.3) into competent *E. coli* BL21 (DE3) cells. Colonies obtained were used to make glycerol stocks (Section 2.8.4) and screened for the presence of the *Tz*CATB gene insert using restriction digests with the appropriate restriction enzymes or screened for the presence of the *Tz*stefinB gene insert using colony PCR (Section 2.8.6).

2.10 Expression of recombinant *Tz*CATB and *Tz*stefinB by IPTG induction

Expression of recombinant proteins was induced with IPTG, which binds to and inhibits the lac repressor allowing for expression of the lac operon. Recombinant *Tz*CATB and *Tz*stefinB were both expressed in the pET-28a expression vector (Fig. 2.4 and Fig. 2.5A), which provides a 6x His-tag on both the N- and C- termini of the expressed protein. Single pET-28a-*Tz*CATB and pET-28a-*Tz*stefinB colonies were obtained by streaking out glycerol stocks (Section 2.9) onto 2 x YT agar plates containing 34 µg/mL of kanamycin. Colonies were used to inoculate 5 mL of 2 x YT liquid medium (Section 2.8.1) containing 34 µg/mL of kanamycin and cultures incubated at 37 ºC with 200 rpm of agitation for 16 h. Cultures were then diluted 1:100 to 50 mL using 2 x YT liquid medium containing kanamycin, and then grown at 37 ºC with 200 rpm of agitation. This was done until cultures reached an OD_{600} of 0.6 - 0.8, at which point IPTG (1 mM) was used to induce protein expression in cultures at 37 ºC with 200 rpm of agitation for 4 h. Cells were then pelleted by centrifugation (6000 x g, 10 min, 4 ºC) and resuspended in 2 mL of PBS containing 1 % (v/v) Triton X-100 and frozen at -20 ºC. Cells were thawed and sonicated on ice 5 times for 30 s (with 30 s intervals) at 20 % amplitude. Insoluble and soluble fractions were separated using centrifugation (10 000 x g, 20 min, 4 ºC). Recombinant *Tz*CATB was additionally expressed within the pCold-1 (Fig. 2.4 and Fig. 2.5B) and pCold-TF (Fig. 2.4 and Fig. 2.5C) expression vectors. These vectors utilise a cold-shock expression system whereby the presence of the cold shock protein A (cspA) promotor allows for increased expression levels and solubility of recombinant protein at low temperature, with lower expression levels of *E. coli* proteins (Bjerga and Williamson, 2015; Sugiki et al., 2017; Li et al., 2018). Expression was conducted the same way as with the pET-28a expression vector, except using 50 µg/mL of ampicillin, and the expression was induced using 0.1 mM IPTG at 4 ºC for 24 h.

A

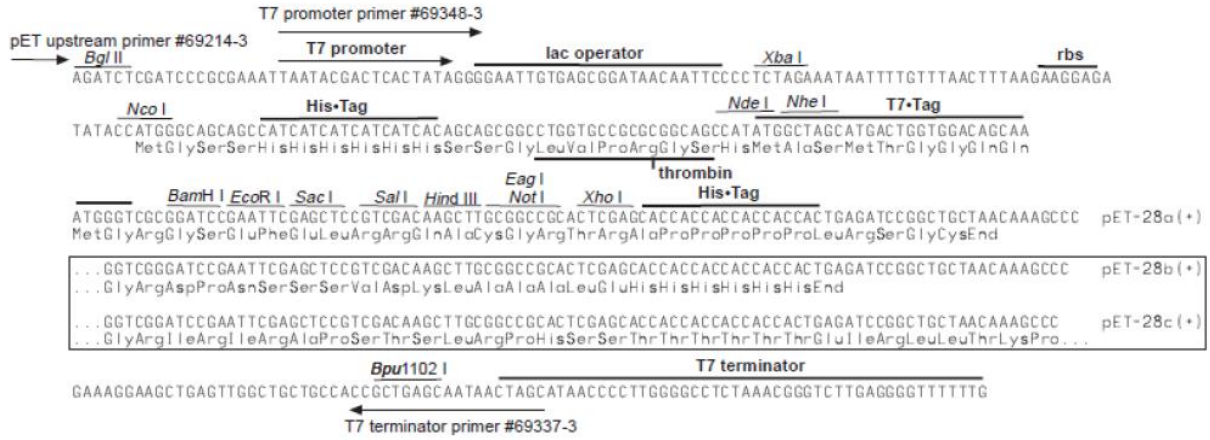

B

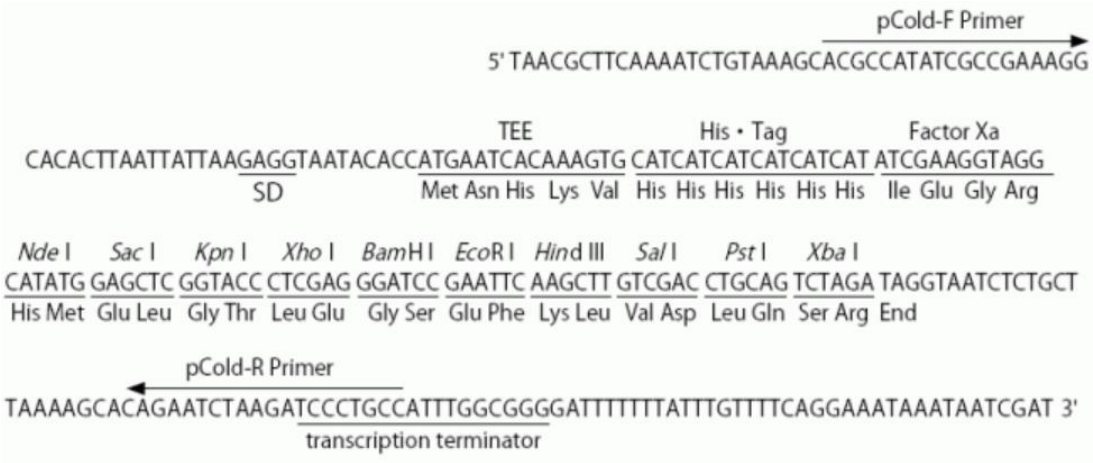

C

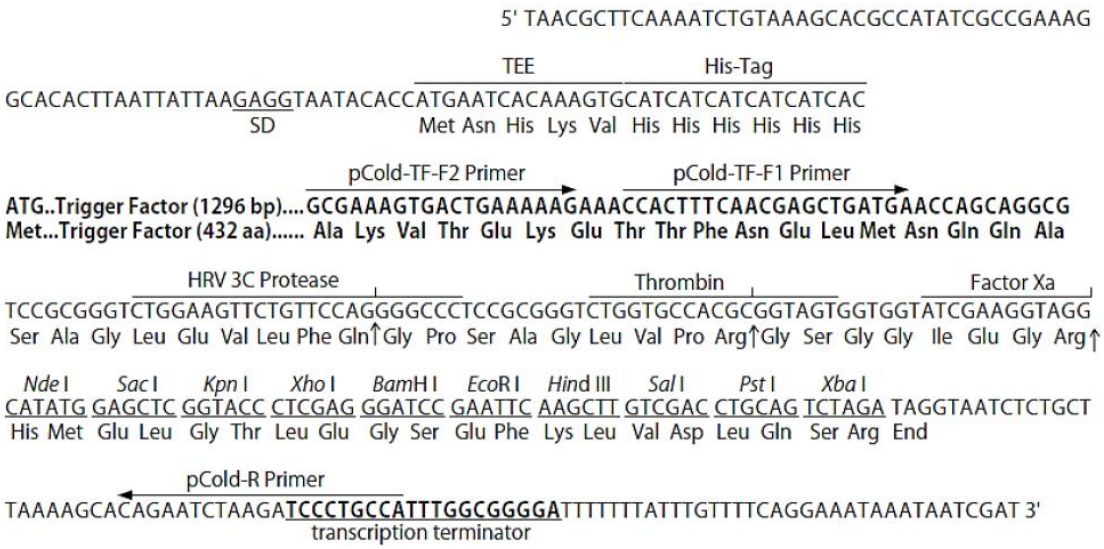

Figure 2.4: Maps showing the multiple cloning sites of the (A) pET-28a, (B) pCold-1 and (C) pCold-TF expression vectors. All expression vectors provide His-tags and restriction enzyme recognition sites, while pCold-TF additionally provides the trigger factor fusion protein. The pET-28a map was obtained from the Novagen user manual and the pCold maps were obtained from the TaKaRa user manuals.

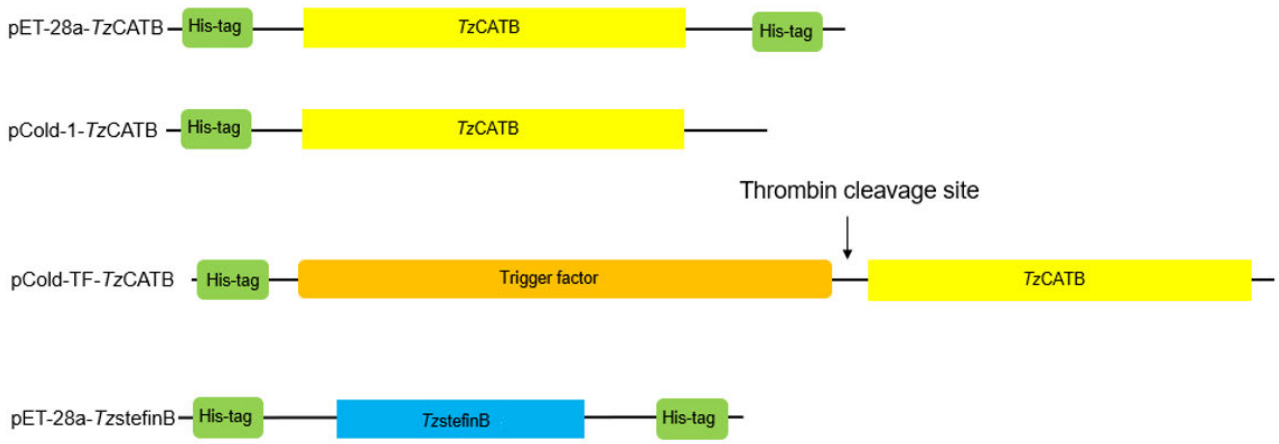

Figure 2.5: Schematic representation of recombinant proteins expressed in the pET-28a, pCold-1 and pCold-TF expression vectors.

2.11 Analysis of recombinant expression

2.11.1 SDS-PAGE analysis of *Tz*CATB and *Tz*stefinB recombinant expression

Sodium dodecyl sulfate-polyacrylamide gel electrophoresis (SDS-PAGE) analysis is a technique which separates proteins based upon their molecular weight and allows for their visualisation. The protein contents of uninduced cultures as well as the insoluble and soluble fractions obtained from protein expressions (Section 2.10) were analysed on 10 % tris-tricine reducing SDS-PAGE gels (Schägger, 2006). Samples were combined 1:1 with reducing treatment buffer (125 mM Tris-HCl, 4 % (w/v) SDS, 20 % (v/v) glycerol, 10 % (v/v) 2-mercaptoethanol, pH 6.8) and boiled for 3 min. Samples were loaded onto gels alongside molecular weight markers. Unstained Protein Molecular Weight Marker was used for analysis of *Tz*CATB expression and Low Range Molecular Weight Marker was used for analysis of *Tz*stefinB expression (markers both manufactured by Thermo Fisher Scientific). Samples were electrophoresed at 80 V until the dye front reached the bottom of the gels. Gels were then stained overnight with Coomassie R-250 and de-stained [50 % (v/v) methanol, 10 % (v/v) acetic acid]. Gels were imaged using the GelDoc imaging system (BioRad) and the distances travelled by the bands of the molecular weight marker were used to calculate relative mobility for each protein, which was plotted against the log(molecular weight) of each protein (Fig. 2.6). These standard curves were calibrated to allow the sizes of proteins to be estimated in experimental samples.

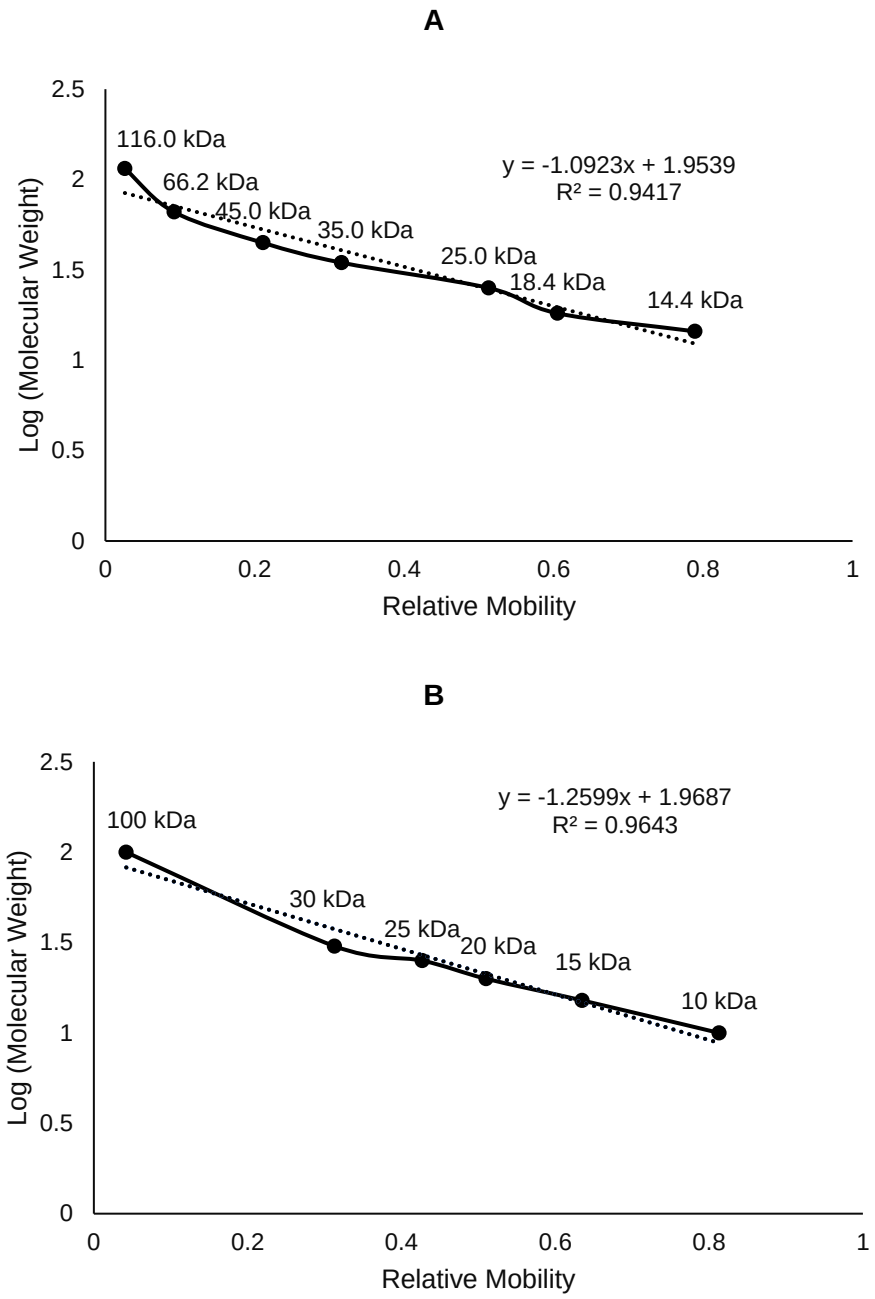

Figure 2.6: Standard curves of relative mobility against log (molecular weight) of proteins. (A): Unstained Protein Molecular Weight Marker (ThermoFisher Scientific). **(B):** Low Range Molecular Weight Marker (ThermoFisher Scientific). Distances travelled by each marker protein were measured, used to calculate relative mobility and plotted against respective log (molecular weight).

2.11.2 Western blotting for detection of recombinant protein

Western blotting was utilised to confirm protein expression by detection of the His-tag(s) present after expression in the pET-28a, pCold-1 and pCold-TF expression vectors. This technique involves the transfer proteins onto a membrane, such as nitrocellulose, and thereafter utilises enzyme-linked antibodies to detect target proteins (Kurien and Scofield, 2006). Additional reducing tris-tricine SDS-PAGE gels (Section 2.11.1) were run with

expression samples and separated proteins then transferred onto nitrocellulose membranes at 20 mA for 16 hours. Membranes were stained with Ponceau S (0.1 % (w/v) in distilled water, with 5 % (v/v) glacial acetic acid) for 10 - 20 min to confirm protein transfer and mark the bands of the molecular weight marker. Membranes were rinsed with distilled water and a few drops of 1 M NaOH and then blocked with 5 % (w/v) non-fat milk powder in TBS (20 mM Tris, 20 mM NaCl, pH 7.4) at RT for 1 h to block non-specific binding sites. Membranes were washed three times with TBS for 5 min before incubating with 10 mL of primary antibody [mouse anti-His antibodies [1:5000 in 0.5 % (w/v) BSA-TBS)] at RT for 2 h. Membranes were washed as before and then incubated with 10 mL of secondary antibody [goat anti-mouse HRPO-conjugate [1:5000 in 0.5 % (w/v) BSA-TBS)] at RT for 1 h. Membranes were washed again before adding 10 mL of 4-chloro-1-naphthol substrate solution [10 % (v/v) 4-chloro-1-naphthol (Sigma-Aldrich), 0.2 % (v/v) of 30 % hydrogen peroxide in PBS, pH 7.4] and placing them in the dark for 5 min. Blots were imaged with the GelDoc imaging system (BioRad).

2.12 Solubilisation and purification of *Tz*CATB expressed in pET-28a and pCold-1

Due to *T*zCATB in pET-28a and pCold-1 expressing predominantly as insoluble protein, solubilsation of this protein was achieved using SDS and sarkosyl (Burgess, 2009). Sarkosyl is anionic detergent which solubilises inclusion bodies but binds protein relatively weakly. Recombinant *Tz*CATB in pET-28a and pCold-1 was expressed and cells collected (Section 2.10) which were lysed with 5 mL of PCL [sarkosyl lysis buffer: 8 mM Na_2HPO_4, 286 mM NaCl, 1.4 mM KH_2PO_4, 2.6 mM KCl, 1% (w/v) SDS, pH 7.4] with 1 mM DTT added before use. Cells were then sonicated on ice (8 x 30 s) and placed on ice for 30 min. Samples were then centrifuged (10000 x g, 20 min, 4ºC) to separate the insoluble and soluble fractions which were analysed on 10 % reducing tris-tricine SDS-PAGE gels (Section 2.11.1). Refolding and purification of solubilised *Tz*CATB was achieved with Ni-IMAC (nickel immobilised metal affinity chromatography), a purification method based on the high affinity of the His-tags for nickel where by electron donor groups on the imidazole ring of histidine form coordination bonds with nickel (Bornhorst and Falke, 2000). Into 10 mL BioRad chromatography columns, 1 mL of Ni-NTA resin (Thermo Fisher Scientific) was poured and allowed to settle. Resins were washed with 10 column volumes of 6M guanidine HCl and 10 column volumes of distilled water, and then with 5 column volumes of PCW [sarkosyl wash buffer: 8 mM Na_2HPO_4, 286 mM NaCl, 1.4 mM KH_2PO_4, 2.6 mM KCl, 0.1% (w/v) sarkosyl, pH 7.4] containing 10 mM imidazole. Solubilised lysates (5 mL) were added to the resins and incubated at 4ºC for 3 h on an end-to-end rotator. Unbound proteins were eluted and columns washed with 50 mL of PCW containing 20 mM imidazole until an A_{280} of 0.03 was reached. Bound proteins were eluted with PCE [sarkosyl elution buffer: 8 mM Na_2HPO_4, 286 mM NaCl, 1.4 mM KH_2PO_4, 2.6 mM

KCl, 0.1% (w/v) sarkosyl, 250 mM imidazole, pH 7.4] and collected in 1 mL fractions. Samples from purifications were analysed on 10 % reducing tris-tricine SDS-PAGE gels (Section 2.11.1).

2.13 Immunoaffinity purification of *Tz*CATB expressed in pCold-TF

Recombinant *Tz*CATB expressed in pCold-TF was purified using Ni-IMAC (Section 2.12) following which no proteolytic activity was obtained. Immunoaffinity chromatography is a method of protein isolation based upon the selective non-covalent binding of antibodies to antigens (Wu et al., 2016a), with antibodies immobilized on a support resin. This method was used as an alternative means of purifying recombinant *Tz*CATB expressed in pCold-TF.

2.13.1 Coupling of anti-*Tz*CATB IgY antibodies to UltraLink Hydrazide resin

Chicken anti-*Tz*CATB IgY antibodies raised in a previous study (Zondo, 2019) were coupled onto UltraLink™ Hydrazide Resin as per the manufacturer's instructions. Antibodies are coupled through oxidised sugar groups on their Fc region, allowing for optimal orientation for binding of antigens. Antibodies were diluted to 10 mg/mL with 1 mL of coupling buffer (100 mM Na_2HPO_4, pH 7.0) and added to 5.35 mg of sodium meta-periodate in an amber vial covered with aluminium foil. This was dissolved gently by briefly swirling, and then incubated at RT for 30 min. The antibodies were then buffer exchanged into new coupling buffer using the Amicon® Ultra centrifugal filter (Merck). During this buffer exchange, 1 mL of UltraLink™ Hydrazide Resin was poured into a 10 mL BioRad chromatography column and allowed to settle. The storage fluid was drained and the resin washed with five resin-bed volumes of coupling buffer. The oxidised antibodies (1 mL) were added to resin, which was incubated on an end-to-end rotator at RT for 1 h and then at 4 ºC for 16 h. The column was then drained and washed with one column volume of coupling buffer to produce the immunoaffinity column. The resin was then washed with five resin-bed volumes of 1 M NaCl and the same volume of PBS with 0.05 % (w/v) NaN_3.

2.13.2 Purification and thrombin cleavage

Recombinant *Tz*CATB was expressed in pCold-TF (Section 2.10) but following induction and centrifugation, cells were resuspended in binding buffer (50 mM Na_2HPO_4, 300 mM NaCl, pH 7.0) and sonicated on ice (5 x 30 s). The resulting lysate (2 mL) was diluted with an equal volume of binding buffer and added to the immunoaffinity column which was equilibrated with five resin-bed volumes of binding buffer. The column was incubated on an end-to-end rotator at 4 ºC for 16 h, following which unbound proteins were collected and the column washed with five resin-bed volumes of binding buffer (1 mL fractions collected). Bound protein was eluted with 300 mM glycine (pH 3.0) and collected fractions neutralised with 1/10th volume of 1 M Tris

(pH 7.5). The column was washed with five resin-bed volumes of binding buffer and then PBS containing 0.05 % (w/v) NaN_3. Purification samples were analysed on 10 % non-reducing tris-tricine gels (Section 2.10.1). Fractions with purified *Tz*CATB were pooled and then subjected to thrombin cleavage to remove the trigger factor fusion protein, producing *Tz*CATB protein alone. To a 1 mL solution of purified *Tz*CATB (5 µM), 13 U of thrombin was added and incubated at RT for 1 h, and at 4 ºC for 23 h. The success of the cleavage was determined using reducing tris-tricine SDS-PAGE (Section 2.11.1). Thrombin was subsequently removed by incubating the cleavage product on a 1 mL p-aminobenzamidine agarose (Sigma) column at 4ºC for 16 h. Benzamidine is a competitive, reversible inhibitor of trypsin-like serine proteases (such as thrombin) with affinity for their substrate binding pocket, allowing for specific purification of these proteases (De-Simone et al., 2005).

2.14 Purification of *Tz*stefinB expressed in pET-28a using Ni-IMAC

Recombinant *Tz*stefinB expressed as soluble protein (Section 2.10) was purified using Ni-IMAC (Section 2.12). After pouring 1 mL of Ni-NTA resin into a 10 mL BioRad column, the resin was washed with 10 column volumes of 6M guanidine HCl and 10 column volumes of distilled water, and then equilibrated with 10 column volumes of Ni-IMAC equilibration buffer (20 mM NaH_2PO_4, 300 mM NaCl, 10 mM imidazole, pH 7.4). Soluble *Tz*stefinB lysate (2 mL) was added to the resin and the purification conducted as before (Section 2.12) but utilising Ni-IMAC buffer with 20 mM and 250 mM imidazole. Purification samples were analysed on a 10 % reducing tris-tricine SDS-PAGE gel (Section 2.11.1).

2.15 Immunisation of chickens with *Tz*StefinB and IgY isolation

2.15.1 Chicken immunisation

Approval for procedures involving experimental animals for antibody production was obtained from the University of KwaZulu-Natal Research Ethics Committee (Reference number AREC/00004250/2022). Permission to do research in terms of Section 20 of the Animal Diseases Act, 1984 (Act No. 35 of 1984) Antibody production Ref Number: 12/11/1/5/MG (1769) was obtained from the South African Department of Agriculture Land Reform and Rural Development.

Two chickens were immunised with *Tz*stefinB and each immunisation was conducted with 50 µg of pure *Tz*stefinB per chicken. For each chicken, pure *Tz*stefinB (50 µg in 1 mL) was mixed with an equal volume of Freund's complete adjuvant and the solution tricurated until obtaining a stable water-in-oil emulsion which was injected into either side of the chicken's breast. Booster injections were given at 2-, 4- and 6-weeks post-immunisation using Freund's

incomplete adjuvant. Eggs were collected prior to immunisation and daily for 12 weeks and stored at 4 ºC.

2.15.2 Isolation of IgY antibodies

Chicken IgY antibodies were isolated from eggs collected during the immunisation period using filtration and PEG precipitation (Goldring and Coetzer, 2003). The egg yolk was separated from the white, punctured and the volume of the yolk measured. Two yolk volumes of PBS (100 mM Na-phosphate, 0.02 % (w/v) NaN_3, pH 7.4) were added to the yolk and mixed, followed by 3.5 % (w/v) PEG (polyethylene glycol) 6000. Upon dissolving the PEG 6000, the solution was filtered through Whatman No.1 filter paper. A further 8.5 % (w/v) of PEG 6000 was added to the filtrate and dissolved before centrifuging (12 000 x g, 10 min, RT). The pellet was resuspended in a volume of PBS equal to the original yolk volume and 12 % (w/v) PEG 6000 added and dissolved. Antibodies were then pelleted by centrifugation (12 000 x g, 10 min, RT), resuspended in PBS equal to 1/6 of the original yolk volume, and the concentration of IgY determined using absorbance at 280 nm, and the extinction coefficient of IgY which is equal to 1.25 (Goldring and Coetzer, 2003).

2.15.3 ELISA tests for detection of anti-*Tz*stefinB antibodies

Indirect ELISA was used to monitor the production of antibodies following immunisation of chickens with *Tz*stefinB. This method allows for detection of target antigens using an antigen-specific primary antibody followed by a secondary enzyme-linked antibody, whereby the product of the enzyme HRPO (horseradish peroxidase) produces light which is measured at 405 nm. The wells of a Nunc-Immuno™ Maxisorp 96-well plate from Nunc Intermed (Roskilde, Denmark) were coated with purified *Tz*stefinB (1 µg/mL, 100 µL per well) for 16 h at 4 ºC. The solution was poured off, and the wells blocked with 0.5 % (w/v) BSA in PBS (300 µL per well) at 37 ºC for 1 h. Wells were then washed 3 times with 1% (v/v) Tween-20-PBS using the BIOTEK ELx50 Microplate washer from BioTek Instruments Inc. (USA), after which 100 µL of primary antibody (100 µg/mL chicken anti-*Tz*stefinB IgY in 0.5 % (w/v) BSA-PBS) was added to the wells and the plate incubated at 37 ºC for 2 h. The wells were then washed as before, and 100 µL of secondary antibody (rabbit anti-chicken IgY HRPO-conjugate 1:5000 in 0.5 % (w/v) BSA-PBS) added to the wells and the plate incubated at 37 ºC for 1 h. The wells were washed as before, after which 100 µL of substrate solution (0.05 % (w/v) ABTS, 0.0015 % (v/v) H_2O_2 in 0.15 M citrate-phosphate buffer, pH 5.0) was added to each well and the plate incubated for 5 min at RT in the dark. Absorbance at 405 nm was measured in each well using the Versamax™ microplate reader purchased from Molecular Devices Inc. (USA). A similar protocol was conducted to find the optimal primary antibody concentration for western blotting but only using primary antibody from the weeks of maximal IgY production, as determined in

the above-mentioned ELISA, and using a series of primary antibody dilutions (0.1, 1, 5, 10, 25 and 50 µg/mL).

2.16 Detection of *Tz*CATB and *Tz*stefinB using Western blotting with chicken IgY

To confirm the presence of *Tz*CATB expressed in pCold-TF and to evaluate anti-*Tz*stefinB IgY antibodies produced (Section 2.15), chicken anti-*Tz*CATB IgY (5 µg/mL) and anti-*Tz*stefinB IgY antibodies (1 µg/mL) were used to detect 10 µg of expressed proteins in western blots (Section 2.11.2). Secondary antibody used for these blots was rabbit anti-chicken IgY HRPO-conjugate (1:5000). Recombinant *Tz*CATB was used in an additional western blot to determine if rabbit anti-human cathepsin B antibodies (1:1000) could detect it, with the secondary antibody being goat anti-rabbit IgG HRPO-conjugate (1:2500). Recombinant *Tz*stefinB was used in an additional blot to determine if chicken anti-sheep stefin B IgY antibodies could detect it, with the secondary antibody being rabbit anti-chicken IgY HRPO-conjugate (1:5000). Sheep stefin B (10 µg) was included in blots alongside *Tz*stefinB as a control.

2.17 Autocatalysis of *Tz*CATB and detection of proteolytic activity

To remove the *Tz*CATB propeptide region, autocatalysis was conducted by incubating *Tz*CATB in cysteine protease assay buffer (100 mM Na-acetate, 1 mM EDTA, pH 5.0) containing 5 mM DTT at 37 ºC for 1 h. Autocatalysed *Tz*CATB (1 µM) was incubated with the synthetic substrate Z-Arg-Arg-AMC (20 µM) at 37 ºC for 15 min, and the fluorescence measured with $Ex_{355\ nm}$ and $Em_{460\ nm}$ using the FLUORStar Optima spectrophotometer. This was conducted in the same assay buffer used for autocatalysis at pH 5.0 and in acetate-MES-tris (AMT) buffer at pH 8.0. Assays were simultaneously conducted with pre-incubation of *Tz*CATB with E-64 (10 µM) for 30 min before digestion of Z-Arg-Arg-AMC.

Additionally, proteolytic activity was tested against gelatin using zymography, a method utilising a gelatin-containing SDS-PAGE (Heussen and Dowdle, 1980). Proteolytic digestion of gelatin is observed after staining, whereby transparent bands against a stained background indicate digestion. Autocatalysed *Tz*CATB was combined 1:1 with non-reducing treatment buffer (125 mM Tris-HCl, 4 % (w/v) SDS, 20 % (v/v) glycerol, pH 6.8) and electrophoresed on a 10 % non-reducing tris-tricine SDS-PAGE gel (Section 2.11.1) containing 0.1 % (w/v) of gelatin. After electrophoresis, the gel was washed with two volumes of 2.5 % (v/v) Triton X-100 over 1 h to remove SDS and thereby renature the proteins separated on the SDS-PAGE gel. The gel was then incubated in cysteine protease assay buffer (100 mM Na-acetate, 1 mM EDTA, pH 5.0) containing 1 mM DTT at 37 ºC for 16 h, stained with amido black [0.1 % (w/v)

in methanol:acetic acid:dH_2O (30:10:60)] for 1h, and de-stained in several changes of methanol:acetic acid:dH_2O (30:10:40).

2.18 Inhibition of cysteine protease activity with *Tz*stefinB

2.18.1 Active site titration of cysteine proteases with E-64

Inhibition of papain from papaya latex and cathepsin L from *Trypanosoma congolense* (*Tc*CATL) by *Tz*stefinB was tested using synthetic substrate assays, prior to which the concentration of active papain and *Tc*CATL was determined using active site titration with E-64 (Barrett and Kirschke, 1981). Prior to assays with *Tc*CATL, this protease was autocatalysed for 1 h in cysteine protease assay buffer (100 mM Na-acetate, 1 mM EDTA, pH 5.0) containing 5 mM DTT. Papain (0.2 µM) and *Tc*CATL (1 µM) were each incubated with 0-1 µM of E-64 at 37 ºC for 10 min, following which proteolytic activity was determined by digestion of the synthetic substrate Z-Phe-Arg-AMC (20 µM) and fluorescence measured with $Ex_{355\ nm}$ and $Em_{460\ nm}$. This assay and subsequent assays were conducted in Z-Phe-Arg-AMC assay buffer [340 mM Na-acetate, 60 mM acetic acid, 4 mM Na_2EDTA, 0.02 % (w/v) NaN_3, pH 5.5] containing 5 mM DTT.

2.18.2 Synthetic substrate assays

Hydrolysis of Z-Phe-Arg-AMC (20 µM) by papain and *Tc*CATL was measured in the presence of *Tz*stefinB (0.1-1 µM) to detect inhibition of cysteine protease activity and determine the optimal concentration of *Tz*stefinB for inhibition of these proteases. Inhibition of papain by *Tz*stefinB was then measured after pre-incubating the inhibitor in AMT buffers (100 mM Na-acetate, 100 mM MES, 200 mM Tris, 4 mM Na_2EDTA) from pH 5.0 - 9.0 to find the optimal pH for inhibitory activity and/or demonstrate the pH stability of the inhibitor. AMT buffers provide constant ionic strength between experiments allowing for pH-dependent processes to be analysed (Ellis and Morrison, 1982). The thermal stability of *Tz*stefinB was also tested by inhibiting papain hydrolysis of Z-Phe-Arg-AMC but after incubating the inhibitor at 99 ºC for up to 30 min or at either RT or 4 ºC for up to 3 weeks.

2.18.3 Reverse zymography

Inhibition of papain by *Tz*stefinB was additionally tested using reverse zymography which detects protease inhibition by incubating a gelatin-containing SDS-PAGE gel in the presence of a protease (Hanspal et al., 1983) after which inhibition of gelatin digestion can be visualised by staining, whereby dark bands against an unstained background indicate inhibitory activity. A zymogram was run as before (Section 2.17) but with 0.5, 1, 5 and 10 µM of *Tz*stefinB, as well as 10 µM of SBTI (soya bean trypsin inhibitor) as a negative control (10 µL of these solutions). Papain (20 µM) was included in the assay buffer for incubation.

Chapter Three

Results

3.1 Bioinformatic analyses

To ascertain the similarity between the *Tz*CATB amino acid sequence (KRZ17844.1) and those of cathepsin B from other species of *Trichinella*, a multiple sequence alignment (Fig. 3.1) was conducted using Clustal Omega (https://www.ebi.ac.uk/jdispatcher/msa/clustalo). The *Tz*CATB sequence was aligned with those from the non-encapsulated *T. pseudospiralis* (KRZ37126.1) and *T. papuae* (KRZ80814.1), as well as those from the encapsulated *T. spiralis* (AGR34128.1), *Trichinella* genotype T8 (KRZ88549.1) and *T. britovi* (KRY60486.1). A similarity of 90.17 % was obtained between *Tz*CATB and *Tps*CATB, while other cathepsin B sequences had sequence identities between 40-50 %. The *Tz*CATB protein is shown to consist of a signal peptide (Fig. 3.1), which was excluded from the gene sequence used for cloning and recombinant expression. The propeptide was included to provide correct protein folding (Section 1.5.1). The amino acid sequences all have the conserved catalytic cysteine, histidine and asparagine residues as part of their active sites, as well as the GC-x-GG motif (Section. 1.5.1) which is a motif that is conserved among the amino acid sequences of all cysteine proteases, confirming their identity.

```
TzCATB      ------------------------------------LC------RIFPQKLKMIASVLLF      18
TpsCATB     -MVG------------------------VIYRNRNAT------KFLAQKLKMIAAVLLF      28
TpCATB      ------------------------------------------------------------      376
T8CATB      YCIGDLSKYKEGKIALRWRIEQEVIKGKGQFICGNKRCEEEENLTSWEVNFAYVEEQEKK      465
TsCATB      ------------------------------------------------------MFLQVVTF      8
TbCATB      ------------------------------------------------------MFLQVVTF      8

TzCATB      TLFLQHSYSAYYEDQFRTFLDKMDKFENKIETDWQNNAKMNEKQNKILFQHEFGLNEYFK      78
TpsCATB     TLFLRHSYSAYYEDQFRTFLDKMDKFENQIQTDWQ-----------------FGLNEYFK      71
TpCATB      -------------------KLLKE--------------IQQKNDLEQLPYTFGKNAYFK      402
T8CATB      NALVKLRLCPDCSEKLNYKKIFEKKKRNKVKTDT--LHAKGEDRKRSVEEDDMGLNPYFS      523
TsCATB      VALIKFSFCGYYED--NYIQL--------I------------KNNQMPKTWKMGLNPYFS      46
TbCATB      VTLIKFSFCGYYED--NYIQL--------I------------KNNQMPKTWKMGLNPYFS      46
                                                       :* * **.

TzCATB      GMSKEDIQIRVDGLSKELAKFKFIN-KGEKEIQNQKNYTDAKSESLPLEKHFDAREKWPQ      137
TpsCATB     GMSKEDIQIRVDGLSKELAKFKFLYKEGVKEIQKQQNYTETKSDSLPLEKHFDAREKWPE      131
TpCATB      GASIETVKRLLGFKENF-PSKTFI----------SS--SKNEHLSVDLPFEMDARKRWPQ      449
T8CATB      GMSKEEILIRMGTKLMN-SSTEFDSK--------LS--NNNEALIKKLPKHFDSREKWPE      572
TsCATB      GMSKEEILIRMGTKLMN-SSTEFDSK--------LS--NNNEALIKKLPKHFDSREKWPE      95
TbCATB      GMSKEEILIRMGTKLMN-SSTEFDSK--------MS--NNNEALIKKLPKHFDSREKWPE      95
            * * * :   :.       .  *           .  .. :     *  .:*:*::**:

TzCATB      CKYIGFIKDQSTCSCCWAMSSASVMTDRTCIAYNGEQQPFLSDEELTSCCTSCGDGCNGG      197
TpsCATB     CKYIGFIKDQSTCSCCWAMSSASVMTDRTCIAYKNQQQPFLSDEELTSCCTSCGDGCSGG      191
TpCATB      CKYIGFIRDQANCGSCWAVSSASVMTDRICIGNNATQQPLLSEEELVSCCKICGNGCDGG      509
T8CATB      CEWIRFIRDQSNCGSCWAVSAASVMTDRHCIASKGQETPYISDEQILSCA-S-SYGCSGG      630
TsCATB      CEWIRFIRDQSNCGSCWAVSAASVMTDRHCIASKGQETPYISDEQILACA-SSSYGCSGG      154
TbCATB      CEWIRFIRDQSNCGSCWAVSAASVMTDRHCIASKGQETPYISDEQILSCA-S-SYGCSGG      153
            *::* **:**:.*..***:*:******* **. :  : * :*:*:: :*.   . **.**
```

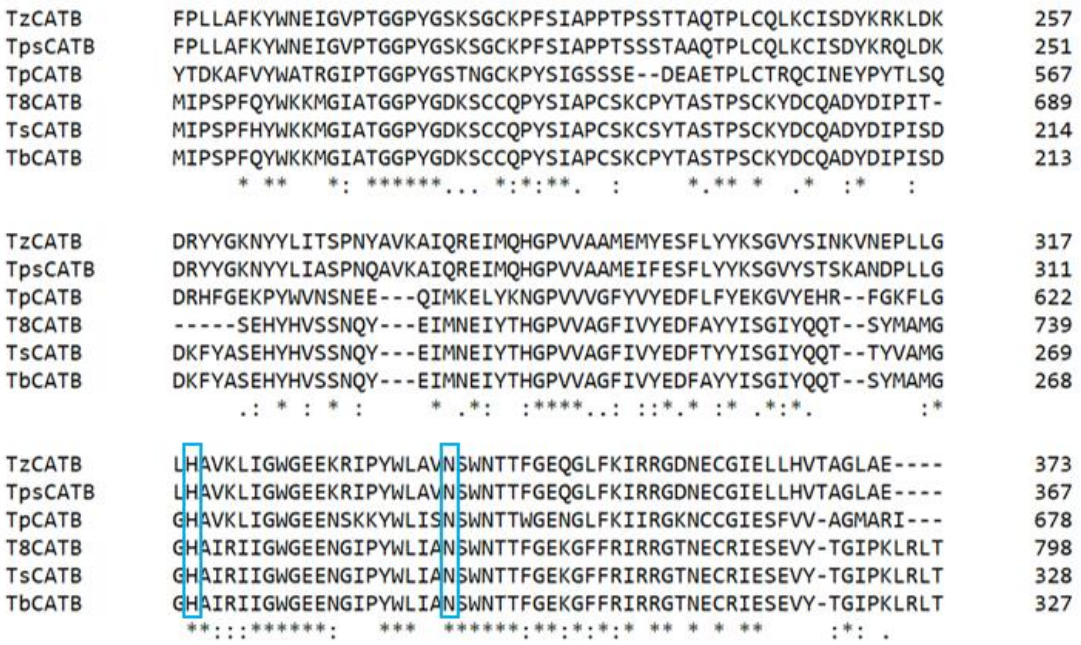

Figure 3.1: ClustalO multiple sequence alignment of *Trichinella* cathepsin B amino acid sequences. Amino acid sequences were obtained in Fasta format from NCBI (www.ncbi.nlm.nih.gov) and aligned with Clustal Omega (https://www.ebi.ac.uk/Tools/msa/clustalo/). The *Tz*CATB amino acid sequence (KRZ17844.1) was aligned with cathepsin B sequences from *Trichinella pseudospiralis* (KRZ37126.1), *Trichinella papuae* (KRZ80814.1), *Trichinella* genotype T8 (KRZ88549.1), *Trichinella spiralis* (AGR34128.1), and *Trichinella britovi* (KRY60486.1). The *Tz*CATB signal peptide is underlined in green and the propeptide is indicated by arrows. The conserved residues of the catalytic triad are in blue boxes and those of the GC-x-GG motif are in a purple box.

To demonstrate whether or not antibodies and drugs that target *Tz*CATB may be expected to cross react with human cathepsin B, the *Tz*CATB amino acid sequence was additionally aligned (Fig. 3.2) with that of human cathepsin B (AAH95408.1) with which it had a sequence identity of 39.75 %. This relatively low similarity indicates potential for this antigen in diagnostics and drug development

Figure 3.2: ClustalO pairwise alignment of the *Tz*CATB and human CATB amino acid sequences. Amino acid sequences were obtained in Fasta format from NCBI (www.ncbi.nlm.nih.gov) and aligned with Clustal Omega (https://www.ebi.ac.uk/Tools/msa/clustalo/). The conserved residues of the catalytic triad are in blue boxes and those of the GC-x-GG motif are in a purple box.

The *Tz*stefinB amino acid sequence (KRZ08317.1) was aligned with stefin B sequences from the non-encapsulated *T. pseudospiralis* (KRZ14801.1) and *T. papuae* (KRZ69001.1), as well as those from the encapsulated *T. spiralis* (XP_003379766.1), *Trichinella* genotype T8 (KRZ83534.1) and *T. britovi* (KRY54242.1). A sequence identity of 100 % was obtained between *Tz*stefinB and *Tp*stefinB, 98.17 % between *Tz*stefinB and both T8stefinB and *Tb*stefinB, 93.81 % between *Tz*stefinB and *Tps*stefinB and 87.63 % between *Tz*stefinB and *Ts*stefinB. The sequences are shown to have the glycine residues as well as the Q-x-V-x-G motif (Fig. 3.3), both of which are important in the binding of these inhibitors to C1 cysteine proteases (Section 1.5.2).

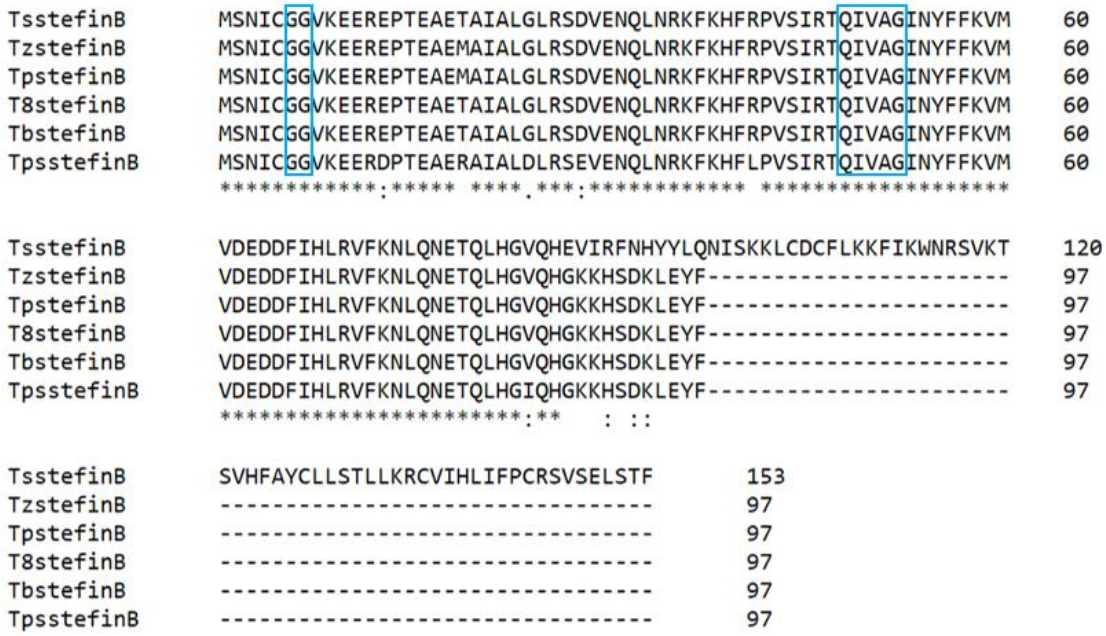

Figure 3.3: ClustalO multiple sequence alignment of *Trichinella* stefin B amino acid sequences. Amino acid sequences were obtained in Fasta format from NCBI (www.ncbi.nlm.nih.gov) and aligned with Clustal Omega (https://www.ebi.ac.uk/Tools/msa/clustalo/). The *Tz*stefinB amino acid sequence was aligned with stefin B sequences from *Trichinella spiralis* (XP_003379766.1), *Trichinella papuae* (KRZ69001.1), *Trichinella* genotype T8 (KRZ83534.1), *Trichinella britovi* (KRY54242.1), and *Trichinella pseudospiralis* (KRZ14801.1). The conserved N-terminal glycine residues and Q-x-V-x-G motif are in blue bloxes.

To demonstrate the potential of *Tz*stefinB as a target antigen in the same manner as with *Tz*CATB (Fig. 3.2), the *Tz*stefinB amino acid sequence was additionally aligned (Fig. 3.4) with that of human stefin B (AAF44059.1) with which it had a sequence identity of 41.05 %, indicating a low level of similarity.

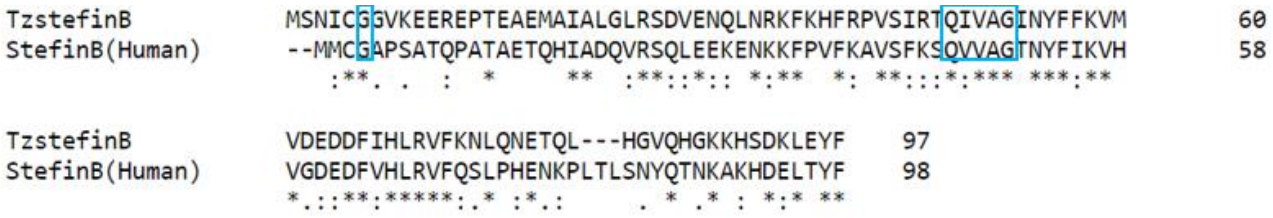

Figure 3.4: ClustalO pairwise alignment of the *Tz*stefinB and human stefin B amino acid sequences. Amino acid sequences were obtained in Fasta format from NCBI (www.ncbi.nlm.nih.gov) and aligned with Clustal Omega (https://www.ebi.ac.uk/Tools/msa/clustalo/). The conserved N-terminal glycine residues and Q-x-V-x-G motif are in blue bloxes.

The biophysical properties of *Tz*CATB and *Tz*stefinB were estimated using the Expasy compute pI and molecular weight tool (www.expasy.org). A pI of 7.43 and molecular weight of 37.85 kDa was estimated for *Tz*CATB, and a pI of 6.97 and molecular weight of 11.32 kDa was estimated for *Tz*stefinB.

3.2 PCR amplification of the *Tz*stefinB gene from *T. zimbabwensis* cDNA and cloning into the pMD-19 simple T-Vector

Specific gene primers were used to amplify the *Tz*stefinB gene sequence from cDNA synthesised from *T. zimbabwensis* RNA. The gene was amplified at approximately 290 bp (Fig. 3.5A) which is the expected size. The *Tz*stefinB gene amplicon was ligated to pMD-19 simple (2693 bp) and the ligation mixture transformed into competent *E. coli* JM109 cells. Blue-white screening was used to select recombinant colonies and the presence of the *Tz*stefinB gene insert was ascertained using colony PCR. An amplicon of the correct size (~290 bp) was obtained for both of the selected recombinant colonies (Fig. 3.5B).

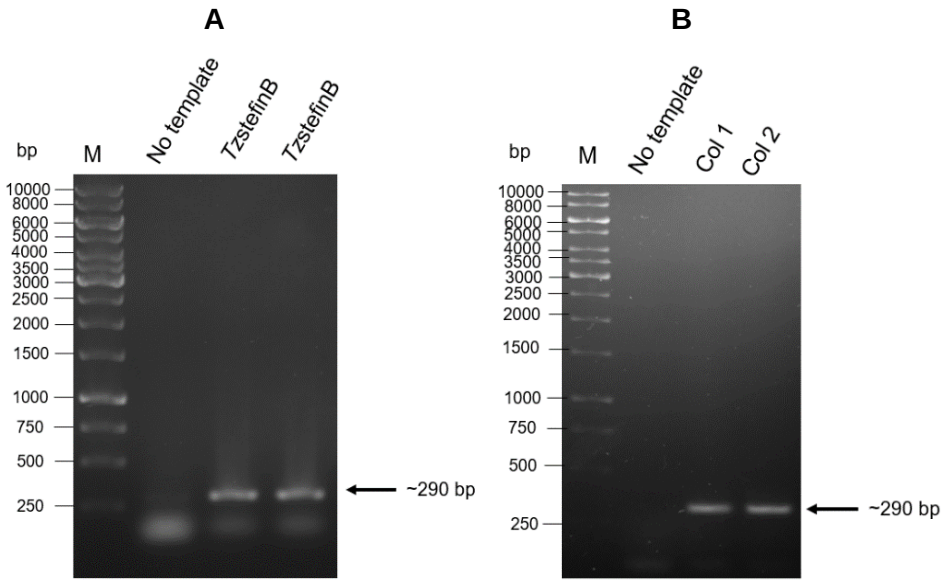

Figure 3.5: Agarose gel analysis of (A) PCR amplification of the *Tz*stefinB gene sequence from *T. zimbabwensis* and (B) colony PCR amplicons from recombinant pMD-19- *Tz*stefinB colonies. Amplicons from PCR reactions were run on a 1 % (w/v) agarose gel alongside a no template control. M: O'GeneRuler$_{TM}$ 1kb DNA ladder. Amplicons and their sizes are indicated by arrows.

3.3 Subcloning of the *Tz*CATB gene into the pET-28a, pCold-1 and pCold-TF expression vectors and the *Tz*stefinB gene into the pET-28a expression vector

The *Tz*CATB gene was synthesised by Thermo Fisher Scientific within the cloning vector pMA-RQ allowing for easy and efficient subcloning for protein expression. The *Tz*CATB gene was subcloned into the pET-28a and pCold-1 expression vectors and the *Tz*stefinB gene (Section 3.2) was subcloned into the pET-28a expression vector to allow recombinant expression of these proteins. Isolated pMA-RQ-*Tz*CATB and pET-28a were restriction digested with BamHI and XhoI, and pCold-1 was restriction digested with BamHI and SalI. Isolated pMD-19-*Tz*stefinB and pET-28a were restriction digested with EcoRI and XhoI restriction enzymes.

This was done to produce compatible ends for ligation. Restriction digestion products were run on agarose gels (Fig. 3.6). Double restriction digestion of pMA-RQ-*Tz*CATB by BamHI and XhoI (Fig. 3.6A) produced a band at the expected size of the *Tz*CATB gene (1000 bp) and both BamHI and XhoI restriction digestions of pET-28a produced single bands at approximately the expected size of this vector (5370 bp). Restriction digestion of pCold-1 by both BamHI and SalI (Fig. 3.6B) produced single bands at approximately the expected size of the vector (4400 bp), with the additional bands present in the double digest lane representing the uncut vector, and the previous gene insert removed by restriction digestion. Restriction digestions of pCold-TF by both BamHI and SalI (Fig. 3.6C) produced single bands, however this vector appeared at higher molecular weight than expected (approximately 8000 bp). Double restriction digestion of pMD-19-*Tz*stefinB by EcoRI and XhoI (Fig. 3.6D) produced a band at approximately the expected size of the *Tz*stefinB gene (290 bp) and both EcoRI and XhoI restriction digestions of pET-28a produced single bands at approximately the expected size of this vector (5370 bp).

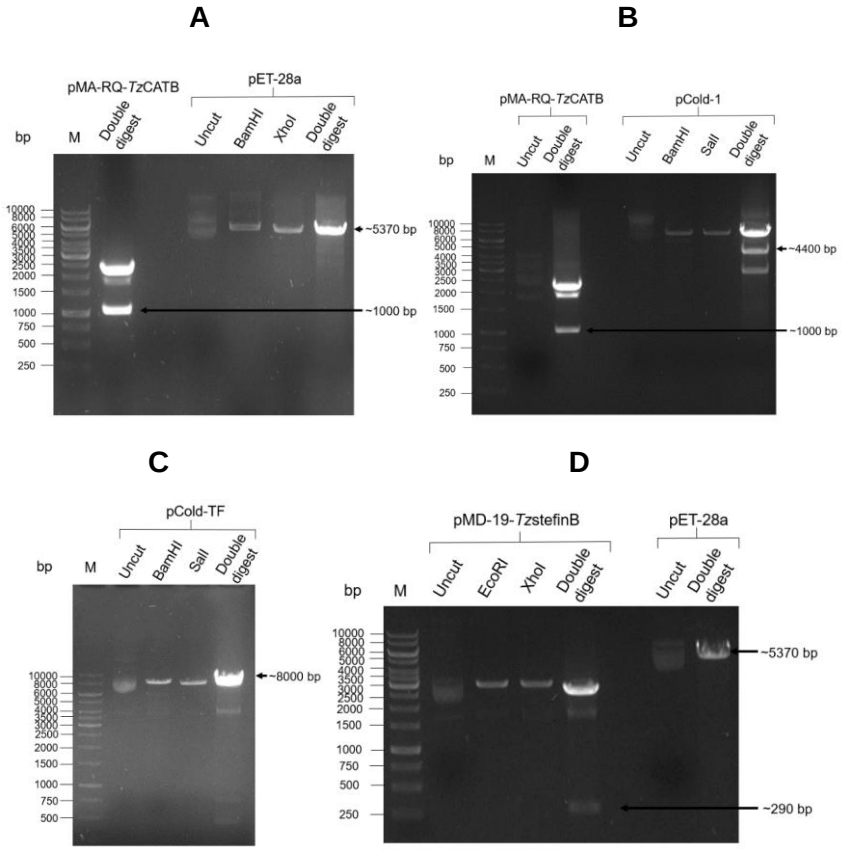

Figure 3.6: Agarose gel analysis of products from restriction digestions of (A) pMA-RQ-*Tz*CATB and pET-28a, (B) pMA-RQ-*Tz*CATB and pCold-1, (C) pCold-TF, and (D) pMD-19-*Tz*stefinB and pET-28a. Plasmid samples were restriction digested at 37 ºC for 1 h and run on 1 % (w/v) agarose gels. Arrows indicate the position and sizes of expression vectors and gene inserts.

After ligating the *Tz*CATB and *Tz*stefinB genes to expression vectors, these constructs were transformed into *E. coli* BL21 DE3 cells and recombinant colonies selected with blue-white screening. The presence of the *Tz*CATB gene was ascertained using restriction digestions whilst the presence of the *Tz*stefinB gene in colonies was ascertained using colony PCR. Restriction digestion of pET-28a-*Tz*CATB clones by BamHI and XhoI produced bands at the expected size of the *Tz*CATB gene (1000 bp) and the pET-28a expression vector (5370 bp) in both clones (Fig, 3.7A). Restriction digestion of pCold-1-*Tz*CATB and pCold-TF-*Tz*CATB clones was done with only BamHI. This is because ligation of the compatible ends from restriction digestion by XhoI and SalI produces a restriction site that is not recognised by either enzyme. However, restriction digestion with one enzyme will reveal the total size of the constructs within clones, revealing the size of the gene insert. Restriction digestion of pCold-1-*Tz*CATB (Fig. 3.7B) produced a band at approximately the expected size of the *Tz*CATB gene (1000 bp) and the pCold-1 expression vector (4400 bp) in all four clones (5400 bp). Restriction digestion of pCold-TF-*Tz*CATB (Fig. 3.7C) produced a band at approximately the expected size of the *Tz*CATB gene (1000 bp) and the pCold-TF vector (8000 bp) in three of four clones (Fig. 3.7C) with the exception of clone 2 in which multiple anomalous bands are observed.

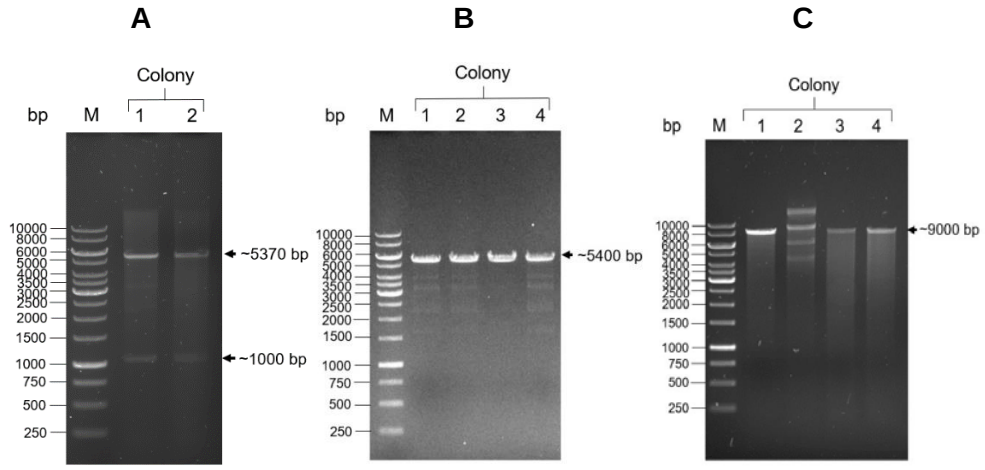

Figure 3.7: Agarose gel analysis of restriction digestions of (A) pET-28a-*Tz*CATB, (B) pCold-1-*Tz*CATB and (C) pCold-TF-*Tz*CATB clones. Plasmid samples were restriction digested at 37 ºC for 1 h and run on 1 % (w/v) agarose gels. Arrows indicate the position and sizes of expression vectors and gene inserts.

Colony PCR using pET-28a-*Tz*stefinB clones produced a band at the expected size of the *Tz*stefinB gene (290 bp) in all eight clones (Fig. 3.8). Results from restriction digests and colony PCR indicated that clones contained the desired constructs with the desired gene inserts for recombinant protein expression.

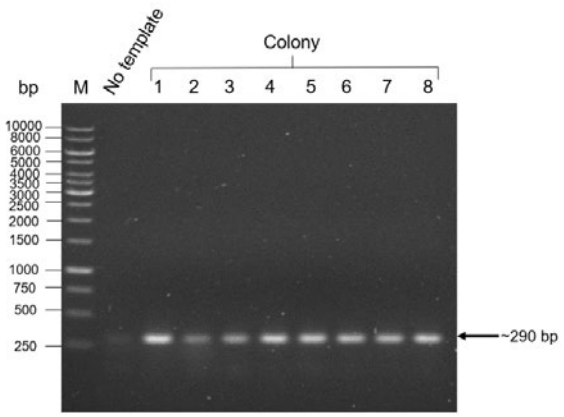

Figure 3.8: Agarose gel analysis of Colony PCR amplicons from pET-28a-*Tz*stefinB colonies. Colony PCR amplicons were run on a 1 % (w/v) agarose gel. Arrows indicate the position and size of the *Tz*stefinB gene insert.

3.4 Recombinant expression of *Tz*CATB

The pET-28a-*Tz*CATB (clones 1 and 2), pCold-1- *Tz*CATB (clones 3 and 4: now referred to as pCold-1- *Tz*CATB clones 1 and 2) and pCold-TF-*Tz*CATB (clones 1 and 4: now referred to as pCold-TF-*Tz*CATB clones 1 and 2) clones (Fig. 3.7) were used for recombinant protein expression of *Tz*CATB. Expression was induced with 1 mM IPTG (or 0.1 mM for pCold-TF). This produced a large band at ~43 kDa as insoluble protein upon expression from both pET-28a clones (Fig. 3.9A). This correlates with the expected size of *Tz*CATB with the attached His-tags. Western blotting with anti-His antibodies against samples from clone 2 confirmed that the recombinant *Tz*CATB expressed from pET-28a possessed the desired His-tags for Nickel affinity purification (Fig. 3.9B).

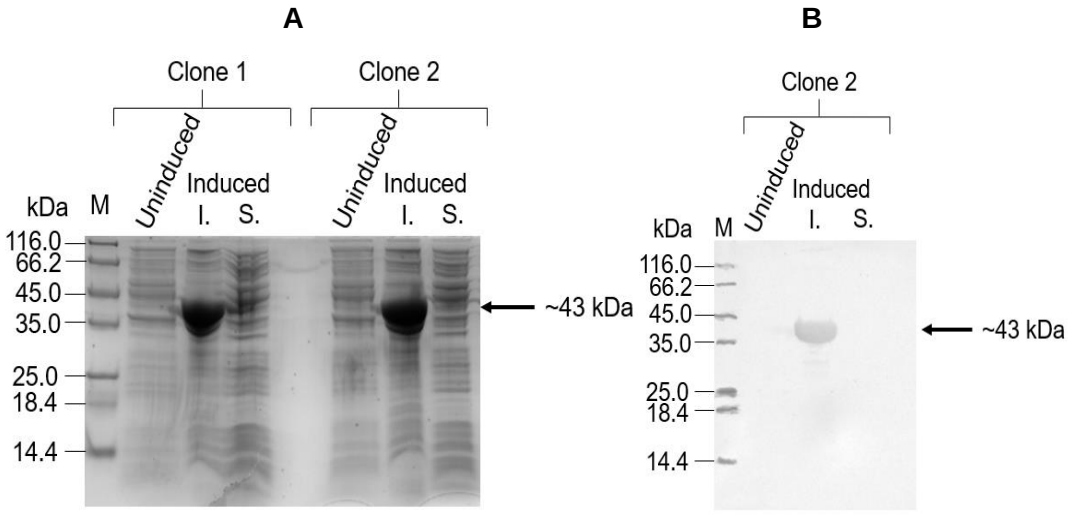

Figure 3.9: SDS-PAGE and western blotting analyses of recombinant expression of *Tz*CATB in pET-28a. (A) 10 % Reducing tris-tricine SDS-PAGE gel run with samples from recombinant expression of *Tz*CATB in pET-28a. I: insoluble fraction; S: soluble fraction. **(B)** Western blotting of pET-28a clone 2 expression samples. Primary antibody: mouse anti-His antibodies (1:5000); secondary antibody: goat anti-mouse HRPO-conjugate (1:5000); chromogenic substrate: 4- chloro-1 naphthol. Arrows indicate the position and size of expressed *Tz*CATB.

Expression from both pCold-1 clones also produced a distinct band in the insoluble fraction (Fig. 3.10A) but at ~42kDa, correlating with the expected size of *Tz*CATB with a single His-tag. Western blotting with anti-His antibodies against samples from clone 2 confirmed that the recombinant *Tz*CATB expressed from pCold-1 possessed the desired His-tag for Nickel affinity purification (Fig. 3.10B).

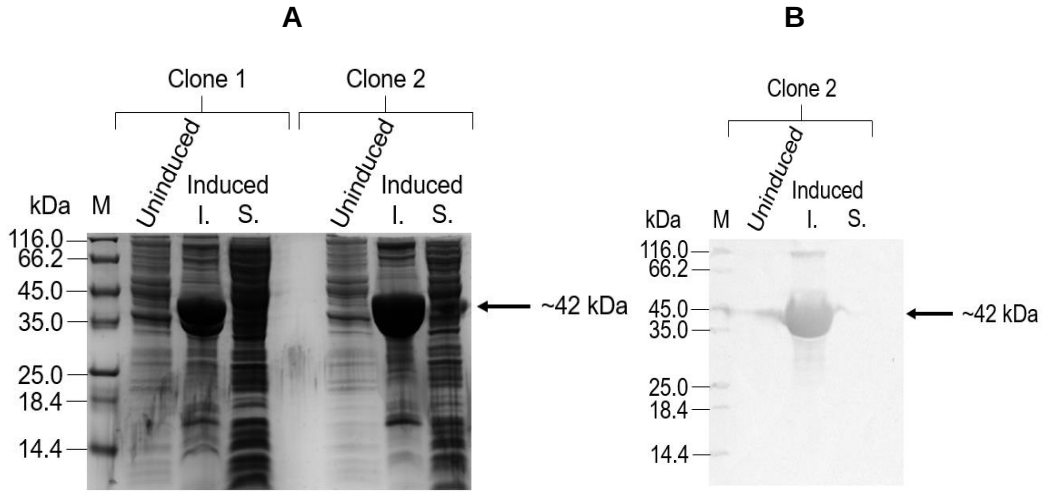

Figure 3.10: SDS-PAGE and western blotting analyses of recombinant expression of *Tz*CATB in pCold-1. (A) 10 % Reducing tris-tricine SDS-PAGE gel run with samples from recombinant expression of *Tz*CATB in pCold-1. I: insoluble fraction; S: soluble fraction. **(B)** Western blotting of pCold-1 (clone 2) expression samples. Primary antibody: mouse anti-His antibodies (1:5000); secondary antibody: goat anti-mouse HRPO-conjugate (1:5000); chromogenic substrate: 4- chloro-1 naphthol. Arrows indicate the position and size of expressed *Tz*CATB.

Expression from pCold-TF yielded a large protein band in both the insoluble and soluble fractions of clone 2 but a less distinct band in clone 1 (Fig. 3.11A). This band was at ~90 kDa, correlating with the expected size of *Tz*CATB with the attached Trigger Factor fusion protein and His-tag. Western blotting with anti-His antibodies against samples from clone 2 confirmed that the recombinant *Tz*CATB expressed from pCold-TF possessed the desired His-tag for Nickel affinity purification (Fig. 3.11B).

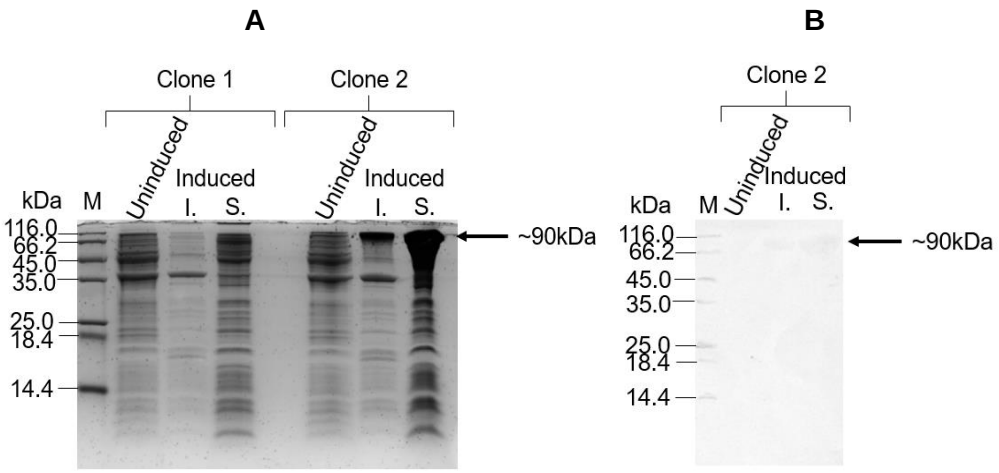

Figure 3.11: SDS-PAGE and western blotting analyses of recombinant expression of *Tz*CATB in pCold-TF. (A) 10 % Reducing tris-tricine SDS-PAGE gel run with samples from recombinant expression of *Tz*CATB in pCold-TF. I: insoluble fraction; S: soluble fraction. **(B)** Western blotting of pCold-TF clone 2 expression samples. Primary antibody: mouse anti-His antibodies (1:5000); secondary antibody: goat anti-mouse HRPO-conjugate (1:5000); chromogenic substrate: 4- chloro-1 naphthol. Arrows indicate the position and size of expressed *Tz*CATB.

3.5 Recombinant expression of *Tz*stefinB

The pET-28a-*Tz*stefinB (clones 4 and 7: now referred to as clones 1 and 2) clones (Fig. 3.8) were used for recombinant protein expression of *Tz*stefinB. Expression was induced with 1 mM IPTG which produced a band at ~16 kDa in both clones (Fig. 3.12A), the expected size of the His-tagged *Tz*stefinB. The protein was expressed in both the insoluble and soluble fractions. Western blotting with anti-His antibodies against samples from clone 2 confirmed that the protein at 16 kDa possessed the desired His-tag for affinity purification (Fig. 3.12B).

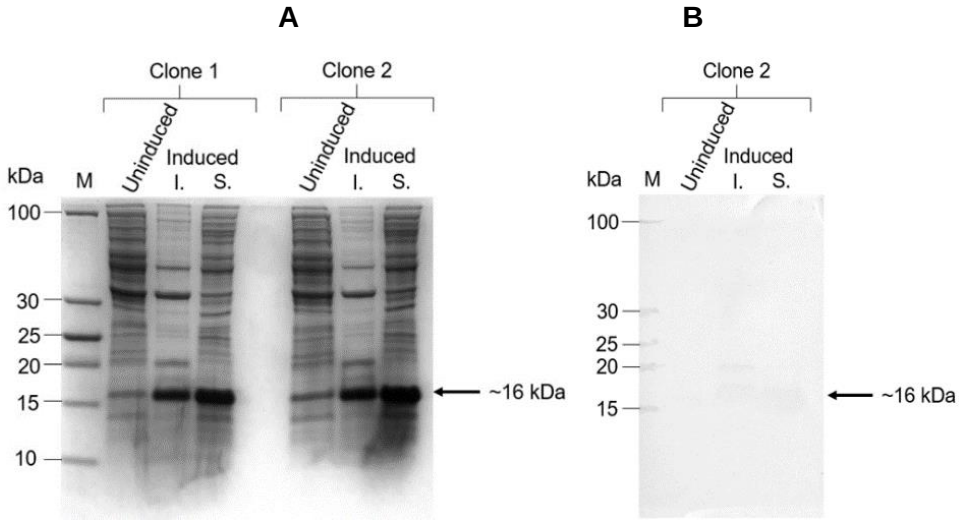

Figure 3.12: SDS-PAGE and western blotting analyses of recombinant expression of *Tz*stefinB in pET-28a. (A) 10 % ris-tricine SDS-PAGE gel run with samples from recombinant expression in two clones. I: insoluble fraction; S: soluble fraction. **(B)** Western blotting of expression samples from clone 2. Primary antibody: mouse anti-His antibodies (1:5000); secondary antibody: goat anti-mouse HRPO-conjugate (1:5000); chromogenic substrate: 4- chloro-1 naphthol. Arrows indicate the position and size of expressed *Tz*stefinB.

3.6 Sarkosyl solubilisation and Ni-IMAC purification of *Tz*CATB expressed in pET-28a and pCold-1

Expression of *Tz*CATB in pET-28a and pCold-1 produced insoluble protein (Section 3.4) which was solubilised using sarkosyl and SDS. Solubilisation of *Tz*CATB from both vectors was successful (Fig. 3.13A and 3.14A). Solubilised protein was then purified using Ni-IMAC. Following binding, unbound fractions were collected from resins, non-specific binders washed off, and bound protein eluted with 250 mM imidazole. From both pET-28a and pCold-1, *Tz*CATB eluted from the column with a small amount of contaminating protein at high and low molecular weight (Fig. 3.13B and 3.14B). Eluted *Tz*CATB-pET28a and *Tz*CATB-pCold-1 fractions were each pooled and buffer exchanged into PBS for subsequent experiments.

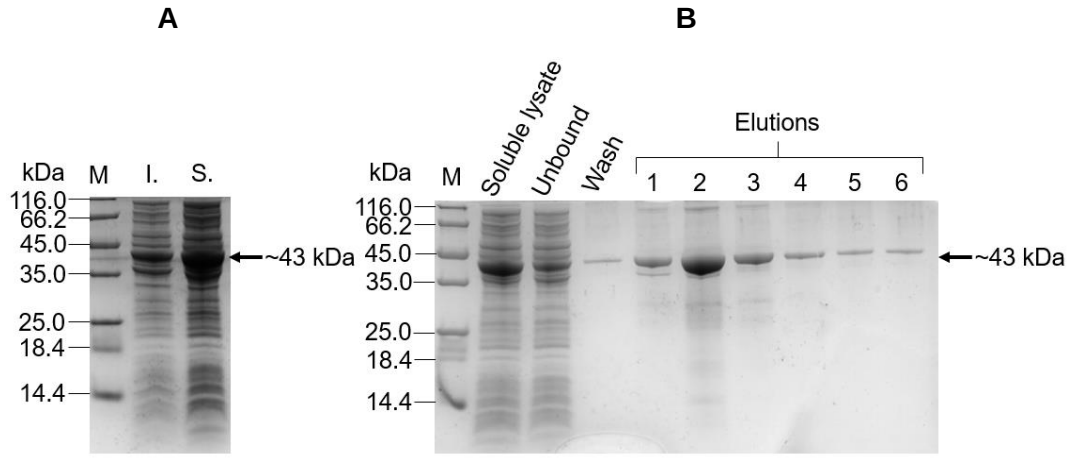

Figure 3.13: SDS-PAGE analysis of (A) sarkosyl solubilisation and (B) Ni-IMAC purification of *Tz*CATB expressed in pET-28a. Samples were run on a 10 % reducing tris-tricine SDS-PAGE. M: molecular weight marker. I: insoluble fraction; S: soluble fraction. Wash fraction refers to the final wash fraction collected before eluting. Arrows indicate the position and size of *Tz*CATB.

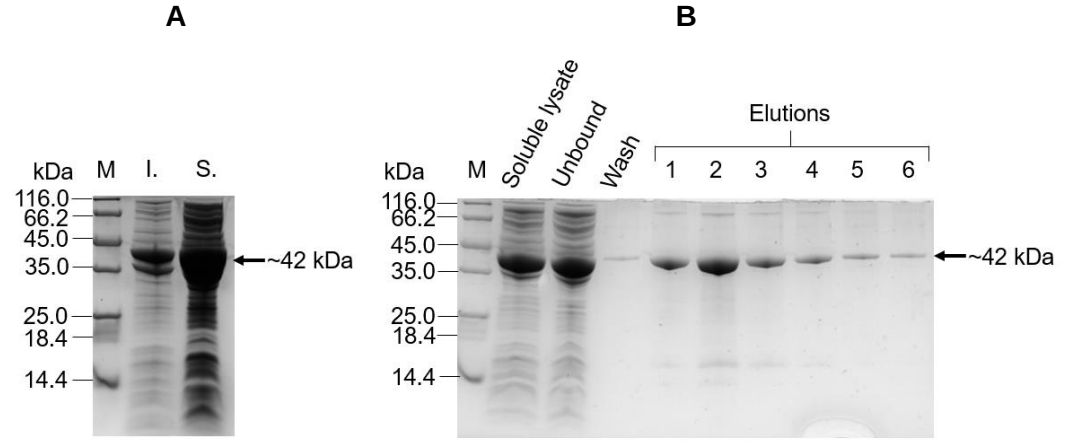

Figure 3.14: SDS-PAGE analysis of (A) sarkosyl solubilisation and (B) Ni-IMAC purification of *Tz*CATB expressed in pCold-1. Samples were run on a 10 % reducing tris-tricine SDS-PAGE. M: molecular weight marker. I: insoluble fraction; S: soluble fraction. Wash fraction refers to the final wash fraction collected before eluting. Arrows indicate the position and size of *Tz*CATB.

3.7 Immuno-affinity purification and thrombin cleavage of *Tz*CATB expressed in pCold-TF

The soluble lysate obtained from expression of *Tz*CATB in the pCold-TF expression vector (Section 3.4) was purified with immunoaffinity chromatography using chicken anti-*Tz*CATB IgY coupled to UltraLink™ Hydrazide Resin. The recombinant *Tz*CATB was not obtained in the fractions eluted from the column using low pH buffer, suggesting that binding to the immunoaffinity column was not effective (Fig. 3.15A), however a significant amount of *Tz*CATB was obtained in the wash fractions with a small amount of protein contamination. Wash fractions were pooled for subsequent thrombin digestion to remove the Trigger factor fusion protein. Incubation of *Tz*CATB-TF with thrombin for 24 h efficiently released the Trigger Factor fusion protein as evidenced by a protein band at approximately 51 kDa on reducing tris-tricine SDS-PAGE, and *Tz*CATB at approximately 39 kDa (Fig. 3.15B).

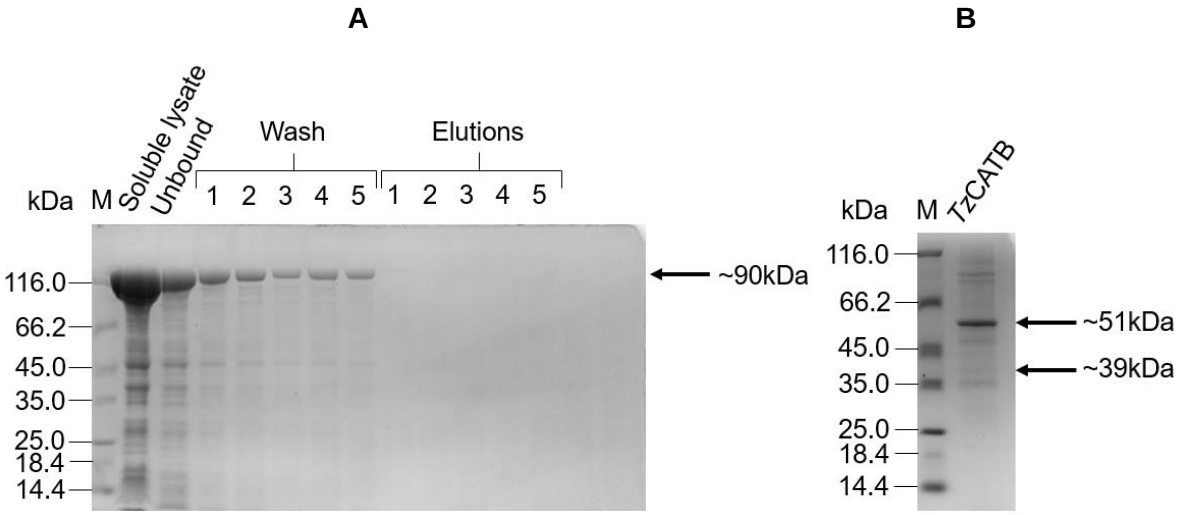

Figure 3.15: SDS-PAGE analysis of (A) immunoaffinity purification of *Tz*CATB expressed in pCold-TF and (B) thrombin cleavage products. Samples were run on a 10 % reducing tris-tricine SDS-PAGE. M: molecular weight marker. Arrows indicate the position and size of *Tz*CATB as well as the trigger factor fusion protein.

3.8 Purification of *Tz*stefinB using Ni-IMAC

The soluble lysate from expression of *Tz*stefinB in clone 4 (Section 3.5) was applied to a Ni-NTA column to purify *Tz*stefinB. The His-tagged protein was allowed to bind the column, and after washing off non-specific contaminating proteins, the bound protein was eluted with a high concentration of imidazole. The ~16 kDa His-tagged protein was eluted from the column along with one lower molecular weight and a few higher molecular weight contaminating proteins represented by faint bands in the first elution fraction analysed on the tris-tricine SDS-PAGE

gel (Fig. 3.16). Elution fractions 1-7 were pooled and buffer exchanged into PBS for subsequent experiments.

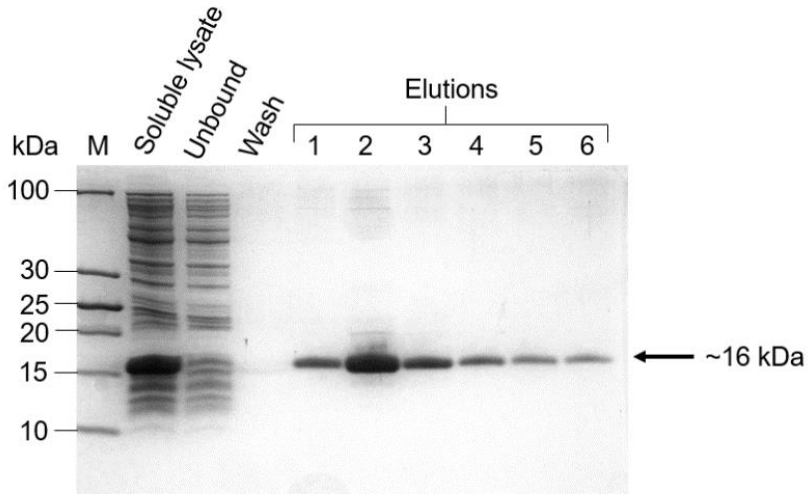

Figure 3.16: SDS-PAGE analysis of Ni-IMAC purification of *Tz*stefinB expressed in pET-28a. Samples were run on a 10 % reducing tris-tricine SDS-PAGE. M: molecular weight marker. Wash fraction refers to the final wash fraction collected before eluting with imidazole (250 mM). The arrow indicates the position and size of *Tz*stefinB.

3.9 Production of anti-*Tz*stefinB antibodies in chickens

Two chickens were immunised with recombinant *Tz*stefinB and IgY antibodies isolated from the yolks of eggs collected from each chicken across a 12-week period. The production of antibodies was monitored using an indirect ELISA with r*Tz*stefinB as the antigen. In both chickens, a significant increase in anti-*Tz*stefinB-IgY was observed from week 6 and IgY production peaked from week 7 onwards, with a greater ELISA signal produced from week 6 by chicken 1 than that produced by chicken 2 (Fig. 3.17A). Anti-*Tz*stefinB-IgY produced between weeks 6 and12 from each chicken were pooled separately for subsequent experiments. To determine a suitable antibody concentration required for western blotting, an ELISA as conducted on each of the two pools of IgY (from chicken 1 and chicken 2) over a range of antibody concentrations (0.1-20 µg/mL). Chicken 1 pooled antibodies produced a significant increase in signal at 1 µg/mL with a slower increase up to 20 µg/mL (Fig. 3.17B). Chicken 2 pooled antibodies produced a significant signal from 10 µg/mL upwards. The results suggest that using the pooled antibodies from chicken 1 may be more effective, and that and antibody concentration as low as 1 µg/mL should produce a suitable signal on a western blot.

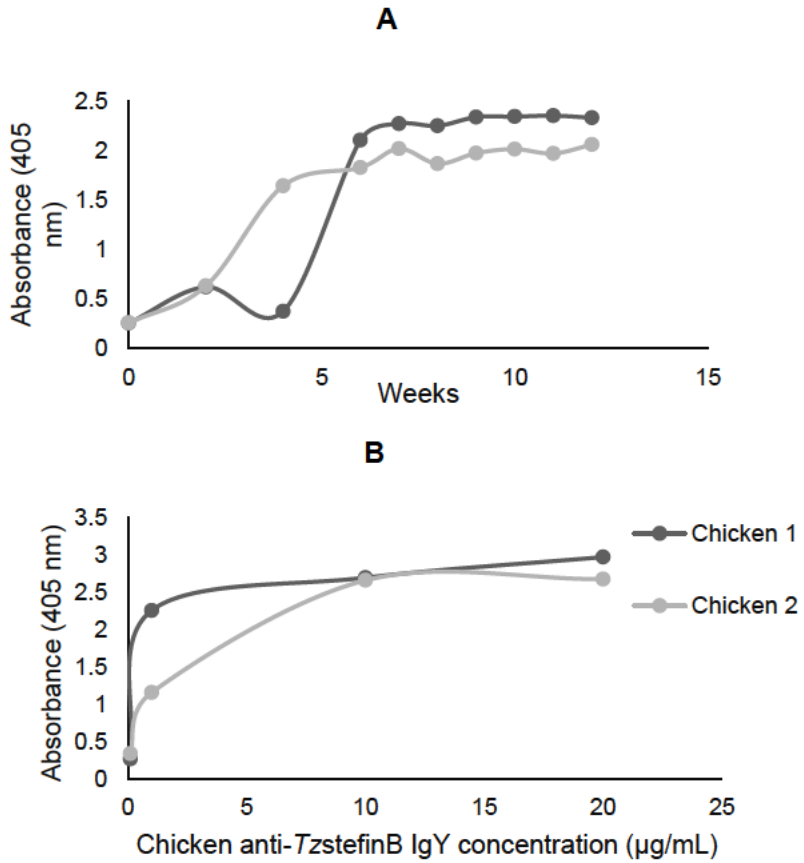

Figure 3.17: Analysis of chicken anti-*Tz*stefinB IgY production using an ELISA. (A): Detection of *Tz*stefinB (coated at 1 µg/mL) using chicken anti-*Tz*stefinB IgY obtained throughout immunisation period. **(B):** Detection of *Tz*stefinB (coated at 1 µg/mL) using week 6-12 pool from each chicken (0,1, 1, 10 and 20 µg/mL). Rabbit anti-chicken IgY HRPO (1:5000) was used as secondary antibody in ELISA tests.

3.10 Detection of *Tz*CATB and *Tz*stefinB using western blotting

Western blotting with anti-*Tz*CATB IgY, produced in a previous study, was used to confirm the identity of the *Tz*CATB recombinantly expressed in the present study. Recognition of recombinant *Tz*stefinB by chicken anti-*Tz*stefinB IgY in an ELISA (Section 3.9) was also confirmed by western blotting. Recombinant *Tz*CATB expressed in pCold-TF was detected by anti-*Tz*CATB IgY antibodies at a concentration of 5 µg/mL (Fig. 3.18B), and additionally was shown not to be detected by anti-human cathepsin B antibodies (Fig. 3.18C). Recombinant *Tz*stefinB was detected by anti-*Tz*stefinB IgY at 1 µg/mL (Fig. 3.19B) confirming this to be an effective concentration for use in western blots (Section 3.9). These antibodies were shown not to recognise stefin B isolated from sheep liver in a previous study, and vice-versa, chicken anti-sheep liver stefin B IgY antibodies did not detect recombinant *Tz*stefinB (Fig. 3.19C). Anti-sheep stefin B antibodies, however, did not detect sheep stefin B either, suggesting that detection with these antibodies was ineffective.

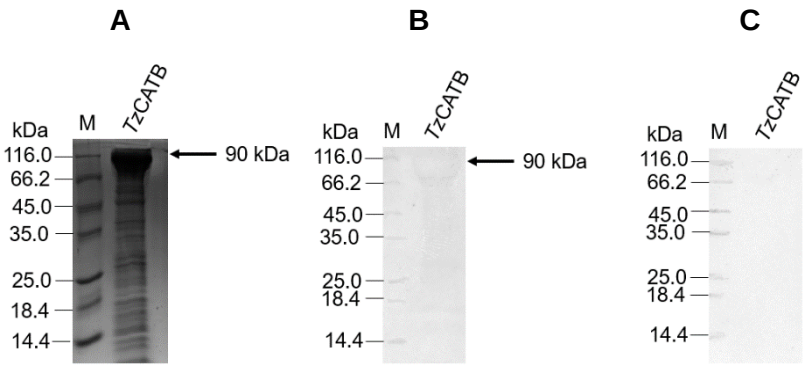

Figure 3.18: Recombinant *Tz*CATB (A) electrophoresed on a 10 % reducing tris-tricine SDS-PAGE gel, and used in western blotting with (B) anti-*Tz*CATB antibodies and (C) anti-human cathepsin B antibodies. On each gel, 10 µg of protein was loaded. **(B):** Primary antibody: chicken anti-*Tz*CATB IgY (5 µg/mL); secondary antibody: rabbit anti-chicken HRPO-conjugate (1:5000). **(C):** Primary antibody: rabbit anti-human cathepsin B IgG (1:1000); secondary antibody: goat anti-rabbit HRPO-conjugate (1:2500). Arrows indicate the position and size of *Tz*CATB.

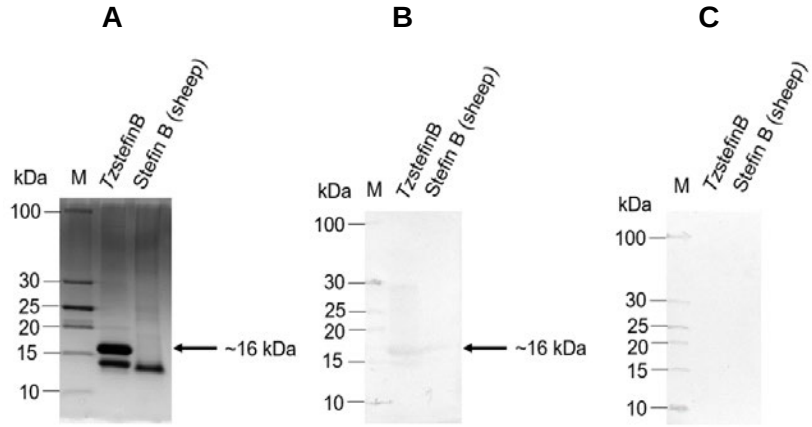

Figure 3.19: Recombinant *Tz*stefinB and stefin B from sheep (A) electrophoresed on a 10 % reducing tris-tricine SDS-PAGE gel, and used in western blotting with (B) anti-*Tz*stefinB antibodies and (C) anti-sheep stefin B antibodies. On each gel, 10 µg of protein was loaded. **(B):** Primary antibody: chicken anti-*Tz*stefinB IgY (1 µg/mL); secondary antibody: rabbit anti-chicken HRPO-conjugate (1:5000). **(C):** Primary antibody: chicken anti-sheep stefin B IgY (5 µg/mL); secondary antibody: rabbit anti-chicken HRPO-conjugate (1:5000). Arrows indicate the position and size of *Tz*CATB.

3.11 Detection of *Tz*CATB activity

Hydrolysis of Z-Arg-Arg-AMC (20 µM) by autocatalysed *Tz*CATB produced an increase in fluorescence of approximately 5000 Arbitrary Fluorescence Units from baseline (result not shown), however this activity was not inhibited by E-64 and was only present at pH 8.0. Digestion of Z-Arg-Arg-AMC by thrombin, at the same concentration as calculated after dilution of the thrombin-cleaved *Tz*CATB preparation (if thrombin removal was not successful), was tested and found to produce a similar increase in fluorescence at pH 8.0. Gelatin-zymography analysis only detected proteolytic digestion of gelatin by a control sample of papain and not by *Tz*CATB (result not shown), affirming that there was no *Tz*CATB activity

present in this preparation. Sequencing of the pCold-TF-*Tz*CATB construct (Appendix B) indicated that the incorrect gene sequence was present, despite western blotting detecting *Tz*CATB in this preparation (Section 3.10).

3.12 Inhibition of cysteine protease activity with *Tz*stefinB

3.12.1 Active site titration of papain and *Tc*CATL

The concentration of active papain and *Tc*CATL was determined using E-64 titration allowing for the proportion of active protease to be reported. The titrations showed that 50 % of papain was active (Fig. 3.20A) and that 80 % of *Tc*CATL was active (Fig. 3.20B). The concentration of these proteases in subsequent results is reported in terms of the active concentration.

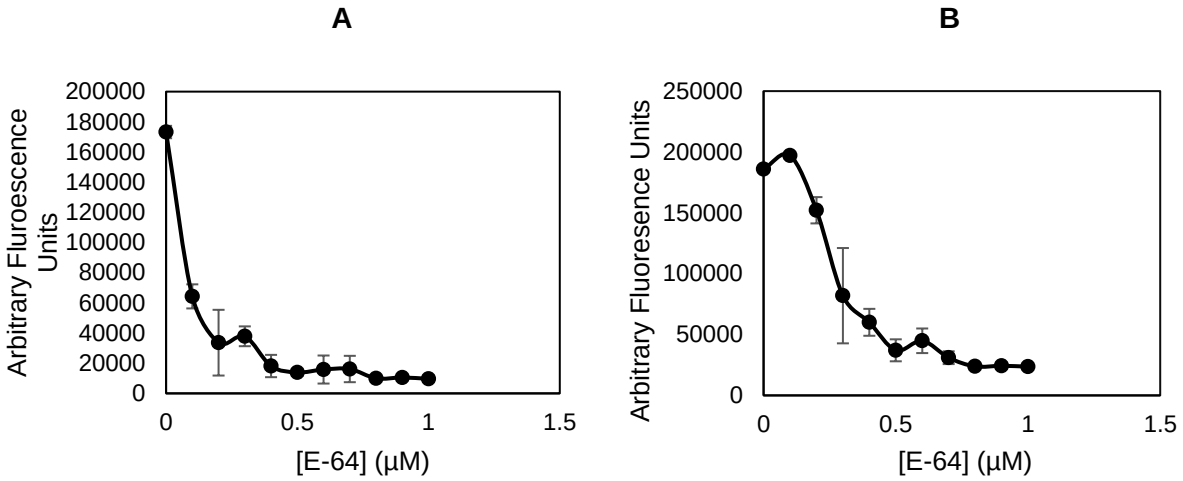

Figure 3.20: Active site titration curves of (A) papain and (B) *Tc*CATL. In triplicate, papain (0.2 μM) and *Tc*CATL (1 μM) were each incubated with E-64 (0.1-1.0 μM) for 15 min and then used to digest Z-Phe-Arg-AMC for 15 min. Fluorescence was measured with $Ex_{355\ nm}$ and $Em_{460\ nm}$.

3.12.2 Titration of papain and *Tc*CATL with *Tz*stefinB

To determine if the recombinantly expressed *Tz*stefinB inhibited cysteine protease activity and to determine the lowest concentration that can effectively inhibit cysteine protease activity, the cysteine proteases papain from papaya latex and cathepsin L from *Trypanosoma congolense* (*Tc*CATL) were titrated with 0.1 – 1 μM of *Tz*stefinB and used to hydrolyse Z-Phe-Arg-AMC. Fluorescence measured was represented as a percentage of that obtained in the absence of inhibitor for each protease. *Tz*stefinB at a concentration of 0.1 μM was observed to inhibit papain by approximately 25 % (Fig. 3.21A), and this residual activity sharply decreased with increasing concentrations of *Tz*stefinB until reaching 0.6 μM at which papain was inhibited by approximately 85 %. Inhibition above this concentration shows a minimal increase with maximal inhibition reached at 0.9 μM of *Tz*stefinB which inhibited papain by approximately 90

%. The equation from the trendline of the graph (Fig. 3.21A) was used to calculate the IC50 of *Tz*stefinB for papain, which was 2.60 µM. *Tz*stefinB at a concentration of 0.1 µM was shown to inhibit *Tc*CATL by also approximately 25 % (Fig. 3.21B), inhibition increases greatly with approximately 75 % inhibition at 0.2 µM after which it begins to plateaux, with maximal inhibition at 0.5 µM which inhibited *Tc*CATL by approximately 90 %. The IC50 of *Tz*stefinB for *Tc*CATL from the equation of the trendline (Fig. 3.21B) was calculated to be 1.49 µM.

A

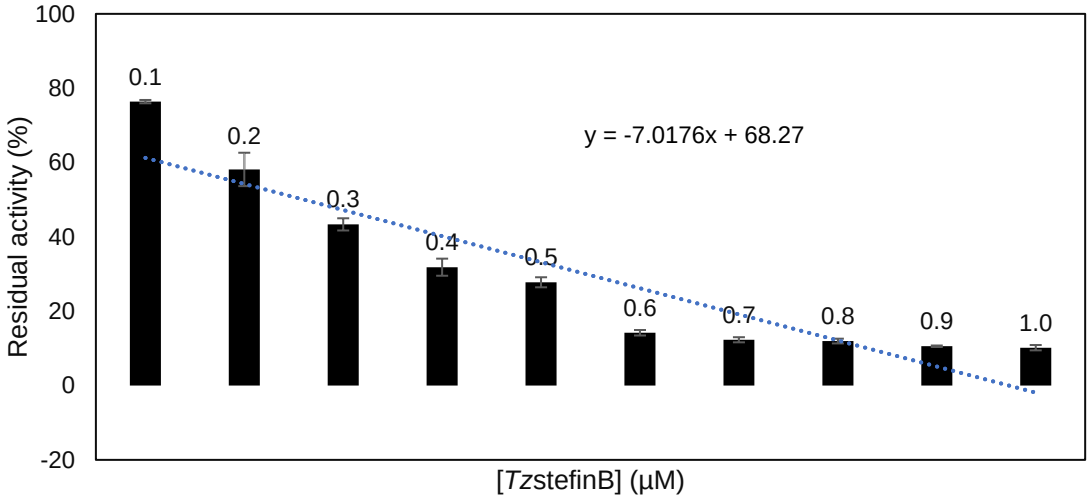

B

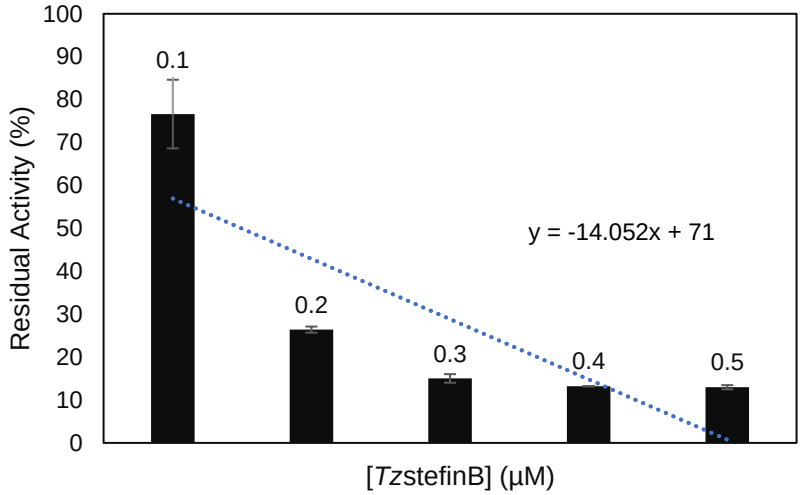

Figure 3.21: Inhibition of (A) papain and (B) TcCATL with *Tz*stefinB. In triplicate, papain (0.1 µM) and *Tc*CATL (0.8 µM) were each incubated with *Tz*stefinB at 37 ºC for 5 min, following which they were used to digest Z-Phe-Arg-AMC at 37 ºC for 15 min and fluorescence measured ($Ex_{355\ nm}$ and $Em_{460\ nm}$).

3.12.3 Optimal pH for *Tz*stefinB inhibitory activity

To determine the optimal pH for inhibition of papain by *Tz*stefinB, the inhibitor was pre-incubated in AMT buffers from pH 5 to 9 and then used (at 1 µM) to inhibit papain hydrolysis of Z-Phe-Arg-AMC. Pre-incubation from pH 5 to 9 was shown to maintain inhibitory activity of *Tz*stefinB (Fig. 3.22), suggesting that the inhibitor is stable across this pH range. Negligible difference was observed in the amount of inhibition obtained between different pH levels.

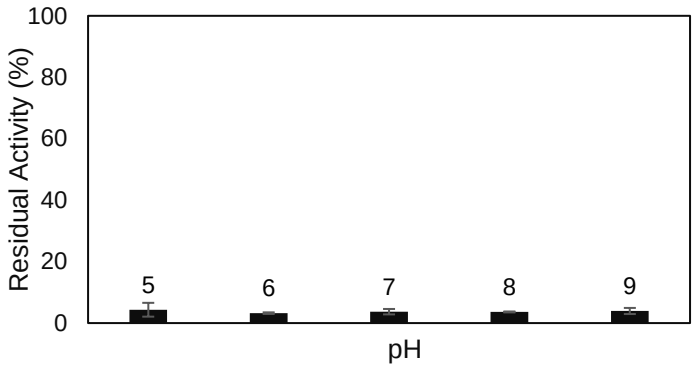

Figure 3.22: Inhibition of papain with *Tz*stefinB pre-incubated at different pH levels. Prior to adding 1 µM *Tz*stefinB to papain and conducting Z-Phe-Arg-AMC hydrolysis in triplicate, *Tz*stefinB was incubated for 30 min in AMT buffer from pH 5 – 9.

3.12.4 Temperature stability of *Tz*stefinB

To determine the temperature stability of *Tz*stefinB, the inhibitor was incubated at 99 ºC for up to 30 min, as well as at RT and 4 ºC for up to 3 weeks, before testing inhibition of papain. Incubation at 99 ºC for 15 min removed the majority of *Tz*stefinB inhibitory activity (Fig. 3.23A), with papain activity only inhibited by approximately 5 %. After 30 min incubation of *Tz*stefin B at 99 ºC, no inhibitory activity remained. Upon storage of *Tz*stefinB at 4 ºC and RT for three weeks, a great deal of variation was observed across results and there appears to be negligible difference between storage at 4 ºC and RT (Fig. 3.23B). Storage of *Tz*stefinB at both 4 ºC and RT for 1 week showed a significant decrease in inhibitory activity from fresh *Tz*stefinB, with papain having 40-50 % of residual activity upon incubation with *Tz*stefinB stored at 4 ºC and approximately 30 % of residual activity upon incubation with *Tz*stefinB stored at RT, as opposed to having less than 10 % of residual activity upon incubation with freshly prepared *Tz*stefinB. Inhibitory activity after storage at these temperatures for 2 and 3 weeks is then observed to be greater, suggesting that the results at 1 week could be subject to error. Upon incubation of papain with *Tz*stefinB stored at 4 ºC and RT for 2 weeks, papain had 10-20 % of residual activity. Following storage of *Tz*stefinB at 4 ºC and RT for 3 weeks, a

significant amount, but not all inhibitory activity of *Tz*stefinB was abolished with papain still having 20-30 % of residual activity.

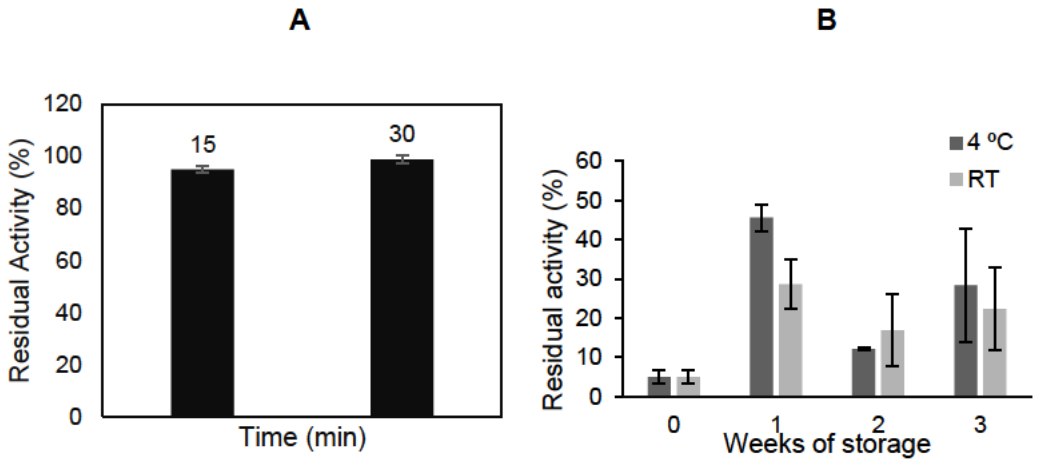

Figure 3.23: Inhibition of papain with *Tz*stefinB pre-incubated at different temperatures. Prior to adding 1 µM *Tz*stefinB to papain and conducting Z-Phe-Arg-AMC hydrolysis in triplicate, *Tz*stefinB was incubated at **(A)** 99 ºC for 15 and 30 min and at **(B)** RT and 4 ºC for 3 weeks.

3.12.5 Reverse zymography detection of *Tz*stefinB inhibitory activity

To further test *Tz*stefinB inhibitory activity, it was used to inhibit papain in a reverse zymogram. This is a gelatin-containing SDS-PAGE which, after renaturation of electrophoresed proteins with Triton X-100, was digested with papain for 16 h and stained to detect inhibition of papain. Inhibition is represented by the retention of stain where gelatin is not digested. Recombinant *Tz*stefinB was detected at 5 µM and more optimally at 10 µM (Fig. 3.24). SBTI, a serine protease inhibitor, was shown not to produce any band of inhibition as expected of this negative control.

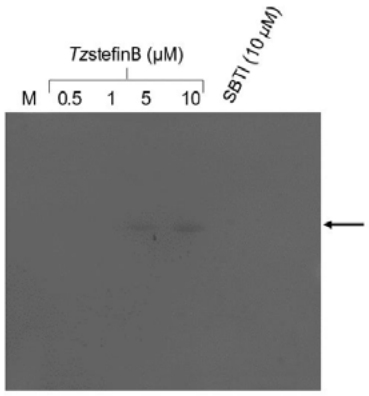

Figure 3.24: Reverse zymography detection of *Tz*stefinB inhibitory activity. Recombinant *Tz*stefinB (10 µL of a 0.5-10 µM solution) was run on a gelatin-containing tris-tricine SDS-PAGE which was incubated with papain (50 µM) at RT for 16 h to digest the gelatin (except at positions where *Tz*stefinB inhibited hydrolysis (arrow). SBTI (10 µM) was included as a negative control. The arrow indicates the position of the *Tz*stefinB inhibitory band.

Chapter Four
General Discussion

Parasitic roundworms of the genus *Trichinella* pose a potential risk to human health, agriculture and economic well-being. The encapsulated *T. spiralis* has received the most attention in research and development, and there is a clear need for advancements to be made in understanding the interaction of non-encapsulated *Trichinella* species with the host immune system, as this has been shown to differ between encapsulated and non-encapsulated species (Asano et al., 2016; Onkoba et al., 2016; Wang et al., 2020). These parasites interact with the immune system in a number of ways, including by means of their ES products (Han et al., 2019) and so differences in the ES products of encapsulated and non-encapsulated members are likely present. The non-encapsulated *T. zimbabwensis* has been reported in reptilian and mammalian hosts across sub-saharan Africa, has been shown to infect primates experimentally and there is currently no diagnostic test for this species of *Trichinella* (La Grange et al., 2010; Ndlovu et al., 2023). Proteases and their inhibitors have been shown to be valuable targets for diagnotics, as well as drug and vaccine development due to their many vital roles in the parasitism of *Trichinella* such as immunomodulation amongst others (Yang et al., 2015; Xu et al., 2017; Yang et al., 2019; Han et al., 2020; Hu et al., 2021; Liu et al., 2022; Song et al., 2022). All of these findings emphasise the importance of conducting research on the ES products of *T. zimbabwensis*, including the characterisation of functional proteins such as the cysteine protease, *Tz*CATB and cysteine protease inhibitor,*Tz*stefinB.

Molecular cloning was implemented in *E. coli* to produce plasmid constructs for recombinant expression of *Tz*CATB and *Tz*stefinB. Agarose gel electrophoresis allowed for observation of successful cloning and subcloning of gene sequences at the approximate expected sizes. Some difficulties in cloning occured in the transformation step, with little or no colonies often being obtained, however optimisation of transformation conditions was effective in obtaining transformations, and these optimal parameters tend to differ with differing sizes of constructs being transformed. Future studies involving transformations should conduct many different transformations at the same with optimised parameters (ratio of ligation mixture:competent cells, incubation times such as the duration of the heat shock step) to obtain successful transformation more quickly. Following sub-cloning into *E. coli* BL21 (DE3) cells, recombinant expression of *Tz*CATB and *Tz*stefinB in the pET-28a expression vector was induced with IPTG. This strain of *E. coli* is widely used for recombinant protein expression due to the deficiency in proteases that may degrade recombinant protein, as well as their high capacity

for T7 polymerase production and in turn, high levels of protein expression (Ratelade et al., 2009). Recombinant expression produced proteins at the expected sizes of His-tagged *Tz*CATB (43 kDa) and *Tz*stefinB (16 kDa) as observed in SDS-PAGE analyses and confirmed by western blotting with anti-His-tag antibodies. While *Tz*stefinB was expressed abundantly in the insoluble and soluble fractions, *Tz*CATB was only expressed in the insoluble fraction. *Tz*CATB was additionally subcloned into, and recombinantly expressed in the pCold-1 expression vector, which utilises the cold shock Protein A promotor to express large amounts of soluble protein at 15 ºC (Bjerga and Williamson, 2015; Sugiki et al., 2017; Li et al., 2018). Expression from this vector produced a band at the expected size of 42 kDa, representing His-tagged *Tz*CATB which was recognised by anti-His-tag antibodies in a western blot. However, this expression system once again produced insoluble *Tz*CATB even upon optimisation of expression parameters (IPTG concentration, culture OD_{600} reached before induction and duration of induction).

Recombinantly expressed proteins were purified using Ni-IMAC which allows purification of His-tagged proteins. This method is rapid and can achieve up to 95 % purity with high yields of protein (Bornhorst and Falke, 2000). Prior to purification, insoluble *Tz*CATB was solubilised using SDS and sarkosyl as per Burgess (2009) and subsequently purified using Ni-IMAC which was also used to purify soluble *Tz*stefinB. Tris-tricine SDS-PAGE analysis indicated that using this method resulted in the purification of a large amount of protein and that there was only minimal contaminating proteins present. Recombinant proteins were exchanged into new buffers and used for downstream analysis, however, recombinant *Tz*CATB (after autocatalysis at pH 5.0 and activation with DTT) had no proteolytic activity against Z-Arg-Arg-AMC. Sequencing of the pET-28a-*Tz*CATB and pCold-1-*Tz*CATB constructs showed the same sequence as shown for pMA-RQ-*Tz*CATB (Appendix A).

The *Tz*CATB gene was subsequently subcloned into, and expressed in the pCold-TF expression vector, which uses the same expression system as pCold-1 but with the addition of an attached trigger factor fusion protein providing improved protein solubility (Bjerga and Williamson, 2015). Recombinant expression of soluble *Tz*CATB in pCold-TF was confirmed (at the expected 90 kDa) by tris-tricine SDS-PAGE and western blotting with anti-His antibodies. After Ni-IMAC purification, the protease again exhibited no hydrolytic activity against Z-Arg-Arg-AMC. Since *Tz*CATB had this time been expressed in a soluble form, there was no need for solubilisation followed by refolding, and thus immunoaffinity chromatography was used as an alternative purification method, utilising chicken anti-*Tz*CATB IgY antibodies raised in a previous study (Zondo, 2019), which were coupled to UltraLink™ Hydrazide Resin. This choice of resin is advantageous because antibodies are coupled by their Fc region with

the antigen-binding site presented outwards, available for binding (Nisnevitch and Firer, 2001). While SDS-PAGE analysis of the purification showed that little *Tz*CATB bound to the immunoaffinity column, the protease eluted in the wash fractions as mostly purified protein with some contaminants. Purified *Tz*CATB was subjected to thrombin hydrolysis to remove the His-tag and trigger factor fusion protein, following which thrombin removal was attempted with a *p*-aminobenzamidine column. Benzamidine is a tight binding, reverisble inhibitor of thrombin and other trypsin-like serine proteases (De-Simone et al., 2005). After autocatalysing this preparation at low pH (5.0) in the presence of DTT and testing it against Z-Arg-Arg-AMC, hydrolysis was observed however the activity was present at pH 8.0 and not at lower pH (5.0 and 6.0), and this activity was not inhibited by E-64, which differs from what is expected of a cysteine protease and what is observed in the literature. The cathepsin B-like HC58 from *Haemonchus contortus* was inhibited by E-64 (Muleke et al., 2006), cathepsin B-like AcCBL1 from *Angiostrongylus cantonensis* had optimal activity at pH 5.0 (Cheng et al., 2012), a cathepsin B from *Schistosoma japonicum* (SjCB2) had optimal activity at pH 4.0 and was inhibited by E-64 (Zhu et al., 2020), and cathepsin B from *T. spiralis* (TsCB) had optimal activity at pH 5.5 and was inhibited by E-64 (Zao et al., 2024). A previous study on *Tz*CATB showed hydrolytic activity against Z-Arg-Arg-AMC after expression from the pCold-TF vector, and was inhibited by E-64 (Zondo, 2019). Since serine proteases are also known to hydrolyse Z-Arg-Arg-AMC (Semashko et al., 2014), thrombin, at the same concentration as used in the fusion protein hydrolysis, was tested alongside the *Tz*CATB-containing sample and showed the same level of fluorescence. This suggested that the activity observed was that of unremoved thrombin and not of recombinant *Tz*CATB. These results suggested that the recombinant *Tz*CATB produced was not active, and that thrombin removal was not successful. The protein present was confirmed to be *Tz*CATB by western blotting with chicken anti-*Tz*CATB IgY antibodies. Additionally, anti-human cathepsin B antibodies were shown not to recognise *Tz*CATB. This suggests that there would likely be no cross-reactivity between anti-*Tz*CATB IgY and mammalian cathepsin B, which is important for diagnostic purposes.

While western blotting confirmed the recombinant expression and purification of *Tz*CATB, sequencing of the pCold-TF-*Tz*CATB construct (Appendix B) produced a sequence with only approximately 40% similarity to the *Tz*CATB gene sequence. Sequencing was repeated on more than one plasmid miniprep, ruling out the possilibity of a miniprep of poor quality. The nucleotide sequences from the forward and reverse reactions from sequencing were translated and subjected to protein BLAST against the NCBI database (https://blast.ncbi.nlm.nih.gov/Blast.cgi), which deteceted similarities between the open reading frames with elongation factors, GTP-binding proteins and uncharacterised proteins from *Mycobacterium tuberculosis*, but not with any sequence from cathepsin B-like proteins

or from *Trichinella*. The primers for the sequencing reaction (pCold-TF-F1 and pCold-R) were available in-house and sent with the minipreps for sequencing, as opposed to other sequencing reactions for which the sequencing facility have the required primers available. Due to the expression of *Tz*CATB at the correct estimated molecular weight and its detection with anti-*Tz*CATB IgY antibodies, it is possible that the primers may have caused incorrect sequencing. This may have been due to primers not remaining stable while shipping. Alternatively, an incorrect gene sequence may indeed be present, but the sequence of the recombinantly expressed gene product was sufficiently similar to allow detection by chicken anti-*Tz*CATB IgY antibodies.

Purifed *Tz*stefinB was used to immunise two chickens over a 12-week period, and IgY isolated from the yolks of their eggs using filtration and PEG precipitation. Chicken IgY present a cost-effective choice of antibodies as they can be obtained in abudance from egg yolks instead of from an animal's blood, and these antibodies have advantages over mammalian antibodies including their increased sensitivity and low background signal in immunological assays, and they do not activate the human complement system (Larsson et al., 1993). Anti-*Tz*stefinB IgY production was shown to peak from week 6 after the first immunisation onwards using an ELISA with *Tz*stefinB as the coated antigen. An additional ELISA showed that 1 µg/mL of anti-*Tz*stefinB IgY was sufficient to produce a sufficiently high signal and this concentration was then used in western blotting. Western blotting confirmed that the chicken anti-*Tz*stefinB IgY antibodies recognised recombinant *Tz*stefinB. These antibodies did not detect stefin B isolated from sheep liver and antibodies raised against this sheep liver stefin B did not recognise *Tz*stefinB, suggesting sufficient immunogenic difference between the *Trichinella* stefin B and the mammalian homologue, that could be exploited in developing a specific diagnostic assay.

Sequencing of the pMD-19-*Tz*stefinB construct showed the correct gene sequence (Appendix C) with the exception of a single thymine instead of a cytosine. This causes Ala20 to change to Val20, adding only two methyl groups, and causing no alteration to conserved motifs of importance for inhibitory activity. Recombinant *T*zstefinB was expressed in the present study as a soluble 16 kDa protein. Parasite cystatins have been recombinantly expressed at similar sizes, such as AcCystatin from *Angiostrongylus cantonensis* at 14 kDa (Liu et al., 2010), SjCystatin from *Schistosoma japonicum* at 11 kDa (He et al., 2011) and TsCstN from *T.spiralis* at 13 kDa (Kobpornchai et al., 2020). Recombinant *Tz*stefinB was shown to have potent inhibitory activity against the cysteine proteases papain from papaya latex and cathepsin L from *Trypanosoma congolense* observed by inhibition of their hydrolysis of Z-Phe-Arg-AMC. The IC50 values of *Tz*stefinB for papain and *Tc*CATL were 2.60 µM and 1.49 µM, respectively. This is potent compared to 3.88 µM as reported for a recombinant cystatin from *T. spiralis*

(Kobpornchai et al., 2020). The stability of the recombinantly expressed *Tz*stefinB was tested by pre-incubation of TzstefinB at a range of pH values and temperatures before testing the effect of the inhibitor on papain activity. Results showed that *Tz*stefinB is stable over a broad pH range, since pre-incubation at different pHs had minimal effect on the inhibition of papain by 1 µM *Tz*stefinB. Conducting the pH-pre-incubation assay with a lower concentration of *Tz*stefinB could reveal an optimal pH level for inhibitory activity. In contrast, the inhibitory activity of *Tz*stefinB was rapidly and totally depleted following incubation at 99 ºC, and approximately 15 – 30 % of inhibitory activity was retained up to 3 weeks following storage at 4ºC and RT. The recombinantly expressed AcCystatin from *A. cantonensis* had maximal inhibitory activity against cathepsin B hydrolysis of Z-Arg-Arg-AMC after pre-incubation at pH 8.0 (Liu et al., 2010) and it retained some inhibitory activity after incubation at 99 ºC. A recombinantly expressed cystatin from *T. spiralis* (TsCstN) was shown to specifically inhibit cathepsin L hydrolysis of Z-Phe-Arg-AMC, while being unable to inhibit cathepsins B and S (Kobpornchai et al., 2020). Protein stability of TzstefinB can be assessed in future studies using methods such as differential scanning calorimetry, thermal shift assays, and far UV circular dichroism (Lepock, 2005; Huynh and Partch, 2015; Haque et al., 2022). Inhibition of papain by *Tz*stefinB was additionally tested using reverse zymography, an effective method for observing inhibitory activity in a qualitative manner to confirm quantitative results from synthetic peptide substrate assays. Reverse zymography showed that inhibition of papain by *Tz*stefinB could be detected with as low as 5 µM (10 µL of *Tz*stefinB at this concentration) being run on the gelatin-containing SDS-PAGE gel, and with 10 µM being the optimal amount of inhibitor for detection. The result was supported by the inclusion of SBTI as a negative control, which produced no band in the gel, i.e. SBTI, a serine protease inhibitor, did not interact with papain to inhibit the hydrolysis of the co-polymerised gelatin.

A past study on *Tz*CATB by Zondo (2019) expressed the cysteine protease from pCold-TF, demonstrated its proteolytic digestion of Z-Arg-Arg-AMC, and conducted a general characterisation of its activity. A past study on *Tz*stefinB by Maseko (2019) expressed the cysteine protease inhibitor from pET-28a and demonstrated its inhibition of cysteine proteases including *Tz*CATB. The present study aimed to express both *Tz*CATB and *Tz*stefinB to conduct a more comprehensive characterisation of their activity and interaction, however, active *Tz*CATB was not obtained. The inhibitory activity of *Tz*stefin was further characterised in the present study by subjecting the inhibitor to different pH levels and temperatures, and by visually demonstrating its inhibitory activity with reverse zymography.

Future studies should aim to completely purify *Tz*CATB and *Tz*stefinB from the minor contaminating proteins observed with the purified proteins in this study. This could be

accomplished with immunoaffinity chromatography. Coupling of the respective antibodies to a hydrazide matrix should be further optimised to improve antibody coupling efficiency. Remaining contaminants (if any) could be removed using size excluson chromatography. Chicken anti-*Tz*CATB and anti-*Tz*stefinB IgY antibodies can be used in western blotting to detect native *Tz*CATB and *Tz*stefinB in *T. zimbabwensis* extracts, to evaluate their potential for diagnostics. Sub-cloning of *Tz*CATB to pCold-TF should be re-attempted to obtain clones with the correct gene sequence. Active *Tz*CATB can then be characterised by conducting enzyme activity assays with the Z-Arg-Arg-AMC substrate over a pH range and in the presence of catalytic class-specific inhibitors. Hydrolysis of this substrate and of further fluorogenic substrates that vary in their P1 and P2 residues can also be used to measure the kinetics of *Tz*CATB activity (k_{cat} and K_m), and to study the interaction of *Tz*CATB and *Tz*stefinB.

A recent study on cathepsin L from *T.* spiralis (Liu et al., 2022) provides insight for further research to be conducted in future studies. In this study, qPCR and fluorescently tagged antibodies showed that cathepsin L was mainly transcribed by intestinal infective larvae (IILs) but also muscle larvae and adult worms and that it was mainly localised in the stichosome and gut. The three-dimensional structure of the cysteine protease was determined with homology modelling and molecular docking was conducted with E-64 which exhibited hydrogen bonding and hydrophobic interactions. The relative expression of *Tz*CATB and *Tz*stefinB at the different stages of the *T. zimbabwensis* life cycle can be determined with qPCR, anti-*Tz*CATB and anti-*Tz*stefinB antibodies could be tagged with a fluorescent marker and used for localisation of native proteins in parasite preparations, and the three-dimensional structures of *Tz*CATB and *Tz*stefinB can be determined using homology modelling, or using the more accurate X-ray crystallography (Ilari and Savino, 2008), after which these proteins can be used in molecular docking analyses for studying binding interactions and finding novel drug candidates. For further evaluation of their potential as vaccine candidates, the recombinant proteins can be used to immunise experimental animals and these animals subsequently challenged with *T. zimbabwensis* infection. A cathepsin B-like protease from *T. spiralis* was shown to be expressed across all stages of the parasite's lifecycle and to provide protective immunity against the parasite in mice (Yang et al., 2018). The proteolytic digestion of different mammalian and reptilian protein substrates by *Tz*CATB can be tested for analysis of the protease's functions in the host. Cathepsin B from *T. spiralis* was shown to degrade collagenase type I, suggesting that the protease plays a role in penetration of the small intestinal wall, of which collagenase I is an important constituent (Zao et al., 2024). Inhibition by *Tz*stefinB can be tested on other cysteine proteases, including *Tz*CATB. Cystatins from *T. spiralis* are involved in modulation of the host immune response (Nutman, 2015; Kobpornchai

et al., 2020), and therefore *Tz*stefinB should be tested for inhibition of cysteine proteases involved in antigen processing.

In conclusion, molecular cloning and sub-cloning of recombinant *Tz*CATB to pCold-1 and pCold-TF was succesful but proteins were insoluble and inactive, while sub-cloning to pCold-TF was unsuccesful as evident by the incorrect gene sequence and lack of activity. Recombinant *Tz*stefinB was succesfully cloned, recombinantly expressed and confirmed to have potent cysteine protease inhibitory activity across a broad pH range. These results will pave the way for further characterisation of *Tz*stefinB. Results obtained were similar to those of cystains from other parasites including *T. spiralis* in which they have been found to play important functions in their parasitism, suggesting that *Tz*stefinB may have potential for developing diagnostics, drugs and a vaccine for *T. zimbabwensis* infections. Chicken anti-*Tz*stefinB IgY antibodies were produced which may be valuable in the production of tests such as ELISAs and immunofluorescent techniques for the diagnosis of infection by *T. zimbabwensis*.

APPENDICES

Appendix A

Synthesis of codon optimised *Tz*CATB within the pMA-RQ cloning vector, as well as sequencing of this construct was conducted by Thermo Fisher Scientific. The gene sequence obtained from sequencing was aligned with the expected *Tz*CATB gene sequence (codon optimised).

Figure A: Pairwise sequence alignment of the codon optimised *Tz*CATB gene sequence with result from sequencing. The expected coding sequence for *Tz*CATB was codon optimised by Thermo Fisher Scientific and synthesised within the pMA-RQ cloning vector.

Appendix B

Sequencing of the pCold-TF-*Tz*CATB construct was conducted by the CAF Sequencing Facility at Stellenbosch University. The forward and reverse reactions from sequencing were aligned with the expected codon optimised *Tz*CATB gene sequence.

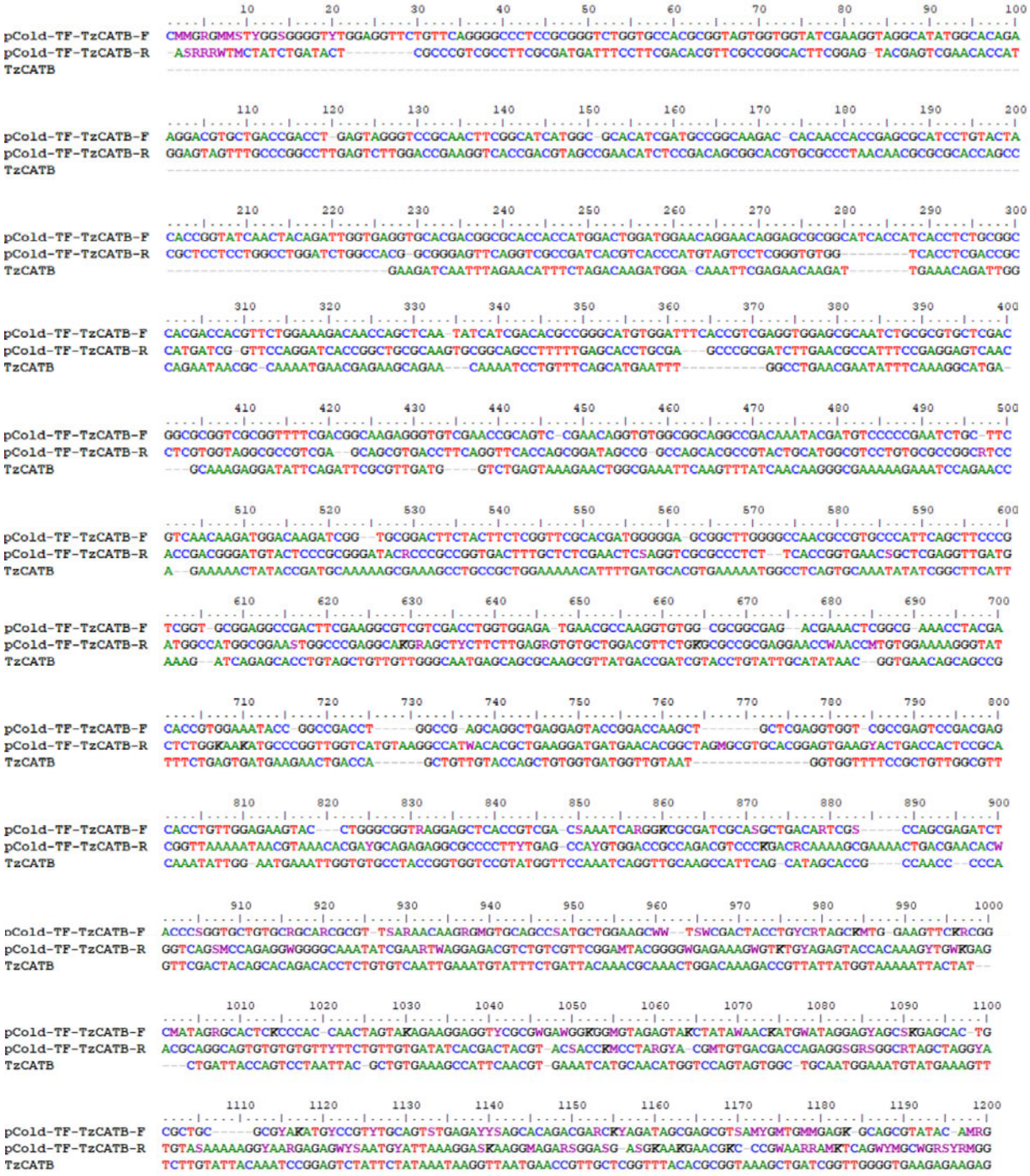

Figure B: Multiple sequence alignment of the codon optimised *Tz*CATB gene sequence with sequencing results. The expected coding sequence for *Tz*CATB was aligned with the forward and reverse reaction from sequencing pCold-TF-*Tz*CATB with the pCold-TF-F1 and pCold-R primers.

Appendix C

Sequencing of the pMD-19-*Tz*stefinB construct was conducted by the CAF Sequencing Facility at Stellenbosch University. The forward and reverse reactions from sequencing were aligned with the expected *Tz*stefinB gene sequence.

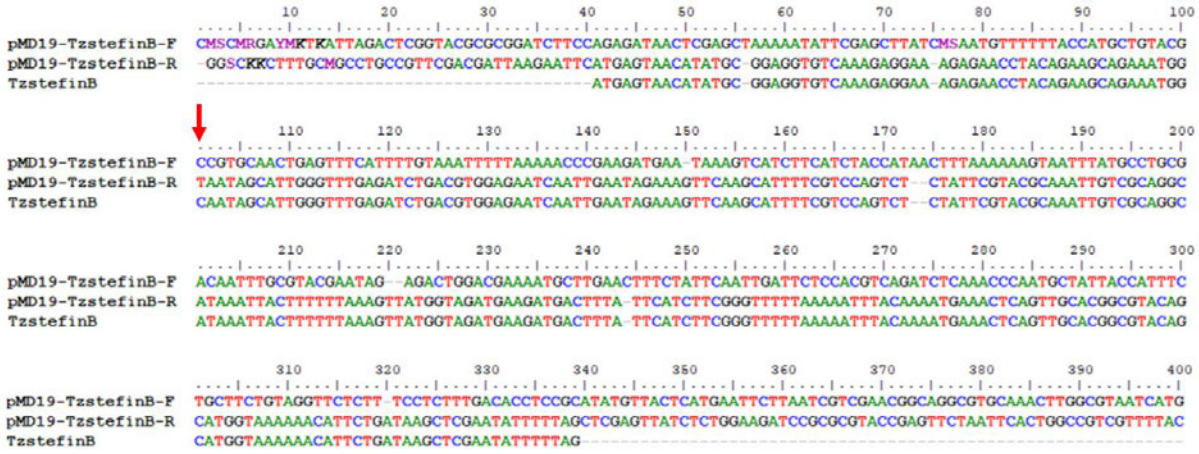

Figure C: Multiple sequence alignment of the *Tz*stefinB gene sequence with sequencing results. The expected coding sequence for *Tz*stefinB was as aligned with the forward and reverse reaction from sequencing pMD19-*Tz*stefinB with the M13 forward and reverse primers. The red arrow indicates the presence of an incorrect residue (in the reverse reaction).

References

Aggarwal, N. & Sloane, B. F. (2014). Cathepsin B: multiple roles in cancer. *Proteomics Clinical Applications,* 8**,** 427-37.

Andrade-Becerra, J. I., Pompa-Mera, E. N., Ribas-Aparicio, R. M. & Yépez-Mulia, L. (2017). Vaccination against *Trichinella spiralis*: potential, limitations and future directions. *Natural Remedies in the Fight Against Parasites,* 219.

Aoun, O., Lacour, S. A., Levieuge, A., Marié, J. L., Vallée, I. & Davoust, B. (2012). Screening for *Trichinella britovi* infection in red fox (*Vulpes vulpes*) and wild boar (*Sus scrofa*) in southeastern France. *Journal of Wildlife Diseases,* 48**,** 223-5.

Asano, K., Wu, Z., Srinontong, P., Ikeda, T., Nagano, I., Morita, H. & Maekawa, Y. (2016). Nonencapsulated *Trichinella pseudospiralis* infection impairs follicular helper T cell differentiation with subclass-selective decreases in antibody responses. *Infection and Immunity,* 84**,** 3550-3556.

Bai, X., Hu, X., Liu, X., Tang, B. & Liu, M. (2017). Current Research of Trichinellosis in China. *Frontiers in Microbiology,* 8.

Barrett, A. J. & Kirschke, H. (1981). Cathepsin B, Cathepsin H, and cathepsin L. *Methods in Enzymology,* 80 Pt C**,** 535-61.

Beveridge, I. & Spratt, D. M. (1996). The Helminth Fauna of Australasian Marsupials: Origins and Evolutionary Biology. *Advances in Parasitology,* 37**,** 135-254.

Bilska-Zając, E., Różycki, M., Grądziel-Krukowska, K., Bełcik, A., Mizak, I., Karamon, J., Sroka, J., Zdybel, J. & Cencek, T. (2020). Diversity of *Trichinella* species in relation to the host species and geographical location. *Veterinary Parasitology,* 279**,** 109052.

Bjerga, G. E. K. & Williamson, A. K. (2015). Cold shock induction of recombinant Arctic environmental genes. *BMC Biotechnology,* 15**,** 1-12.

Bolas-Fernández, F., Dea-Ayuela, M. A., Connolly, B. & Robinson, M. W. (2009). Micro-environmental conditions modulate protein secretion and infectivity of the *Trichinella spiralis* L1 larva. *Veterinary Parasitology,* 159**,** 236-239.

Bolás-Fernandez, F. & Corral Bezara, L. D. (2006). TSL-1 antigens of *Trichinella*: An overview of their potential role in parasite invasion, survival and serodiagnosis of trichinellosis. *Research in Veterinary Science,* 81**,** 297-303.

Boris, T., Dusan, T. & Guy, S. S. (2002). Regulating Cysteine Protease Activity: Essential Role of Protease Inhibitors As Guardians and Regulators. *Current Pharmaceutical Design,* 8**,** 1623-1637.

Bornhorst, J. A. & Falke, J. J. (2000). Purification of proteins using polyhistidine affinity tags. *Methods in Enzymology,* 326**,** 245-54.

Bradford, M. M. (1976). A rapid and sensitive method for the quantitation of microgram quantities of protein utilizing the principle of protein-dye binding. *Analytical Biochemistry,* 72**,** 248-254.

Brix, K. (2018). Host cell proteases: Cathepsins. *Activation of Viruses by Host Proteases***,** 249-276.

Brömme, D. (2000). Papain-like Cysteine Proteases. *Current Protocols in Protein Science,* 21**,** 21.2.1-21.2.14.

Bruschi, F. & Murrell, K. D. (2002). New aspects of human trichinellosis: the impact of new *Trichinella* species. *Postgraduate Medical Journal,* 78**,** 15-22.

Bruschi, F. & Pozio, E. (2019). Trichinella britovi.

Burgess, R. R. (2009). Refolding solubilized inclusion body proteins. *Methods in Enzymology,* 463**,** 259-82.

Buttle, D. J. & Mort, J. S. (2013). Cysteine Proteases. In: Lennarz, W. J. & Lane, M. D. (eds.) Encyclopedia of Biological Chemistry (Second Edition). Waltham: Academic Press.

Capó, V. & Despommier, D. D. (1996). Clinical aspects of infection with *Trichinella* spp. *Clinical Microbiology Reviews,* 9**,** 47-54.

Caron, Y., Bory, S., Pluot, M., Nheb, M., Chan, S., Prum, S. H., Lim, S. B. H., Sim, M., Sengdoeurn, Y., Sovann, L., Khieu, V., Vallée, I. & Yera, H. (2020). Human Outbreak of Trichinellosis Caused by *Trichinella papuae* Nematodes, Central Kampong Thom Province, Cambodia. *Emerging Infectious Diseases,* 26**,** 1759-1766.

Castro, G. A. (1996). Helminths: Structure, Classification, Growth, and Development. 4th ed.: University of Texas Medical Branch at Galveston, Galveston (TX).

Cavallo-Medved, D., Moin, K. & Sloane, B. (2011). Cathepsin B: Basis Sequence: Mouse. *AFCS Nature Molecule Pages,* 2011.

Cheng, M., Yang, X., Li, Z., He, H., Qu, Z., He, A., Wu, Z. & Zhan, X. (2012). Cloning and characterization of a novel cathepsin B-like cysteine proteinase from *Angiostrongylus cantonensis*. *Parasitology Research,* 110**,** 2413-2422.

Chmurzyńska, E., Różycki, M., Bilska-Zając, E., Nöckler, K., Mayer-Scholl, A., Pozio, E., Cencek, T. & Karamon, J. (2013). *Trichinella nativa* in red foxes (*Vulpes vulpes*) of Germany and Poland: possible different origins. *Veterinary Parasitology,* 198**,** 254-7.

Cooper, D. & Eleftherianos, I. (2016). Parasitic Nematode Immunomodulatory Strategies: Recent Advances and Perspectives. *Pathogens,* 5.

Cui, J., Wang, L., Sun, G. G., Liu, L. N., Zhang, S. B., Liu, R. D., Zhang, X., Jiang, P. & Wang, Z. Q. (2015). Characterization of a *Trichinella spiralis* 31 kDa protein and its potential application for the serodiagnosis of trichinellosis. *Acta Tropica,* 142**,** 57-63.

De-Simone, S. G., Correa-Netto, C., Antunes, O. a. C., De-Alencastro, R. B. & Silva, F. P. (2005). Biochemical and molecular modeling analysis of the ability of two p-aminobenzamidine-based sorbents to selectively purify serine proteases (fibrinogenases) from snake venoms. *Journal of Chromatography B,* 822**,** 1-9.

De Ley, P. (2006). A quick tour of nematode diversity and the backbone of nematode phylogeny. *WormBook : the online review of C. elegans biology***,** 1-8.

Demchik, L. L., Sameni, M., Nelson, K., Mikkelsen, T. & Sloane, B. F. (1999). Cathepsin B and glioma invasion. *International Journal of Developmental Neuroscience,* 17**,** 483-494.

Despommier, D. D. (1998). How Does *Trichinella spiralis* Make Itself at Home? *Parasitology Today,* 14**,** 318-323.

Diemert, D. J. (2012). 366 - Tissue Nematode Infections. In: Goldman, L. & Schafer, A. I. (eds.) Goldman's Cecil Medicine (Twenty Fourth Edition). Philadelphia: W.B. Saunders.

Dilcheva, V. & Petkova, S. (2018). *Trichinella britovi*, etiologic agent of trichinellosis in wild carnivores in Bulgaria. *Acta morphologica et anthropologica,* 25**,** 3-4.

Ellis, K. J. & Morrison, J. F. (1982). Buffers of constant ionic strength for studying pH-dependent processes. *Methods in Enzymology,* 87**,** 405-26.

Fabre, M., Beiting, D., Bliss, S. & Appleton, J. (2009). Immunity to *Trichinella spiralis* muscle infection. *Veterinary Parasitology,* 159**,** 245-248.

Farid, A. S., Fath, E. M., Mido, S., Nonaka, N. & Horii, Y. (2019). Hepatoprotective immune response during *Trichinella spiralis* infection in mice. *Journal of Veterinary Medicinal Science,* 81**,** 169-176.

Feidas, H., Kouam, M. K., Kantzoura, V. & Theodoropoulos, G. (2014). Global geographic distribution of *Trichinella* species and genotypes. *Infection, Genetics and Evolution,* 26**,** 255-266.

Fernández-Lucas, J., Castañeda, D. & Hormigo, D. (2017). New trends for a classical enzyme: Papain, a biotechnological success story in the food industry. *Trends in Food Science & Technology,* 68**,** 91-101.

Franssen, F., Swart, A., Van Der Giessen, J., Havelaar, A. & Takumi, K. (2017). Parasite to patient: A quantitative risk model for *Trichinella* spp. in pork and wild boar meat. *International Journal of Food Microbiology,* 241**,** 262-275.

Gajadhar, A. A., Pozio, E., Gamble, H. R., Nöckler, K., Maddox-Hyttel, C., Forbes, L. B., Vallée, I., Rossi, P., Marinculić, A. & Boireau, P. (2009). *Trichinella* diagnostics and control: mandatory and best practices for ensuring food safety. *Veterinary Parasitology,* 159**,** 197-205.

Gajadhar, A. A. & Forbes, L. B. (2010). A 10-year wildlife survey of 15 species of Canadian carnivores identifies new hosts or geographic locations for *Trichinella* genotypes T2, T4, T5, and T6. *Veterinary Parasitology,* 168**,** 78-83.

Gamble, H., Bessonov, A., Cuperlovic, K., Gajadhar, A., Van Knapen, F., Noeckler, K., Schenone, H. & Zhu, X. (2000). International Commission on Trichinellosis: recommendations on methods for the control of *Trichinella* in domestic and wild animals intended for human consumption. *Veterinary Parasitology,* 93**,** 393-408.

Goldring, J. P. D. & Coetzer, T. H. T. (2003). Isolation of chicken immunoglobulins (IgY) from egg yolk. *Biochemistry and Molecular Biology Education,* 31**,** 185-187.

Gómez-Morales, M. A., Ludovisi, A., Amati, M., Bandino, E., Capelli, G., Corrias, F., Gelmini, L., Nardi, A., Sacchi, C., Cherchi, S., Lalle, M. & Pozio, E. (2014). Indirect versus direct detection methods of *Trichinella* spp. infection in wild boar (*Sus scrofa*). *Parasites & Vectors,* 7**,** 171.

Gottstein, B., Pozio, E. & Nöckler, K. (2009). Epidemiology, diagnosis, treatment, and control of trichinellosis. *Clinical Microbiology Reviews,* 22**,** 127-145.

Gruden-Movsesijan, A., Ilic, N., Colic, M., Majstorovic, I., Vasilev, S., Radovic, I. & Sofronic-Milosavljevic, L. (2011). The impact of *Trichinella spiralis* excretory–secretory products on dendritic cells. *Comparative Immunology, Microbiology and Infectious Diseases,* 34**,** 429-439.

Han, C., Yu, J., Zhang, Z., Zhai, P., Zhang, Y., Meng, S., Yu, Y., Li, X. & Song, M. (2019). Immunomodulatory effects of *Trichinella spiralis* excretory-secretory antigens on macrophages. *Experimental Parasitology,* 196**,** 68-72.

Han, Y., Yue, X., Hu, C. X., Liu, F., Liu, R. D., He, M. M., Long, S. R., Cui, J. & Wang, Z. Q. (2020). Interaction of a *Trichinella spiralis* cathepsin B with enterocytes promotes the larval intrusion into the cells. *Research in Veterinary Science,* 130**,** 110-117.

Hanspal, J. S., Bushell, G. R. & Ghosh, P. (1983). Detection of protease inhibitors using substrate-containing sodium dodecyl sulfate-polyacrylamide gel electrophoresis. *Analytical Biochemistry,* 132**,** 288-293.

Haque, M. A., Kaur, P., Islam, A. & Hassan, M. I. (2022). Chapter 14 - Application of circular dichroism spectroscopy in studying protein folding, stability, and interaction. In: Tripathi, T. & Dubey, V. K. (eds.) *Advances in Protein Molecular and Structural Biology Methods.* Academic Press.

He, B., Cai, G., Ni, Y., Li, Y., Zong, H. & He, L. (2011). Characterization and expression of a novel cystatin gene from *Schistosoma japonicum*. *Molecular and Cellular Probes,* 25**,** 186-193.

Hernández-Ancheyta, L., Salinas-Tobón, M. D. R., Cifuentes-Goches, J. C. & Hernández-Sánchez, J. (2018). *Trichinella spiralis* muscle larvae excretory–secretory products induce changes in cytoskeletal and myogenic transcription factors in primary myoblast cultures. *International Journal for Parasitology,* 48**,** 275-285.

Heussen, C. & Dowdle, E. B. (1980). Electrophoretic analysis of plasminogen activators in polyacrylamide gels containing sodium dodecyl sulfate and copolymerized substrates. *Analytical Biochemistry,* 102**,** 196-202.

Hu, Y. Y., Zhang, R., Yan, S. W., Yue, W. W., Zhang, J. H., Liu, R. D., Long, S. R., Cui, J. & Wang, Z. Q. (2021). Characterization of a novel cysteine protease in *Trichinella spiralis* and its role in larval intrusion, development and fecundity. *Veterinary Research,* 52**,** 113.

Huynh, K. & Partch, C. L. (2015). Analysis of Protein Stability and Ligand Interactions by Thermal Shift Assay. *Current Protocols in Protein Science,* 79**,** 28.9.1-28.9.14.

Ilari, A. & Savino, C. (2008). Protein Structure Determination by X-Ray Crystallography. In: Keith, J. M. (ed.) *Bioinformatics: Data, Sequence Analysis and Evolution.* Totowa, NJ: Humana Press.

Ilic, N., Gruden-Movsesijan, A. & Sofronic-Milosavljevic, L. (2012). *Trichinella spiralis*: shaping the immune response. *Immunological Research,* 52**,** 111-9.

Iqbal, S. & Jones, M. G. K. (2017). Nematodes. In: Thomas, B., Murray, B. G. & Murphy, D. J. (eds.) Encyclopedia of Applied Plant Sciences (Second Edition). Oxford: Academic Press.

Ji, P., Hu, H., Yang, X., Wei, X., Zhu, C., Liu, J., Feng, Y., Yang, F., Okanurak, K., Li, N., Zeng, X., Zheng, H., Wu, Z. & Lv, Z. (2015). AcCystatin, an immunoregulatory molecule from *Angiostrongylus cantonensis*, ameliorates the asthmatic response in an aluminium hydroxide/ovalbumin-induced rat model of asthma. *Parasitology Research,* 114**,** 613-624.

Jongwutiwes, S., Chantachum, N., Kraivichian, P., Siriyasatien, P., Putaporntip, C., Tamburrini, A., La Rosa, G., Sreesunpasirikul, C., Yingyourd, P. & Pozio, E. (1998). First outbreak of human trichinellosis caused by *Trichinella pseudospiralis*. *Clinical Infectious Diseases,* 26**,** 111-115.

Kanai, Y., Nonaka, N., Katakura, K. & Oku, Y. (2006). *Trichinella nativa* and *Trichinella* T9 in the Hokkaido island, Japan. *Parasitology International,* 55**,** 313-315.

Karrer, K. M., Peiffer, S. L. & Ditomas, M. E. (1993). Two distinct gene subfamilies within the family of cysteine protease genes. *Proceedings of the National Academy of Sciences,* 90**,** 3063-3067.

Kędzior, M., Seredyński, R. & Gutowicz, J. (2016). Microbial inhibitors of cysteine proteases. *Medical Microbiology and Immunology,* 205**,** 275-296.

Khan, A. R. & James, M. N. G. (1998). Molecular mechanisms for the conversion of zymogens to active proteolytic enzymes. *Protein Science,* 7**,** 815-836.

Khan, I., Qayyum, S., Ahmed, S., Niaz, Z., Fatima, N. & Chi, Z.-M. (2016). Molecular cloning and sequence analysis of a PVGOX gene encoding glucose oxidase in *Penicillium viticola* F1 strain and it's expression quantitation. *Gene,* 592**,** 291-302.

Khumjui, C., Choomkasien, P., Dekumyoy, P., Kusolsuk, T., Kongkaew, W., Chalamaat, M. & Jones, J. L. (2008). Outbreak of trichinellosis caused by *Trichinella papuae*, Thailand, 2006. *Emerging Infectious Diseases,* 14**,** 1913-5.

Khurana, S., Datta, P., Sharma, B., Singh, C., Mewara, A., Johnson, N., Pilania, R. K., Singh, S. & Sehgal, R. (2021). Clinical and laboratory profile of trichinellosis from a non-endemic country. *Indian Journal of Medical Microbiology,* 39**,** 235-239.

Kim, M. J., Yamamoto, D., Matsumoto, K., Inoue, M., Ishida, T., Mizuno, H., Sumiya, S. & Kitamura, K. (1992). Crystal structure of papain-E64-c complex. Binding diversity of E64-c to papain S2 and S3 subsites. *Biochemical Journal,* 287**,** 797-803.

Kimmel, J. R. & Smith, E. L. (1954). Crystalline papain I. Preparation, specificity, and activation. *Journal of Biological Chemistry,* 207**,** 515-531.

Kobayashi, T., Kanai, Y., Ono, Y., Matoba, Y., Suzuki, K., Okamoto, M., Taniyama, H., Yagi, K., Oku, Y. & Katakura, K. (2007). Epidemiology, histpathology, and muscle distribution of *Trichinella* T9 in feral raccoons (*Procyon lotor*) and wildlife of Japan. *Parasitology Research,* 100**,** 1287-1291.

Kobpornchai, P., Flynn, R. J., Reamtong, O., Rittisoonthorn, N., Kosoltanapiwat, N., Boonnak, K., Boonyuen, U., Ampawong, S., Jiratanh, M., Tattiyapong, M. & Adisakwattana, P. (2020). A novel cystatin derived from *Trichinella spiralis* suppresses macrophage-mediated inflammatory responses. *PLoS Neglected Tropical Diseases,* 14**,** e0008192.

Kocięcka, W. (2000). Trichinellosis: human disease, diagnosis and treatment. *Veterinary Parasitology,* 93**,** 365-383.

Krivokapich, S. J., Gatti, G. M., Prous, C. L. G., Degese, M. F., Arbusti, P. A., Ayesa, G. E., Bello, G. V. & Salomón, M. C. (2019). Detection of *Trichinella britovi* in pork sausage suspected to be implicated in a human outbreak in Mendoza, Argentina. *Parasitology International,* 71**,** 53-55.

Kurien, B. T. & Scofield, R. H. (2006). Western blotting. *Methods,* 38**,** 283-293.

La Grange, L. J., Marucci, G. & Pozio, E. (2010). *Trichinella zimbabwensis* in a naturally infected mammal. *Journal of Helminthology,* 84**,** 35-38.

La Grange, L. J. & Mukaratirwa, S. (2020). Epidemiology and hypothetical transmission cycles of *Trichinella* infections in the Greater Kruger National Park of South Africa: an example of host-parasite interactions in an environment with minimal human interactions. *Parasite,* 27**,** 13.

Larsson, A., Bålöw, R.-M., Lindahl, T. L. & Forsberg, P.-O. (1993). Chicken Antibodies: Taking Advantage of Evolution—A Review. *Poultry Science,* 72**,** 1807-1812.

Lecaille, F., Kaleta, J. & Brömme, D. (2002). Human and Parasitic Papain-Like Cysteine Proteases: Their Role in Physiology and Pathology and Recent Developments in Inhibitor Design. *Chemical Reviews,* 102**,** 4459-4488.

Lepock, J. R. (2005). Measurement of protein stability and protein denaturation in cells using differential scanning calorimetry. *Methods,* 35**,** 117-125.

Li, J., Han, Q., Zhang, T., Du, J., Sun, Q. & Pang, Y. (2018). Expression of soluble native protein in *Escherichia coli* using a cold-shock SUMO tag-fused expression vector. *Biotechnology Reports,* 19**,** e00261.

Liu, R. D., Qi, X., Sun, G. G., Jiang, P., Zhang, X., Wang, L. A., Liu, X. L., Wang, Z. Q. & Cui, J. (2016). Proteomic analysis of *Trichinella spiralis* adult worm excretory-secretory proteins recognized by early infection sera. *Veterinary Parasitology,* 231**,** 43-46.

Liu, R. D., Meng, X. Y., Li, C. L., Long, S. R., Cui, J. & Wang, Z. Q. (2022). Molecular characterization and determination of the biochemical properties of cathepsin L of *Trichinella spiralis*. *Veterinary Research,* 53**,** 48.

Liu, X., Liu, L., Wang, Y., Wang, X., Ma, Y. & Li, Y. (2014). The Study on the factors affecting transformation efficiency of *E. coli* competent cells. *Pakistan Journal of Pharmaceutical Sciences,* 27**,** 679-84.

Liu, Y.-H., Han, Y.-P., Li, Z.-Y., Wei, J., He, H.-J., Xu, C.-Z., Zheng, H.-Q., Zhan, X.-M., Wu, Z.-D. & Lv, Z.-Y. (2010). Molecular cloning and characterization of cystatin, a cysteine protease inhibitor, from *Angiostrongylus cantonensis*. *Parasitology Research,* 107**,** 915-922.

Maity, A., Kesh, S. S., Palai, S. & Egbuna, C. (2022). Chapter 4 - Electrophoretic techniques. In: Egbuna, C., Patrick-Iwuanyanwu, K. C., Shah, M. A., Ifemeje, J. C. & Rasul, A. (eds.) Analytical Techniques in Biosciences*.* Academic Press.

Marucci, G., La Grange, L. J., La Rosa, G. & Pozio, E. (2009). *Trichinella nelsoni* and *Trichinella* T8 mixed infection in a lion (*Panthera leo*) of the Kruger National Park (South Africa). *Veterinary Parasitology,* 159**,** 225-228.

Maseko, T. G. (2019). Molecular cloning, recombinant expression and characterisation of serine and cysteine protease inhibitors from *Trichinella zimbabwensis.* University of KwaZulu-Natal, Pietermaritzburg, MSc.

Mitreva, M. & Jasmer, D. P. (2006). Biology and genome of *Trichinella spiralis*. *WormBook***,** 1-21.

Mort, J. S. & Buttle, D. J. (1997). Cathepsin B. *International Journal of Biochemistry & Cell Biology,* 29**,** 715-20.

Mukaratirwa, S., La Grange, L. & Pfukenyi, D. M. (2013). *Trichinella* infections in animals and humans in sub-Saharan Africa: a review. *Acta Tropica,* 125**,** 82-9.

Mukaratirwa, S., La Grange, L. J., Malatji, M. P., Reininghaus, B. & Lamb, J. (2019). Prevalence and molecular identification of *Trichinella* species isolated from wildlife originating from Limpopo and Mpumalanga provinces of South Africa. *Journal of Helminthology,* 93**,** 50-56.

Muleke, C. I., Ruofeng, Y., Lixin, X., Yanming, S. & Xiangrui, L. (2006). Characterization of HC58cDNA, a putative cysteine protease from the parasite *Haemonchus contortus*. *Journal of Veterinary Science,* 7**,** 249-55.

Musil, D., Zucic, D., Turk, D., Engh, R. A., Mayr, I., Huber, R., Popovic, T., Turk, V., Towatari, T., Katunuma, N. & Et Al. (1991). The refined 2.15 A X-ray crystal structure of human liver cathepsin B: the structural basis for its specificity. *The EMBO Journal,* 10**,** 2321-30.

Nagano, I., Wu, Z. & Takahashi, Y. (2009). Functional genes and proteins of *Trichinella* spp. *Parasitology Research,* 104**,** 197-207.

Ndlovu, I. S., Silas, E., Tshilwane, S. I., Chaisi, M., Vosloo, A. & Mukaratirwa, S. (2023). Preliminary insights on the metabolomics of *Trichinella zimbabwensis* infection in Sprague Dawley rats using GCxGC-TOF-MS (untargeted approach). *Frontiers in Molecular Biosciences,* 10.

Nisnevitch, M. & Firer, M. A. (2001). The solid phase in affinity chromatography: strategies for antibody attachment. *Journal of Biochemical and Biophysical Methods,* 49**,** 467-480.

Nöckler, K., Pozio, E., Voigt, W. P. & Heidrich, J. (2000). Detection of *Trichinella* infection in food animals. *Veterinary Parasitology,* 93**,** 335-50.

Nöckler, K., Reckinger, S., Broglia, A., Mayer-Scholl, A. & Bahn, P. (2009). Evaluation of a Western Blot and ELISA for the detection of anti-*Trichinella*-IgG in pig sera. *Veterinary Parasitology,* 163**,** 341-7.

Novinec, M. & Lenarčič, B. (2013). Papain-like peptidases: structure, function, and evolution. *Biomolecular Concepts,* 4**,** 287-308.

Nutman, T. B. (2015). Looking beyond the induction of Th2 responses to explain immunomodulation by helminths. *Parasite Immunology,* 37**,** 304-13.

Onkoba, W. N., Chimbari, M. J., Kamau, J. M. & Mukaratirwa, S. (2016). Differential immune responses in mice infected with the tissue-dwelling nematode *Trichinella zimbabwensis*. *Journal of Helminthology,* 90**,** 547-54.

Otto, H.-H. & Schirmeister, T. (1997). Cysteine Proteases and Their Inhibitors. *Chemical Reviews,* 97**,** 133-172.

Park, J. N., Park, S. K., Cho, M. K., Park, M.-K., Kang, S. A., Kim, D.-H. & Yu, H. S. (2012). Molecular characterization of 45kDa aspartic protease of *Trichinella spiralis*. *Veterinary Parasitology,* 190**,** 510-518.

Park, M. K., Cho, M. K., Kang, S. A., Kim, B. Y. & Yu, H. S. (2016). The induction of the collagen capsule synthesis by *Trichinella spiralis* is closely related to protease-activated receptor 2. *Veterinary Parasitology,* 230**,** 56-61.

Pavic, S., Andric, A., Sofronic-Milosavljevic, L., Gnjatovic, M., Mitić, I., Vasilev, S., Sparic, R. & Pavic, A. (2020). *Trichinella britovi* outbreak: Epidemiological, clinical, and biological features. *Médecine et Maladies Infectieuses,* 50**,** 520-524.

Petushkova, A. I., Savvateeva, L. V. & Zamyatnin, A. A. (2022). Structure determinants defining the specificity of papain-like cysteine proteases. *Computational and Structural Biotechnology Journal,* 20**,** 6552-6569.

Polgár, L. (2005). The catalytic triad of serine peptidases. *Cellular and Molecular Life Sciences,* 62**,** 2161-2172.

Powers, J. C., Asgian, J. L., Ekici, Ö. D. & James, K. E. (2002). Irreversible Inhibitors of Serine, Cysteine, and Threonine Proteases. *Chemical Reviews,* 102**,** 4639-4750.

Pozio, E., La Rosa, G., Murrell, K. D. & Lichtenfels, J. R. (1992). Taxonomic revision of the genus *Trichinella*. *The Journal of Parasitology***,** 654-659.

Pozio, E. & Kapel, C. (1999). *Trichinella nativa* in sylvatic wild boars. *Journal of helminthology,* 73**,** 87-89.

Pozio, E., Owen, I., La Rosa, G., Sacchi, L., Rossi, P. & Corona, S. (1999). *Trichinella papuae* n. sp.(Nematoda), a new non-encapsulated species from domestic and sylvatic swine of Papua New Guinea. *International Journal for Parasitology,* 29**,** 1825-1839.

Pozio, E. (2001). Taxonomy of *Trichinella* and the epidemiology of infection in the Southeast Asia and Australian regions. *Southeast Asian Journal of Tropical Medicine and Public Health,* 32 Suppl 2**,** 129-32.

Pozio, E., Zarlenga, D. & La Rosa, G. (2001). The detection of encapsulated and non-encapsulated species of *Trichinella* suggests the existence of two evolutive lines in the genus. *Parasite,* 8**,** S27-S29.

Pozio, E., Foggin, C. M., Marucci, G., La Rosa, G., Sacchi, L., Corona, S., Rossi, P. & Mukaratirwa, S. (2002). *Trichinella zimbabwensis* n.sp. (Nematoda), a new non-encapsulated species from crocodiles (*Crocodylus niloticus*) in Zimbabwe also infecting mammals. *International Journal for Parasitology,* 32**,** 1787-99.

Pozio, E., Gomez Morales, M. A. & Dupouy-Camet, J. (2003). Clinical aspects, diagnosis and treatment of trichinellosis. *Expert Review of Anti-Infective Therapy,* 1**,** 471-82.

Pozio, E., Owen, I. L., Marucci, G. & La Rosa, G. (2005). Inappropriate feeding practice favors the transmission of *Trichinella papuae* from wild pigs to saltwater crocodiles in Papua New Guinea. *Veterinary Parasitology,* 127**,** 245-251.

Pozio, E., Foggin, C. M., Gelanew, T., Marucci, G., Hailu, A., Rossi, P. & Morales, M. a. G. (2007). *Trichinella zimbabwensis* in wild reptiles of Zimbabwe and Mozambique and farmed reptiles of Ethiopia. *Veterinary Parasitology,* 143**,** 305-310.

Pozio, E., Rinaldi, L., Marucci, G., Musella, V., Galati, F., Cringoli, G., Boireau, P. & La Rosa, G. (2009). Hosts and habitats of *Trichinella spiralis* and *Trichinella britovi* in Europe. *International Journal for Parasitology,* 39**,** 71-79.

Ramirez Merlano, J. A. & Almeida, D. V. (2022). Heterologous Production and Evaluation of the Biological Activity of Cystatin-B From the Red Piranha *Pygocentrus nattereri*. *Frontiers in Genetics,* 13**,** 812971.

Ranque, S., Faugère, B., Pozio, E., La Rosa, G., Tamburrini, A., Pellissier, J. F. & Brouqui, P. (2000). *Trichinella pseudospiralis* outbreak in France. *Emerging Infectious Diseases,* 6**,** 543-7.

Ratelade, J., Miot, M. C., Johnson, E., Betton, J. M., Mazodier, P. & Benaroudj, N. (2009). Production of recombinant proteins in the lon-deficient BL21(DE3) strain of *Escherichia coli* in the absence of the DnaK chaperone. *Applied and Environmental Microbiology,* 75**,** 3803-7.

Rawlings, N. D. & Barrett, A. J. (1994). Families of cysteine peptidases. *Methods in Enzymology,* 244**,** 461-86.

Rawlings, N. D., Barrett, A. J. & Bateman, A. (2011). Asparagine peptide lyases: a seventh catalytic type of proteolytic enzymes. *Journal of Biological Chemistry,* 286**,** 38321-38328.

Rawlings, N. D. (2020). Twenty-five years of nomenclature and classification of proteolytic enzymes. *Biochimica et Biophysica Acta Proteins and Proteomics,* 1868**,** 140345.

Reichard, M. V., Torretti, L., Snider, T. A., Garvon, J. M., Marucci, G. & Pozio, E. (2008). *Trichinella* T6 and *Trichinella nativa* in wolverines (*Gulo gulo*) from Nunavut, Canada. *Parasitology Research,* 103**,** 657-661.

Reichard, M. V., Sanders, T. L., Prentiss, N. L., Cotey, S. R., Koch, R. W., Fairbanks, W. S., Interisano, M., La Rosa, G. & Pozio, E. (2021). Detection of *Trichinella murrelli* and *Trichinella pseudospiralis* in bobcats (*Lynx rufus*) from Oklahoma. *Veterinary Parasitology: Regional Studies and Reports,* 25**,** 100609.

Roberts, R. J., Belfort, M., Bestor, T., Bhagwat, A. S., Bickle, T. A., Bitinaite, J., Blumenthal, R. M., Degtyarev, S., Dryden, D. T., Dybvig, K., Firman, K., Gromova, E. S., Gumport, R. I., Halford, S. E., Hattman, S., Heitman, J., Hornby, D. P., Janulaitis, A., Jeltsch, A., Josephsen, J., Kiss, A., Klaenhammer, T. R., Kobayashi, I., Kong, H., Krüger, D. H., Lacks, S., Marinus, M. G., Miyahara, M., Morgan, R. D., Murray, N. E., Nagaraja, V., Piekarowicz, A., Pingoud, A., Raleigh, E., Rao, D. N., Reich, N., Repin, V. E., Selker, E. U., Shaw, P. C., Stein, D. C., Stoddard, B. L., Szybalski, W., Trautner, T. A., Van Etten, J. L., Vitor, J. M., Wilson, G. G. & Xu, S. Y. (2003). A nomenclature for restriction enzymes, DNA methyltransferases, homing endonucleases and their genes. *Nucleic Acids Research,* 31**,** 1805-12.

Satoskar, A. R., Simon, G. L., Hotez, P. J. & Tsuji, M. (2009). Medical Parasitology, CRC Press.

Schägger, H. (2006). Tricine-SDS-PAGE. *Nature Protocols,* 1**,** 16-22.

Schechter, I. & Berger, A. (1967). On the size of the active site in proteases. I. Papain. *Biochemical and Biophysical Research Communications,* 27**,** 157-62.

Semashko, T. A., Vorotnikova, E. A., Sharikova, V. F., Vinokurov, K. S., Smirnova, Y. A., Dunaevsky, Y. E., Belozersky, M. A., Oppert, B., Elpidina, E. N. & Filippova, I. Y. (2014). Selective chromogenic and fluorogenic peptide substrates for the assay of cysteine peptidases in complex mixtures. *Analytical Biochemistry,* 449**,** 179-187.

Sharma, R., Harms, N. J., Kukka, P. M., Parker, S. E., Gajadhar, A. A., Jung, T. S. & Jenkins, E. J. (2018). Tongue has higher larval burden of *Trichinella* spp. than diaphragm in wolverines (*Gulo gulo*). *Veterinary Parasitology,* 253**,** 94-97.

Sharma, R., Thompson, P. C., Hoberg, E. P., Scandrett, W. B., Konecsni, K., Harms, N. J., Kukka, P. M., Jung, T. S., Elkin, B. & Mulders, R. (2020). Hiding in plain sight: discovery and phylogeography of a cryptic species of *Trichinella* (Nematoda: Trichinellidae) in wolverine (*Gulo gulo*). *International Journal for Parasitology,* 50**,** 277-287.

Sharma, R., Harms, N. J., Kukka, P. M., Jung, T. S., Parker, S. E., Ross, S., Thompson, P., Rosenthal, B., Hoberg, E. P. & Jenkins, E. J. (2021). High prevalence, intensity, and genetic diversity of *Trichinella* spp. in wolverine (*Gulo gulo*) from Yukon, Canada. *Parasites & Vectors,* 14**,** 146.

Smythe, A. B., Holovachov, O. & Kocot, K. M. (2019). Improved phylogenomic sampling of free-living nematodes enhances resolution of higher-level nematode phylogeny. *BMC Evolutionary Biology,* 19**,** 121.

Sofronic-Milosavljevic, L., Ilic, N., Pinelli, E. & Gruden-Movsesijan, A. (2015). Secretory Products of *Trichinella spiralis* Muscle Larvae and Immunomodulation: Implication for Autoimmune Diseases, Allergies, and Malignancies. *Journal of Immunology Research,* 2015**,** 523875.

Song, Y. Y., Lu, Q. Q., Han, L. L., Yan, S. W., Zhang, X. Z., Liu, R. D., Long, S. R., Cui, J. & Wang, Z. Q. (2022). Proteases secreted by *Trichinella spiralis* intestinal infective larvae damage the junctions of the intestinal epithelial cell monolayer and mediate larval invasion. *Veterinary Research,* 53**,** 19.

Sorimachi, H., Hata, S. & Ono, Y. (2013). Calpain. In: Lennarz, W. J. & Lane, M. D. (eds.) Encyclopedia of Biological Chemistry (Second Edition). Waltham: Academic Press.

Storer, A. C. & Ménard, R. (2013). Chapter 419 - Papain. In: Rawlings, N. D. & Salvesen, G. (eds.) Handbook of Proteolytic Enzymes (Third Edition). Academic Press.

Sugiki, T., Fujiwara, T. & Kojima, C. (2017). Cold-Shock Expression System in *E. coli* for Protein NMR Studies. *Methods in Molecular Biology,* 1586**,** 345-357.

Tacias-Pascacio, V. G., Morellon-Sterling, R., Castaneda-Valbuena, D., Berenguer-Murcia, Á., Kamli, M. R., Tavano, O. & Fernandez-Lafuente, R. (2021). Immobilization of papain: A review. *International Journal of Biological Macromolecules,* 188**,** 94-113.

Tang, B., Liu, M., Wang, L., Yu, S., Shi, H., Boireau, P., Cozma, V., Wu, X. & Liu, X. (2015). Characterisation of a high-frequency gene encoding a strongly antigenic cystatin-like protein from *Trichinella spiralis* at its early invasion stage. *Parasites & Vectors,* 8**,** 78.

Todorova, V., Knox, D. & Kennedy, M. (1995). Proteinases in the excretory/secretory products (ES) of adult *Trichinella spiralis*. *Parasitology,* 111**,** 201-208.

Todorova, V. K. (2000). Proteolytic enzymes secreted by larval stage of the parasitic nematode *Trichinella spiralis*. *Folia Parasitologica,* 47**,** 141-5.

Tominaga, T., Aoki, M., Biswas, P. G., Hatta, T. & Itagaki, T. (2021). Prevalence of *Trichinella* T9 in Japanese black bears (*Ursus thibetanus japonicus*) in Iwate prefecture, Japan. *Parasitology International,* 80**,** 102217.

Turk, D., Podobnik, M., Popovic, T., Katunuma, N., Bode, W., Huber, R. & Turk, V. (1995). Crystal structure of cathepsin B inhibited with CA030 at 2.0-.ANG. resolution: A basis for the design of specific epoxysuccinyl inhibitors. *Biochemistry,* 34**,** 4791-4797.

Turk, V., Stoka, V., Vasiljeva, O., Renko, M., Sun, T., Turk, B. & Turk, D. (2012). Cysteine cathepsins: from structure, function and regulation to new frontiers. *Biochimica et Biophysica Acta Proteins and Proteomics,* 1824**,** 68-88.

Turk, V., Turk, D., Dolenc, I. & Stoka, V. (2019). Characteristics, Structure, and Biological Role of Stefins (Type-1 Cystatins) of Human. *Acta Chimica Slovenica,* 66**,** 5-17.

Van Der Giessen, J., Rombout, Y., Franchimont, H., La Rosa, G. & Pozio, E. (1998). *Trichinella britovi* in foxes in The Netherlands. *The Journal of Parasitology***,** 1065-1068.

Vutova, K., Velev, V., Chipeva, R., Yancheva, N., Petkova, S., Tomov, T., Pozio, E. & Robertson, L. J. (2020). Clinical and epidemiological descriptions from trichinellosis outbreaks in Bulgaria. *Experimental Parasitology,* 212**,** 107874.

Wang, N., Bai, X., Tang, B., Yang, Y., Wang, X., Zhu, H., Luo, X., Yan, H., Jia, H. & Liu, M. (2020). Primary characterization of the immune response in pigs infected with *Trichinella spiralis*. *Veterinary Research,* 51**,** 1-14.

Wang, Y., Wen, Y., Wang, S., Ehsan, M., Yan, R., Song, X., Xu, L. & Li, X. (2017a). Modulation of goat monocyte function by HCcyst-2, a secreted cystatin from *Haemonchus contortus*. *Oncotarget,* 8**,** 44108-44120.

Wang, Y., Wu, L., Liu, X., Wang, S., Ehsan, M., Yan, R., Song, X., Xu, L. & Li, X. (2017b). Characterization of a secreted cystatin of the parasitic nematode *Haemonchus contortus* and its immune-modulatory effect on goat monocytes. *Parasites & Vectors,* 10**,** 425.

Wu, C., Duan, J., Liu, T., Smith, R. D. & Qian, W.-J. (2016a). Contributions of immunoaffinity chromatography to deep proteome profiling of human biofluids. *Journal of Chromatography B,* 1021**,** 57-68.

Wu, Z., Nagano, I. & Takahashi, Y. (2013). *Trichinella*: What is going on during nurse cell formation? *Veterinary Parasitology,* 194**,** 155-159.

Wu, Z., Nagano, I., Takahashi, Y. & Maekawa, Y. (2016b). Practical methods for collecting *Trichinella* parasites and their excretory-secretory products. *Parasitology International,* 65**,** 591-595.

Xu, N., Liu, X., Tang, B., Wang, L., Shi, H. N., Boireau, P., Liu, M. & Bai, X. (2017). Recombinant *Trichinella pseudospiralis* Serine Protease Inhibitors Alter Macrophage Polarization In Vitro. *Frontiers in Microbiology,* 8.

Xu, N., Bai, X., Liu, Y., Yang, Y., Tang, B., Shi, H. N., Vallee, I., Boireau, P., Liu, X. & Liu, M. (2021). The Anti-Inflammatory Immune Response in Early *Trichinella spiralis* Intestinal Infection Depends on Serine Protease Inhibitor-Mediated Alternative Activation of Macrophages. *Journal of Immunology,* 206**,** 963-977.

Yang, F., Yang, D. Q., Song, Y. Y., Guo, K. X., Li, Y. L., Long, S. R., Jiang, P., Cui, J. & Wang, Z. Q. (2019). In vitro silencing of a serine protease inhibitor suppresses *Trichinella spiralis* invasion, development, and fecundity. *Parasitology Research,* 118**,** 2247-2255.

Yang, N., Matthew, M. A. & Yao, C. (2023). Roles of Cysteine Proteases in Biology and Pathogenesis of Parasites. *Microorganisms,* 11**,** 1397.

Yang, Y., Wen, Y., Cai, Y. N., Vallée, I., Boireau, P., Liu, M. Y. & Cheng, S. P. (2015). Serine proteases of parasitic helminths. *Korean Journal of Parasitology,* 53**,** 1-11.

Yang, Z., Li, W., Yang, Z., Pan, A., Liao, W. & Zhou, X. (2018). A novel antigenic cathepsin B protease induces protective immunity in *Trichinella*-infected mice. *Vaccine,* 36**,** 248-255.

Zao, Y. J., Cheng, G., Feng, M. M., Wang, Y. X., Zhang, Z. F., Zhang, X. & Jiang, P. (2024). *Trichinella spiralis* cathepsin B bound and degraded host's intestinal type I collagen. *International Journal of Biological Macromolecules,* 257**,** 128728.

Zarlenga, D., Thompson, P. & Pozio, E. (2020). *Trichinella* species and genotypes. *Research in Veterinary Science,* 133**,** 289-296.

Zhan, J. H., Yao, J. P., Liu, W., Hu, X. C., Wu, Z. D. & Zhou, X. W. (2013). Analysis of a novel cathepsin B circulating antigen and its response to drug treatment in *Trichinella*-infected mice. *Parasitology Research,* 112**,** 3213-22.

Zhang, N., Li, W. & Fu, B. (2018). Vaccines against *Trichinella spiralis*: Progress, challenges and future prospects. *Transboundary and Emerging Diseases,* 65**,** 1447-1458.

Zhang, X. Z., Wang, Z. Q. & Cui, J. (2022). Epidemiology of trichinellosis in the People's Republic of China during 2009–2020. *Acta Tropica,* 229**,** 106388.

Zhou, L., Li, M., Du, Q., Yang, S., Li, J., Fan, Y., Mao, K., Zhang, J., Xiao, H. & Wang, J. (2023). Genome-wide identification of PLCPs in pepper and the functional characterization of CaCP34 in resistance to salt- and osmotic-induced leaf senescence. *Scientia Horticulturae,* 309**,** 111624.

Zhou, M.-Y. & Gomez-Sanchez, C. E. (2000). Universal TA cloning. *Current Issues in Molecular Biology,* 2**,** 1-7.

Zhu, B., Luo, F., Shen, Y., Yang, W., Sun, C., Wang, J., Li, J., Mo, X., Xu, B., Zhang, X., Li, Y. & Hu, W. (2020). *Schistosoma japonicum* cathepsin B2 (SjCB2) facilitates parasite invasion through the skin. *PLoS Neglected Tropical Diseases,* 14**,** e0008810.

Zondo, N. M. (2019). Molecular cloning, expression, purification and characterisation of a cathepsin B cysteine protease from *Trichinella zimbabwensis* as a potential diagnostics and vaccine candidate*.* University of KwaZulu-Natal, Pietermaritzburg, MSc.